STUDIES ON THE SYNTHESIS OF MAIN GROUP AND LATE TRANSITION ELEMENT FRAMEWORKS

by

CHRISTIAN SAMANAMU

Bachelor of Sciences with mention in Chemistry, January 2004
Pontificia Universidad Católica del Perú
Lima, Perú

Submitted to the Graduate Faculty of
College of Science and Engineering
Texas Christian University
in partial fulfillment of the requirements
for the degree of

Doctor of Philosophy

May 2009

ACKNOWLEDGEMENTS

It is my pleasure to express my gratitude to Dr. Anne F. Richards, for her efficacious, thoughtful guidance, encouragement and inspiration which helped me fulfill the goal of completing my graduate studies.

I would like to thank Prof. Jean-Luc Montchamp, Prof. Jeffery L. Coffer, Prof. David E. Minter and Prof. Robert H. Neilson for their helpful suggestions and guidance towards my thesis.

My gratitude is also attributed to my group members for their help.

TCU Department of Chemistry, Welch Foundation and TCU-Research and Creative Activities are also thanked for their supporting salary and research funding.

TABLE OF CONTENTS

CHAPTER 5.

Synthesis of homo and hetero metal-phosphonate frameworks from bi-functional aminomethylphosphonic acid

LIST OF ABBREVIATIONS

Ampa	Aminomethylphosphonic acid
ArX	Aryl halide
Adipic acid	Hexanedioic acid
H_2BDC	1,4-benzenedicarboxylic acid
H_3BTC	1,3,5-benzenetricarboxylic acid
4-btapa	1,3,5-benzenetricarboxylic acid tris[N-(4-pyridyl)amide]
H_3BTT	1,3,5-benzenetristetrazol-5-yl
2,2'-bipy	2,2'-Bipyridine
4,4'-bipy	4,4'-Bipyridine
Bib	1,4-bis(1-imidazolyl)benzene
Bpa	1,2-bis-(4-pyridyl)bipyridylethane
$(PyS)_2CH_2$	Bis(2-pyridylthio)methane
$(PymS)_2CH_2$	Bis(pyrimidylthio)methane
$(PymS)_2$	Bipyrimidyldisulfide
CCDC	Cambridge Crystallographic Database Centre
Cys	Cysteine
DB24C8	Dibenzo-[24]-crown-8-ether
DEF	N,N'-Diethylformamide
1D	One dimension, unidimensional
2D	Two dimensions, bidimensional
3D	Three dimensions, tridimensional

DMF	N,N′-Dimethylformamide
DMSO	Dimethylsulfoxide
Dpds	Dipyridyl disulfide
diPyNI	N,N'-di-(4-pyridyl)-1,4,5,8-napthalenetetracarboxydiimide
EtOH	Ethanol
EDX	Energy dispersive X-ray
Gly	Glycine
HRMS	High resolution mass spectra
*p*H	Hydrogen potential
Hys	Hystidine
Im	Imidazole
IR	Infrared
m.p.	Melting point
MOFs	Metal organic frameworks
Met	Methionine
MAO	Methyl aluminoxane
Ndc	2,6-napthalenedicarboxylate
NMR	Nuclear magnetic resonance
phen	o-phenanthroline
pyz	Pyrazine, 1,4-diazabenzene
pyzca	Pyrazine-2-carboxylic acid
H_3pdc	3,5-pyrazoledicarboxylic acid
$4PyCH_2PO_3H_2$	4-pyridylmethylphosphonic acid

$2PyPOH_2$	2-pyridylphosphonic acid
$4PyPOH_2$	4-pyridylphosphonic acid
pym	Pyrimidine, 1,3-diazabenzene
$5\text{-}PymPO_3H_2$	5-pyrimidylphosphonic acid
rrdW	Van der Waals radii
RX	Alkyl halide
oxalic acid	Ethanedioic acid
thf	Tetrahydrofuran
$^tBu_3Ga$	tris(tertbutyl) gallium
TGA	Thermogravimetric analysis
Triflate	Trifluoromethanesulfonate
TMSBr	Trimethylbromosilane
UV	Ultraviolet

LIST OF FIGURES

LIST OF SCHEMES

LIST OF TABLES

Chapter 1

Metal organic frameworks

1.1 Introduction

In 1990, Hoskins and Robson[1] published a pioneering paper presenting their results for the design and the construction of a new class of solid materials with infinite tridimensional framework structures containing copper or zinc atoms. At that time they realized that these extended structures, with their large internal surface area and open pores could have plentiful applications, in addition to having potential for further chemical functionalization.

Their first approach was based on the construction of extended ordered structures using molecular units that provided efficient ligation to tetrahedral metallic centers of copper(I) or zinc(II).[1] In order to synthesize these frameworks, they realized the need to link together units with selected tetrahedral arrays through some appropriate connectivity process. To this end they employed cyanide rodlike molecular units, which are reactive at both ends to link together those arrays by a substitution process at a second tetrahedral center. The result of this approach was the construction of the single diamond-related framework $[N(CH_3)_4][Cu^{I}Zn^{II}(CN)_4]$ by substitution of every other Zn^{2+} of a single $Zn(CN)_2$ framework by Cu^{+} (See Figure 1.1).[1]

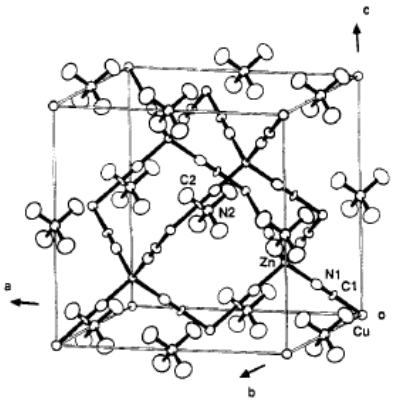

Figure 1.1 Cubic unit cell of $[N(CH_3)_4][Cu^{I}Zn^{II}(CN)_4]$ showing part of its contents.Taken from reference 1.

In the following years, this idea attracted growing interest in the chemical community leading to the creation of a new class of synthetic materials called metal organic frameworks (MOFs).[2]

MOFs are crystalline compounds that consist of metal ions or metallic clusters coordinated to rigid or non-rigid organic molecules (organic spacers or organic linkers) to form often porous (microporous[3] and mesoporous[4]) one-, two- or three-dimensional structures (See Figure 1.2).

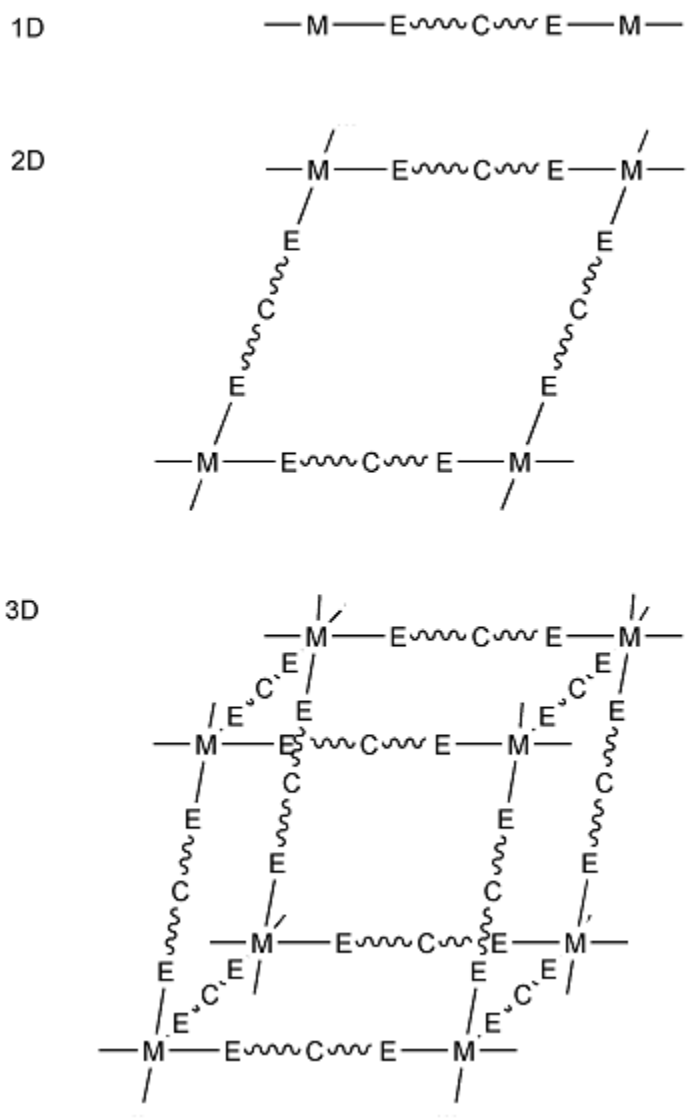

Figure 1.2 Representation of the definition of 1D, 2D or 3D coordination polymers having organic bridging ligands with at least one carbon atom in-between the donor atoms (E). M = metal and the donor atoms (E) can be O, N, S, Se, etc. Taken from reference 2.

Compared with inorganic porous materials (i.e. zeolites)[5] the construction of these frameworks allows control over their pore size, their corresponding shape and the chemical environment of the voids.[6-8] Today the number of research papers related to the synthesis of this class of materials stands at more than 3000[9] with more than 12000 reported structures.[10] The interest in these compounds is explained by their fascinating architectures and their increasing use as functional materials due to their promising properties such as: high porosity,[11] host-guest exchange,[12] catalysis,[13] gas storage,[14] photoluminescence,[15] chirality[16] and magnetic properties.[17]

1.2 Mechanism of formation of metal organic frameworks

In 1993, Stein[18] recognized the importance of completely understanding the chemical reactions for the synthesis of MOFs in order to achieve specific functionalized materials. In this context, Ramanan and Whittingham[19] proposed a simple mechanism for the formation of MOFs. According to their hypothesis,[19] when the metallic precursor is dissolved in the corresponding reaction solvent, a soluble metallic complex is formed. Based on Lewis acid-base interactions, this initial complex will interact with the organic groups present in the medium in order to produce reversible or irreversible bonds. The final solid is formed through a continuous series of solvolysis and condensations. To explain the formation of this resultant solid, the condensation process is believed to occur when point zero charge (PZC) molecules are formed at the isoelectric point. This event produces extended frameworks. The recognition of these PZC molecules as primary building blocks allows the identification of geometrical patterns in a particular structure and to explain the phenomenon of interpenetration which appears when the frameworks interweave, thereby reducing or eliminating their porosity (See Figure 1.3).[20] In conclusion, this hypothesis states that all these events are a manifestation of the way these PZCs interconnect to each other and condense through the elimination of solvent molecules.

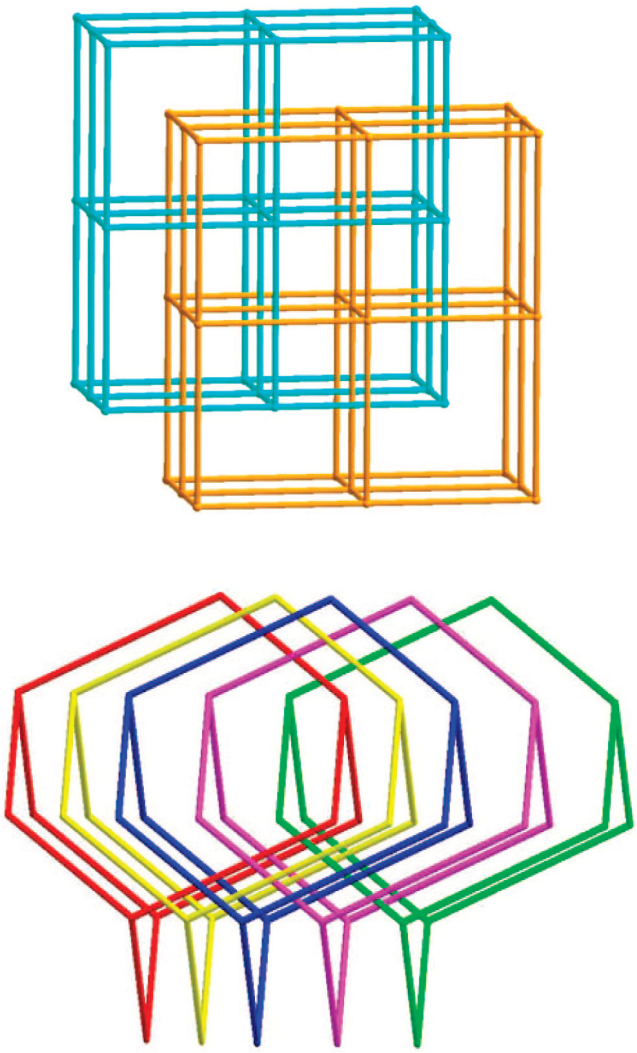

Figure 1.3 Examples of interpenetration in MOFs. Top, [Mn(bib)(HBTC)]. Bottom, $[Ni_2(bib)_2(BDC)_2.2H_2O].H_2O$. H_3BTC = 1,3,5-benzenetricarboxylic acid, H_2BDC = 1,4-benzenedicarboxylic acid) and bib=1,4-bis(1-imidazolyl)benzene. Taken from reference 20.

1.3 Methods for the synthesis of metal organic frameworks

The synthesis of metal organic frameworks is through careful control of numerous factors such as: molar concentration of the reactants, physical state of the reactants, number of ligands involved in the reaction, solvent polarity, *p*H, temperature and reaction times.[21,22] The stoichiometric combination of reactants leads to the production of crystalline material suitable for further characterization by single crystal X-ray crystallography and powder X-ray diffraction. Among the methods for the synthesis of metal organic frameworks are:

(a) Solvothermal methods: This method involves the heating of a mixture of the organic spacer and the metallic salt in a solvent at high temperature and pressure.[23] Such a method often yields crystals suitable for single crystal X-ray diffraction analysis; but the disadvantages are that they require long reaction times and the use, in some cases, of controlled temperature devices. Furthermore, these solvothermal conditions can produce the decomposition of thermally sensitive starting materials. In this category it is noteworthy to mention the "microwave-assisted solvothermal synthesis" which involves the use of microwave radiation that helps to reduce the reaction time compared to common solvothermal methods.[24]

(b) Room temperature methods: In this method, the metallic precursor is slowly added to a solution containing the organic spacer, dissolved in a suitable solvent and, in some cases, a base under vigorous stirring.[10] Included in this category is the slow vapor diffusion technique for framework synthesis. This technique consists of slow vapor diffusion at room temperature of a selected solvent (in some cases containing a volatile base such as triethylamine)[25] into a solution containing the dissolved metal salt and organic spacer. In order to promote the crystallization of the MOF, the product must have limited solubility in the solvent that has been diffused.

(c) Solvent-free synthesis: This process uses mechanochemical procedures (grinding) to produce the desired multidimensional framework[26] or by direct fusion of the reactants.

1.4 Building blocks of metal organic frameworks

The synthesis of MOFs requires assembling repeat units, known as the building blocks which are connected to give rise to a final solid structure with defined symmetry and dimensionality.[27] A common theme in MOF synthesis is to employ a multidentate organic molecule for reactions with metal salts.[27] Through specific geometrical ligand (spacer) selection it is possible to attempt final product structure manipulation. A selection of common organic molecules (spacers) used for this purpose is shown in Figure 1.4.

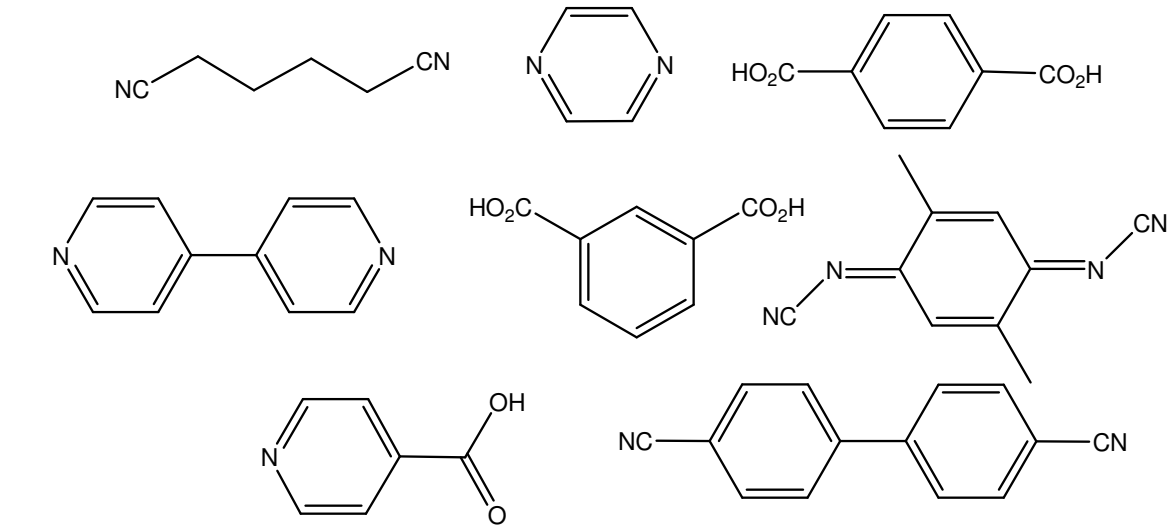

Bidentate ligands

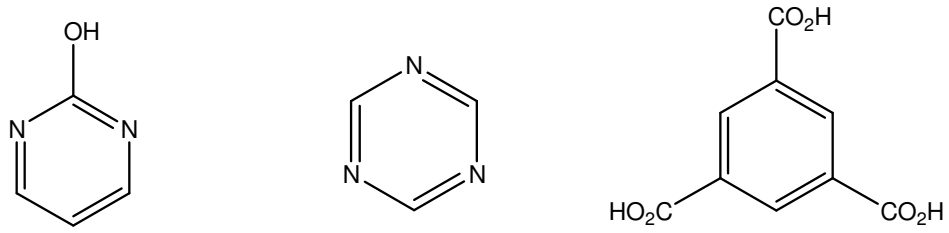

Tridentate ligands

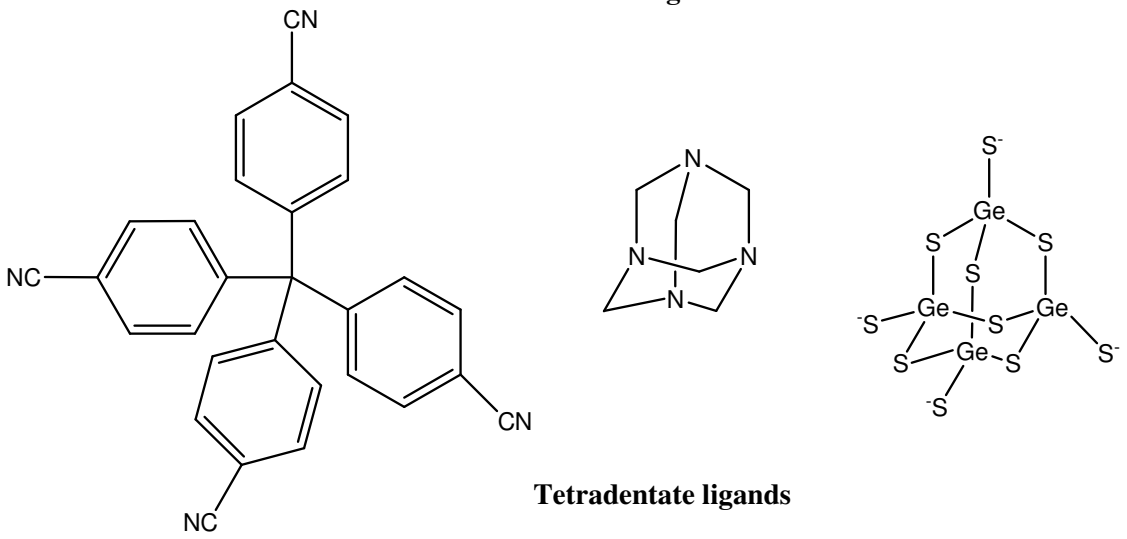

Tetradentate ligands

Figure 1.4 Different ligands used in the construction of MOFs.

At this point it is important to distinguish between two important constituents of these frameworks: building unit and asymmetric unit. The former, in an ionic approach, is

associated with anionic coordination of one or several cations defining the metallic centers of the building unit, whereas the latter refers to crystallographic sites and therefore to symmetry.

1.5 Structural diversity

The last 10 years have witnessed an increased interest and a rapid evolution in the field of MOFs.[28] The chemical preferences of the metallic centers coupled with the geometrical requirements and coordination abilities of the organic spacers have made possible the synthesis of a vast number of metal organic frameworks with 1D, 2D and 3D arrangements formed via coordination bonds.[19] Due to the huge variety of synthesized frameworks, the following section will deal only with descriptions of selected examples that illustrate special features of these n-dimensional arrays.

1.5.1 Unidimensional metal organic frameworks (1D MOFs)

In 1978 Basolo and coworkers synthesized octaethylporphyrinato manganese(III) tetracyanoethenide, a 1D manganese porphyrin coordination polymer.[29] Later, Epstein and coworkers[30] characterized this linear porphyrin in which the porphyrinic planar MnN_4 arrangements are parallel to each other (See Figure 1.5). These planes are linked through the manganese atoms by tetracyanoethenide ligands which lead to a weak ferromagnetic coupling that is explained by the presence of slightly tilted tetracyanoethenide anions giving a non uniformity in the monodimensional chain.

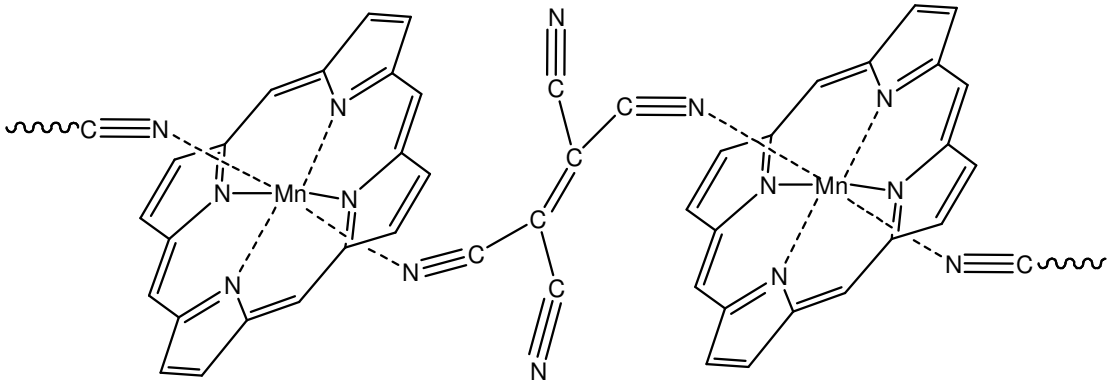

Figure 1.5 Molecular structure of the 1D polymer, octaethylporphyrinato manganese(III) tetracyanoethenide. (Ethyl groups omitted for clarity. Modified from reference 30.

In order to explore the possibility of synthesizing novel 1D frameworks using polynuclear metallic precursors, the use of copper(II) acetate in conjunction with the flexible spacer 1,3-di-4-pyridylpropane was investigated and yielded a zigzag chain containing a dimeric center of copper atoms.[31] The spatial behavior of this 1D chain is due to the *anti* torsion angles of the propyl group in the organic spacer. In these chains it is possible to find the copper atoms directly bonded to the nitrogen atoms of the 1,3-di-4-pyridylpropane that displaced water molecules from the original copper acetate structure. The X-ray diffraction analysis of this material revealed that the chains form layers, and that the angle at which an adjacent layer of chains crosses the layer beneath is of 49.1°. Between the layers of chains are channels of methanol that run perpendicular to each layer (Figure 1.6).

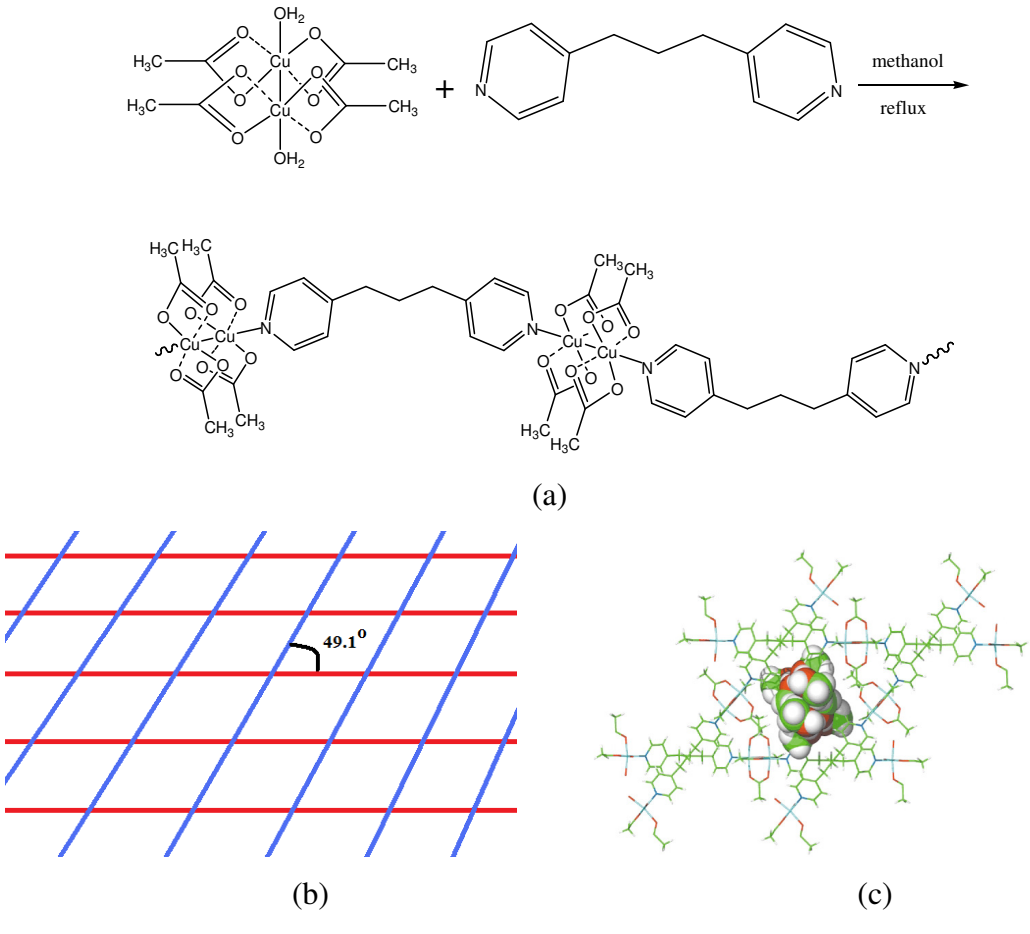

(a)

(b)

(c)

Figure 1.6 (a) Reaction between copper acetate and 1,3-di-4-pyridylpropane which leads to the formation of a 1D zigzag chain. Modified from reference 17 (b) Scheme showing two different layers of chains (blue and red) and the corresponding angle formed between adjacent layers of these non-interpenetration 1D chains. (c) Space-filling plot of the infinite channels viewed along the channel axis showing the included pair of ordered four-fold helices of methanol. Taken from reference 31.

In contrast to the flexible nature of 1,3-di-4-pyridylpropane, mechanically interlocked molecules can be used as rigid spacers for the construction of MOFs. An example is the use of rotaxanes. Rotaxanes are formed when acyclic molecules are inserted inside the cavity of macrocyclic molecules.[32a] The use of rotaxanes as spacers in the construction of extended frameworks provides an opportunity for the insertion of rotaxane based molecular machines into multidimensional MOFs.[32b] 1,2-bis(pyridinium)ethane dications can act as axles for the efficient formation of rotaxanes when employing crown ethers as the wheel component. The two components are held together by a series of C-H···O interactions and significant ion-dipole interactions between the positive charge on the pyridinium nitrogen atoms and the electronegative oxygen atoms of the crown ether (Figure 1.7). Using crown ethers with aromatic rings increases the association by the introduction of π-stacking between the pyridinium rings and the catechol rings.

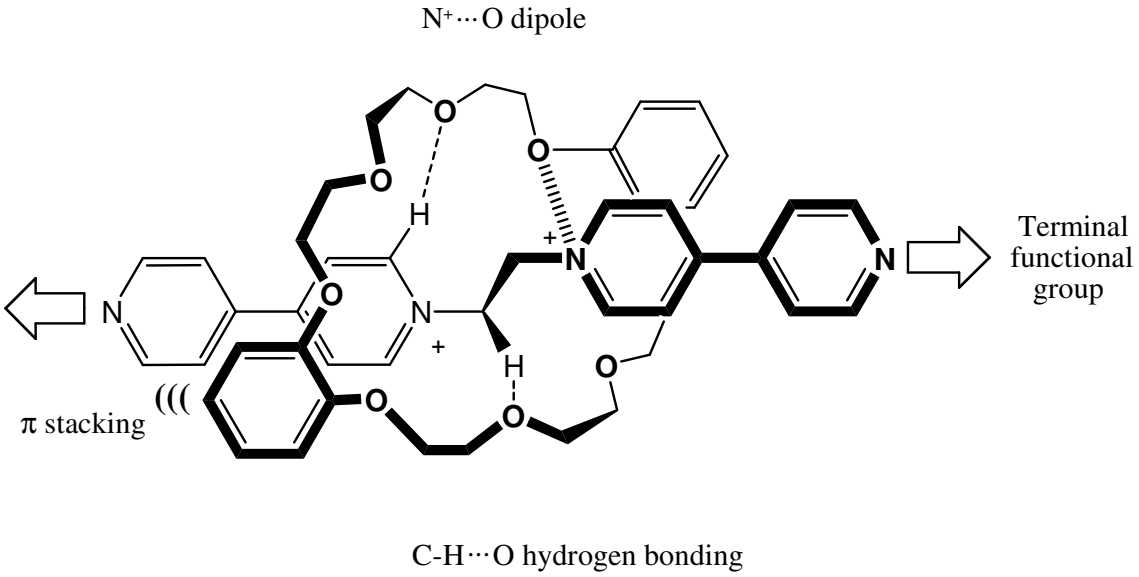

Figure 1.7 Example of non covalent interactions in a rotaxane. Interaction between 1,2-bis(4,4'-bipyridinium)ethane dication, (blue) and dibenzo-[24]-crown-8-ether (DB24C8) (red). Taken from reference 32b.

Davidson and Loeb[33] synthesized a polyrotaxane using a pyridinium salt, dibenzo-[24]-crown-8-ether (DB24C8), and cobalt(II) tetrafluoroborate hexahydrate. The result was a one dimensional chain containing octahedral cobalt(II) atoms coordinated to two polyrotaxane molecules, two molecules of acetonitrile and two molecules of water (See Figure 1.8). This approach opened the possibility of using mechanically interlocked

molecules for constructing n-dimensional frameworks that could be used to introduce controlled molecular motion in order to affect their resultant bulk properties.[32]

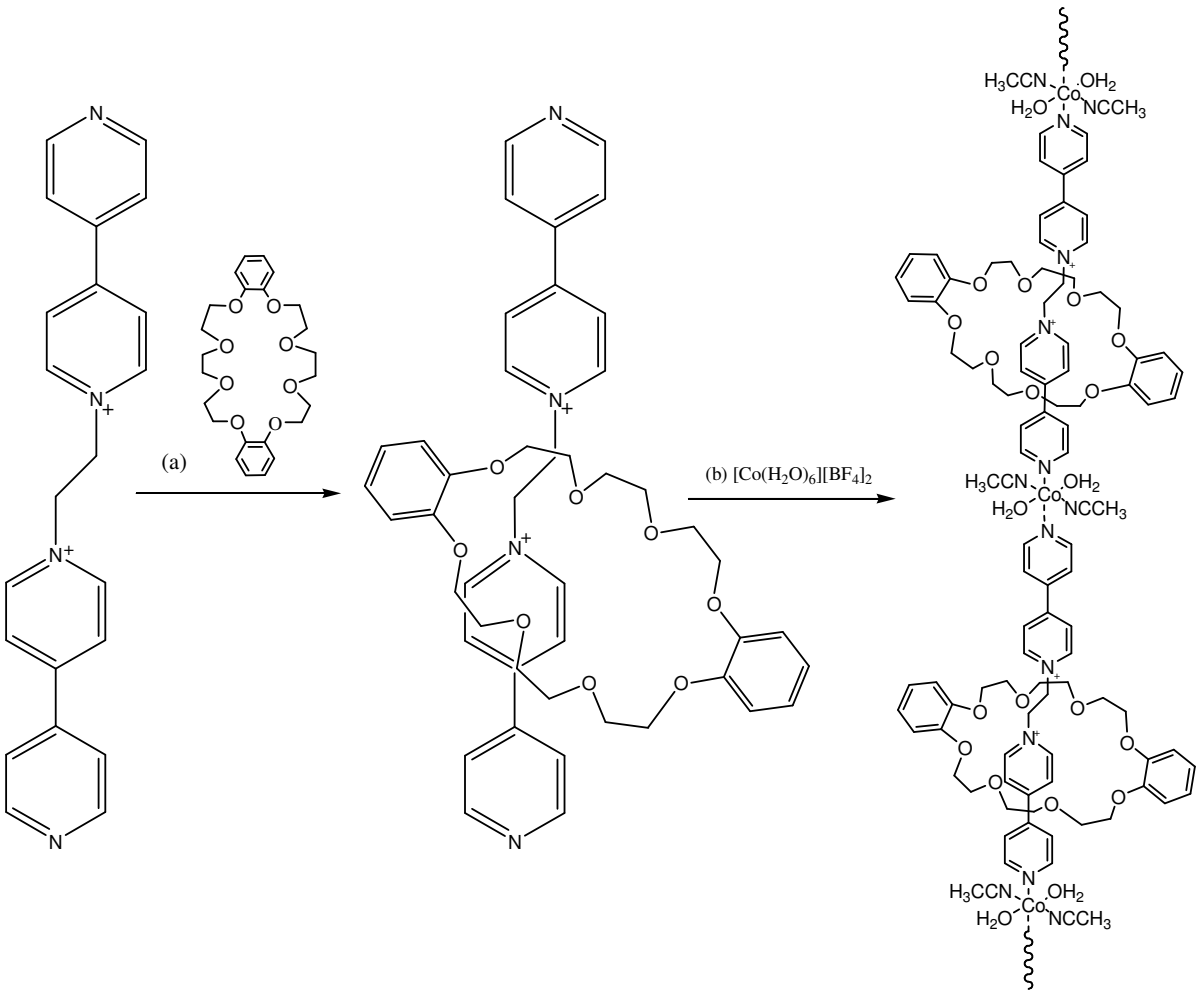

Figure 1.8 Example of the synthesis of a 1D MOF using polyrotaxane molecules. (a) The dipyridinium salt is reacted with DB24C8 giving the polyrotaxane moiety. (b) The subsequent reaction with $[Co(H_2O)_6][BF_4]_2$ yields the 1D chain containing the polyrotaxanes. Adapted from reference 33.

1.5.2 Bidimensional metal organic frameworks (2D MOFs)

2D MOFs have been synthesized using numerous approaches in which the ratio of metal and ligand and the nature of the coordination of the ligands are the primary factors that determine the topology of the framework.[34] For example, the reaction of zinc(II) chlorate and 3-cyanopyridine in a mixture of water and ethanol leads to the formation of a chiral 2D square grid structure.[35] The employed bifunctional ligand was hydrolyzed under solvothermal conditions of the reaction to obtain the carboxylate derivative.[35] The square

grid polymer crystallizes in the chiral space group $P4_32_12$ with the zinc atoms found in distorted octahedral environments coordinated to two carboxylate groups and two pyridyl nitrogen atoms of four different m-carboxypyridine ligands (See Figure 1.9).

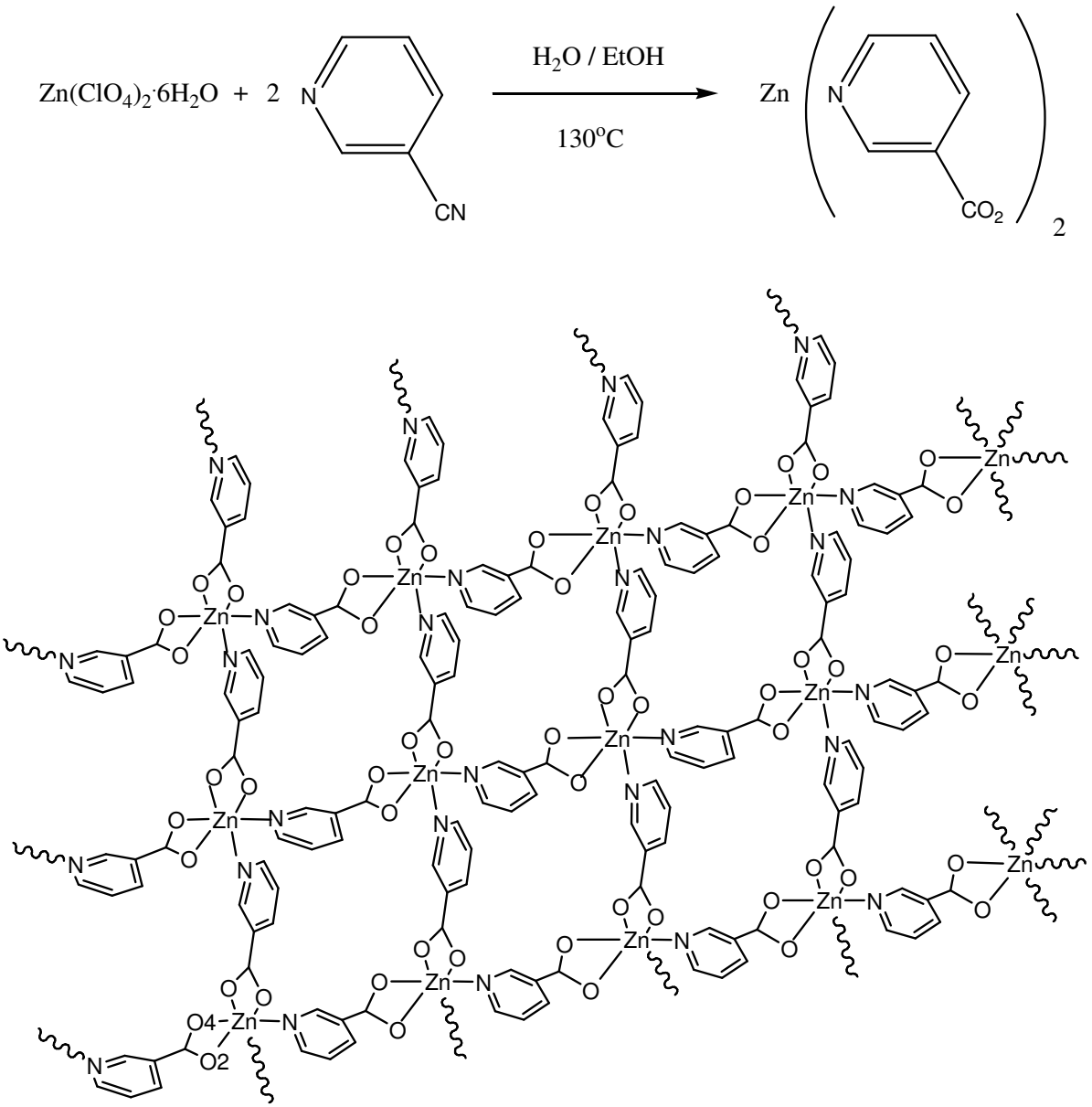

Figure 1.9 Conditions for the reaction between zinc(II) chlorate and 3-cyanopyridine. The resultant 2D chiral molecular grid is also presented. Modified from reference 35.

In another approach to obtain a 2D MOF with open voids, the addition of solid nickel(II) acetate to an aqueous solution of imidazole (im), followed by heating at 180°C in a Teflon-lined autoclave yielded α-Ni(im)$_2$ as a crystalline material.[36] In this material the imidazole ligands and the Ni(II) atoms form 2D arrays of square meshes (See Figure 1.10).

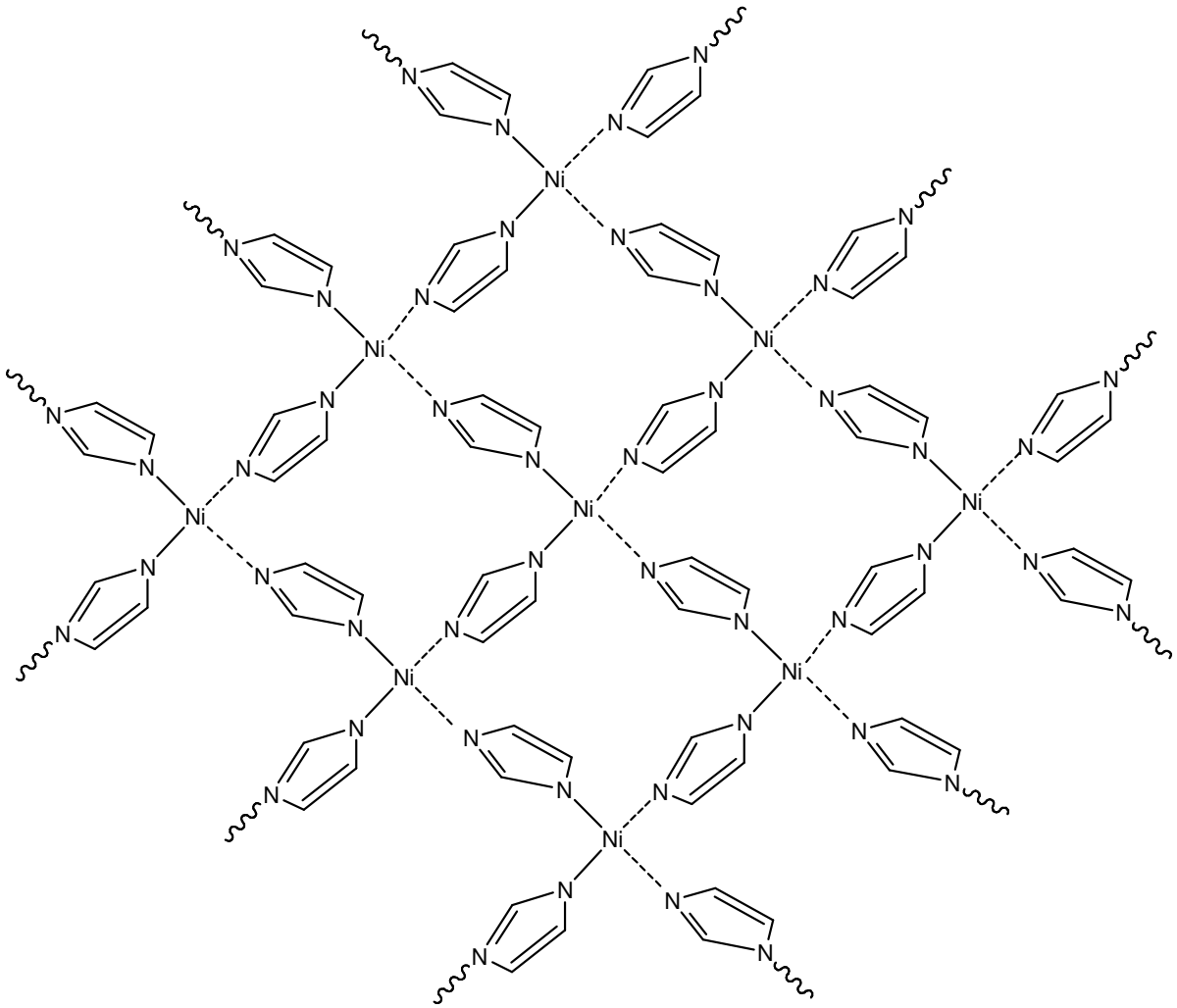

Figure 1.10 Representation of the 2D array of open square meshes in the phase α-Ni(im)$_2$. Modified from reference 36.

The distance between adjacent Ni(II) atoms is ~5.73Å which is comparable to other compounds containing nickel in a square planar geometry.[37] A further example of a 2D polymer was reported by Frisch and Cahill who studied the coordinating abilities of the multidentate ligand 3,5-pyrazoledicarboxylic acid (H_3pdc) for the synthesis of bimetallic MOFs.[38a] This ligand has "hard" carboxylic acid groups and "soft" pyrazole nitrogens

making it ideal for the construction of heterometallic MOFs.[38b] From the equimolar reaction of H_3pdc, copper(II) nitrate and uranium(VI) dinitrate oxide in water under hydrothermal conditions. The framework, $[(UO_2)Cu(C_5H_2N_2O_4)_2(H_2O)_2]$, features a UO_2^{2+} cation bound to four different ligand units of H_3pdc through the carboxylate moiety. The uranium centers are found in a square bipyramidal geometry while the copper centers are found in a distorted octahedral geometry. The vertices of this octahedron are occupied by two different H_2pdc ligands coordinating through nitrogen and oxygen atoms (See Figure 1.11).

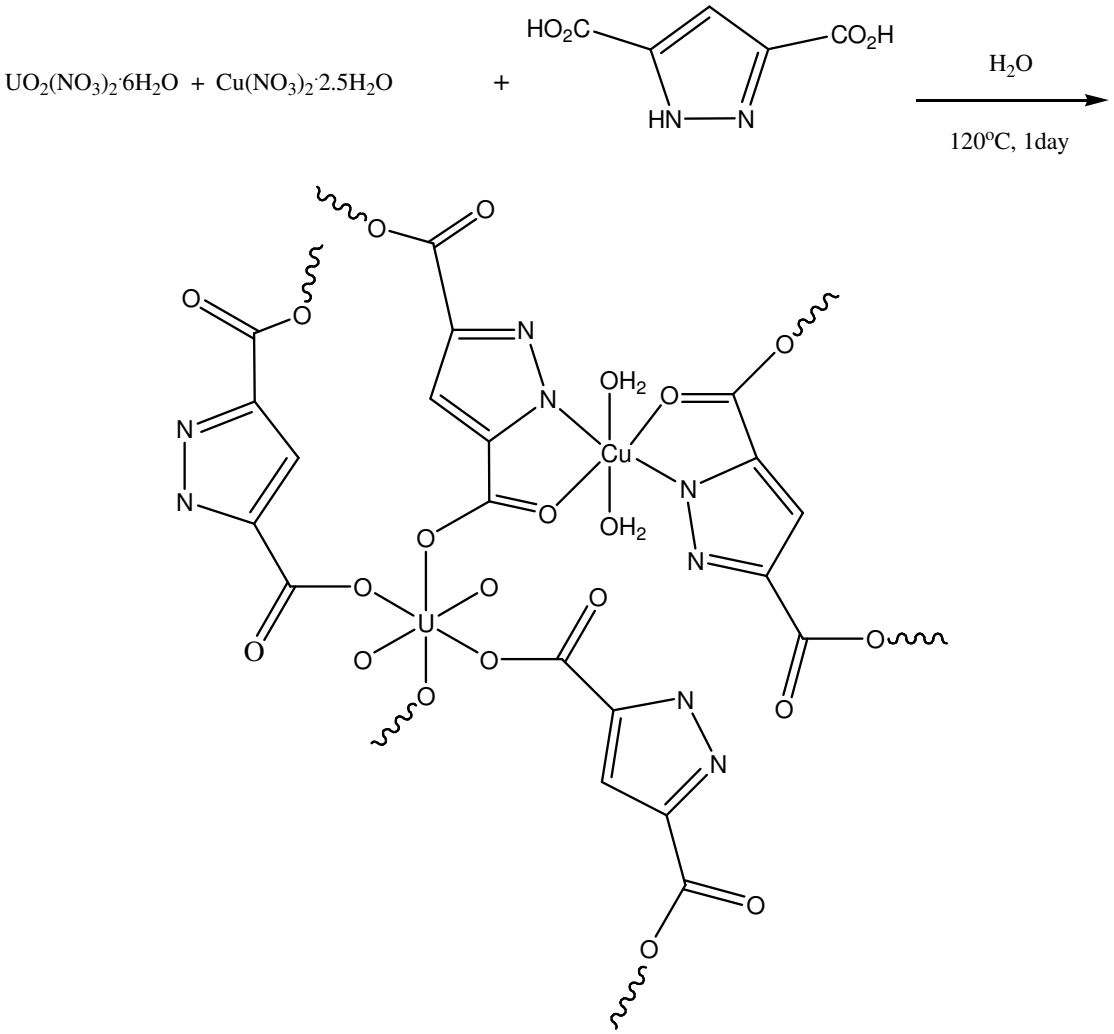

Figure 1.11 Conditions for the synthesis of $[(UO_2)Cu(C_5H_2N_2O_4)_2(H_2O)_2]$. Taken from reference 38a.

This uranium/copper polymer joins a limited group of characterized bimetallic polymers with very useful technological applications[38b] and it represents the first example of a heterometallic H_3pdc containing polymer structure.[38a]

1.5.3 Tridimensional metal organic frameworks (3D MOFs)

In 1999, Yaghi *et al.* synthesized one of the most significant 3D metal organic frameworks, $[Zn_4O(BDC)_3(DMF)_8(C_6H_5Cl)]$ (See Figure 1.12) subsequently defined as MOF-5.[39] MOF-5 is synthesized from the reaction of zinc(II) nitrate, 1,4-benzenedicarboxylic acid (BDC), triethylamine and hydrogen peroxide in a solvent mixture of N,N'-dimethylformamide and chlorobenzene.[39] MOF-5 has ZnO_4 tetrahedra which are capped by CO_2 groups to form a $Zn_4(O)(CO_2)_6$ cluster. These clusters are interconnected by the bidentate ligand, BDC, to form a 3D structure that has guest molecules of N,N'-dimethylformamide and chlorobenzene within the pores. MOF-5 has become a benchmark material because of its very large surface area, its ability to retain crystallinity on loss of guest molecules as well as its superior absorption properties and catalytic activity.[39]

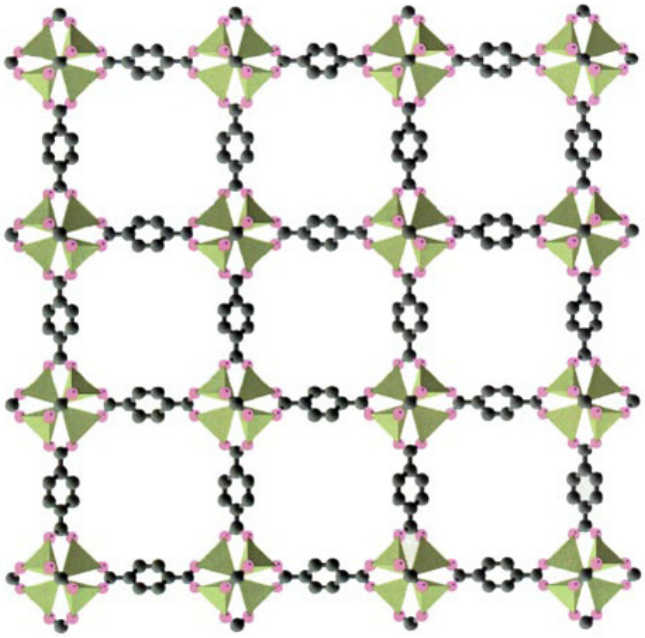

Figure 1.12 Representation of a {100} layer of the MOF-5 framework shown along the a-axis (C, black; O, pink). The ZnO_4 tetrahedra are indicated in green. Taken from reference 39.

1.5.3.1 Heteroleptic metal organic frameworks

Heteroleptic MOFs were first explored by the group of Rao by reacting adipic acid, oxalic acid and $LaCl_3$ in water under hydrothermal conditions.[40] The result was a 3D framework containing the La atom in a 9-coordinated environment coordinated to four oxygen atoms from two oxalate groups, four oxygens of three adipate groups and one water molecule (See Figure 1.13). The formed structure can be described as La-oxalate dimers that are connected by bridging adipate oxygen atoms to form interconnected layers. The connectivity between the layers results in the formation of channels down the c-axis of the unit cell, with both the oxalate and adipate groups forming the walls of the channel.

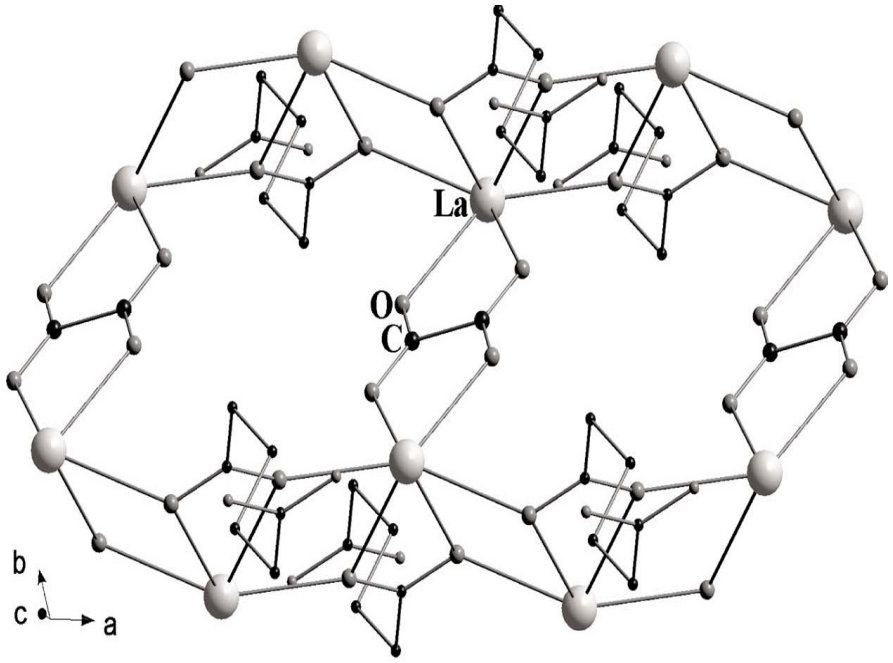

Figure 1.13 A view of the three-dimensional structure of $[La_2(C_2O_4)_2(C_6H_8O_4)(H_2O)_2]$ down the *b*-axis of the unit cell. Taken from reference 40.

1.6 Applications of metal organic frameworks

MOFs have wide and diverse applications that are too plentiful to detail here. To highlight the broad range of applications, a select group of examples will be described below.

1.6.1 Gas storage

In comparison with related compounds such as zeolites, the applications of the metal organic frameworks are an emerging field.[41] An attractive application of MOFs is related to the storage of hydrogen gas which is an alternative future energy source due its high energy content, clean burning and its renewable characteristic.[42] According to the requirements of the US Department of Energy,[43] future hydrogen-fueled cars should be able to operate at ambient conditions, allowing safe and efficient fueling systems, be comparable to gasoline and have a high mileage per load. To fulfill these requirements the storage system must present a highly reversible uptake capacity.[43]

The inclusion of coordinatively unsaturated metal centers in MOFs, acting as Lewis acid sites, inside the pores (chemisorption) or over the surface (physisorption) of the MOFs can allow the binding of hydrogen molecules.[44] A drawback of this approach resides in the generally weak interaction between the metal center and the $H_2(g)$ molecule which is mainly characterized by dispersion forces.[45] For that reason, the majority of these materials work at low temperatures and in some cases their applicability is limited to cryogenic temperatures.[45] A possible solution to this problem is to combine these acid sites with a consequent reduction of the size of the pore, in order to strengthen the Van der Waals contact with the $H_2(g)$ molecules,[46] or with the use of flexible MOFs in order to desorb them later at higher temperatures.[47] Three strategies are postulated to incorporate unsaturated metal centers:

(i) removal of metal-bound solvent molecule

(ii) incorporation of metallic species within the oganic spacer, and

(iii) impregnation of a given framework with excess metal cations.

The most widely used method is the removal of metal-bound solvent molecules such as N,N'-dimethylformamide, water or methanol creating unsaturated metal centers.[45] The majority of MOFs synthesized by this approach are based on small metal clusters bridged by carboxylate groups such as the paddlewheel unit $\{M_2(O_2CR)_4\}$ in which M is usually Cu^{2+} or Zn^{2+}.[48]

Another method for the introduction of unsaturated metal centers is to attach the desired metal to the organic spacer. In contrast to the strategy previously described, the unsaturated metal centers produced in this manner would not be part of the metal-building unit of a given MOF.[45] An example of this approach is the use of a half-sandwich unit such

as {(BDC)Cr(CO)$_3$} inside $Zn_4O(BDC)_3$ (See Figure 1.14). The elimination of all the three CO molecules from the {Cr(CO)$_3$} moiety leads to vacant sites for H_2 coordination.[49]

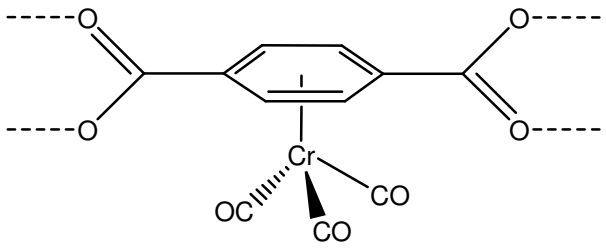

Figure 1.14 Molecular structures of the bridging ligand {(BDC)Cr(CO)$_3$} that can give rise to metal-H_2 binding sites. Taken from reference 45.

The third method consists of doping the synthesized MOF in order to obtain new and stronger binding sites. For example, Mulfort and Hupp used a suspension of Li metal in DMF to reduce $Zn_2(ndc)_2(diPyNI)$, (ndc = 2,6-naphthalenedicarboxylate; diPyNI = N,N'-di-(4-pyridyl)-1,4,5,8- naphthalenetetracarboxydiimide),[50] thus doping the synthesized MOF with approximately 5 mol% of Li cations which led to an increase in the H_2 adsorption capacity.

1.6.2 Chemical separation

Another field of interest is related to separation processes. An example is the separation of alkane isomers using the MOF, $Zn(BDC)(4,4\text{-Bipy})_{0.5}$, (BDC = 1,4-benzenedicarboxylic acid, 4,4'-Bipy = 4,4'-bipyridine) which was synthesized by the solvothermal reaction of $Zn(NO_3)_2.6H_2O$, BDC and 4,4'-Bipy.[51] The synthesized framework presents the paddle-wheel dinuclear zinc carboxylate units {$Zn_2(CO_2)_4$}. The 2D square grids are pillared by 4,4'-Bipy molecules, whose nitrogen atoms occupy the axial sites of the {$Zn_2(COO)_4$} paddle wheels, to form a 3D framework. The separation capacity of the synthesized framework is a result of the degree of the strength of interaction between the alkane isomers and the micropores of the framework.

1.6.3 Magnetism

In the field of magnetism, MOFs have found wide application due the possibility of synthesizing structures containing magnetically coupled metallic centers[52] and in that way

obtaining frameworks with variable magnetic properties.[52b] An example is the synthesis of the magnetic metal organic framework $[Mn_2(C_8H_4O_4)_2(C_3H_7NO)_2]$ (See Figure 1.15).[53] This framework was synthesized by the reaction of 1,4-benzenedicarboxylic acid ($C_8H_6O_4$), $Mn(NO_3)_2.6H_2O$ and DMF at 108°C for 18 days in an autoclave affording a MOF that consists in chains of Mn atoms interconnected by the carboxylate linker forming rombic cavities. The structure shows antiferromagnetic behavior but does not reach magnetic ordering down to 2 K.

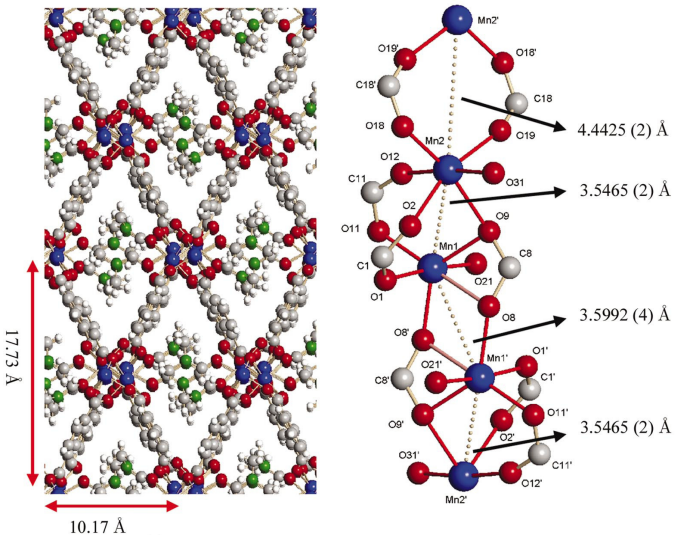

(a) (b)

Figure 1.15 The crystal structure of $[Mn_2(C_8H_4O_4)_2(C_3H_7NO)_2]$ at 16 K. (a) The crystal structure along the a axis. The DMF molecules coordinated to Mn occupy the voids. (b) The Mn chain interconnected by carboxylate groups. Taken from reference 53.

This framework does not present direct Mn-Mn bonds and its magnetic ordering is due to super-exchange via carboxylate bridges between the Mn atoms within the polymeric structure.

1.6.4 Catalysis

In the field of catalysis, MOFs have found great utility.[54] The strategy for catalysis is to functionalize the channel surfaces of the MOFs by two methods, firstly by the introduction of organic groups in order to provide guest-accesible functional organic sites,[55] and secondly to immobilize unsaturated metal sites.[56] The attractiveness of the first strategy is that it is relatively easy to create functional groups that can behave as base-type catalysts.[57] The

disadvantage is that in some cases the donating functional organic sites tend to coordinate metal centers.[58]

In 2007, Hasegawa *et al.*[59] created a 3D porous MOF from the reaction of $Cd(NO_3)_2.4H_2O$ and 1,3,5-benzene tricarboxylic acid tris[N-(4-pyridyl)amide], (4-btapa), a tridentate amide ligand, as the organic spacer (See Figure 1.16). The synthesized framework displayed a free amide functionality that was able to interact with different organic substrates in order to catalyze Knoevenagel condensations.[59]

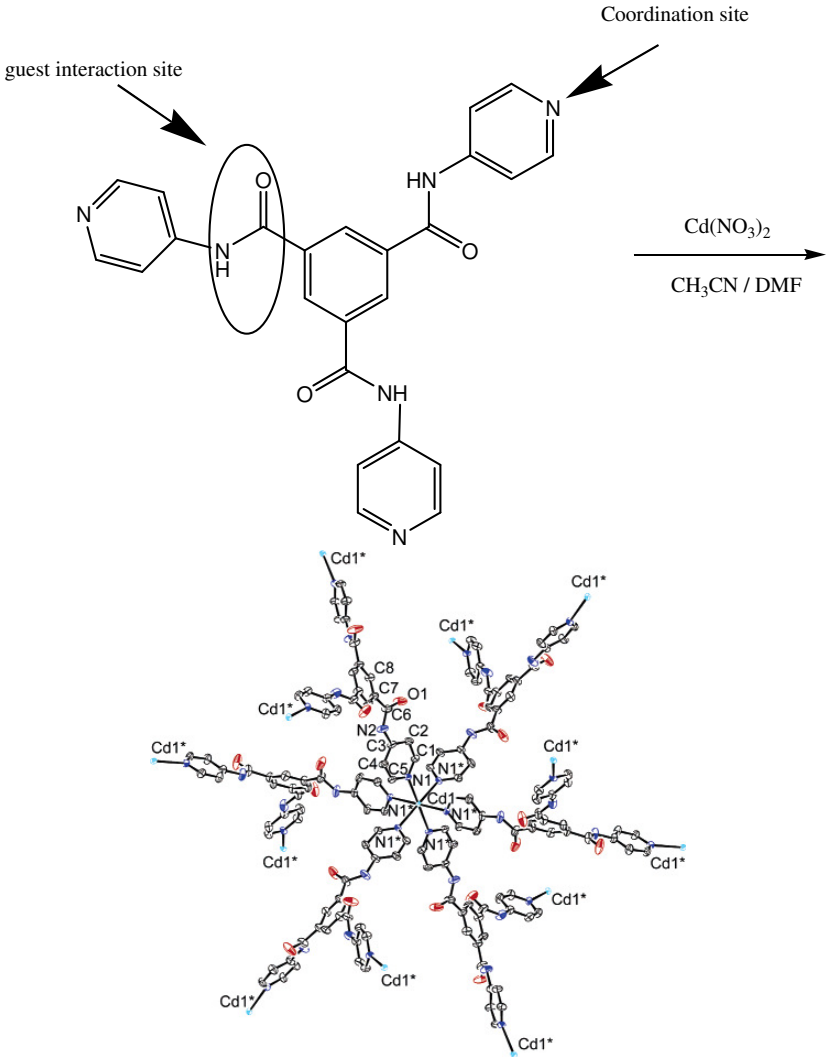

Figure 1.16. 1,3,5-Benzenetricarboxylic acid tris[N-(4-pyridyl)amide] (4-btapa) in reaction with $Cd(NO_3)_2$ affords the polymer $\{[Cd(4\text{-btapa})_2(NO_3)_2]6H_2O.2DMF\}_n$, in which Cd(II) centers are octahedrally coordinated to N atoms of different six 4-btapa. H_2O molecules and hydrogen atoms are omitted for clarity. Taken from reference 59.

MOFs containing well defined pores with unsaturated metal centers are an alternative option for catalysis reactions. The first report of this approach was related to enantioselective catalysis. For this purpose, Long *et al.* used $Mn_3[(Mn_4Cl)_3(BTT)_8(CH_3OH)_{10}]_2$, H_3BTT = 1,3,5-benzenetristetrazol-5-yl, (See Figure 1.17) and examined its catalytic properties with substrates that are of comparable size to the polymer pore dimensions.[60] This framework has two different types of Mn nuclei. One Mn center has one chloride and four bridging tetrasolate ligands with a sixth methanol ligand that projects into the pore. The second Mn site is bound by just two tetrazolate ligands. These Mn sites act as Lewis acid sites aiding the heterogeneous catalysis for the cyanosilylation of aromatic aldehydes and in the Mukaiyama-aldol reaction.[61]

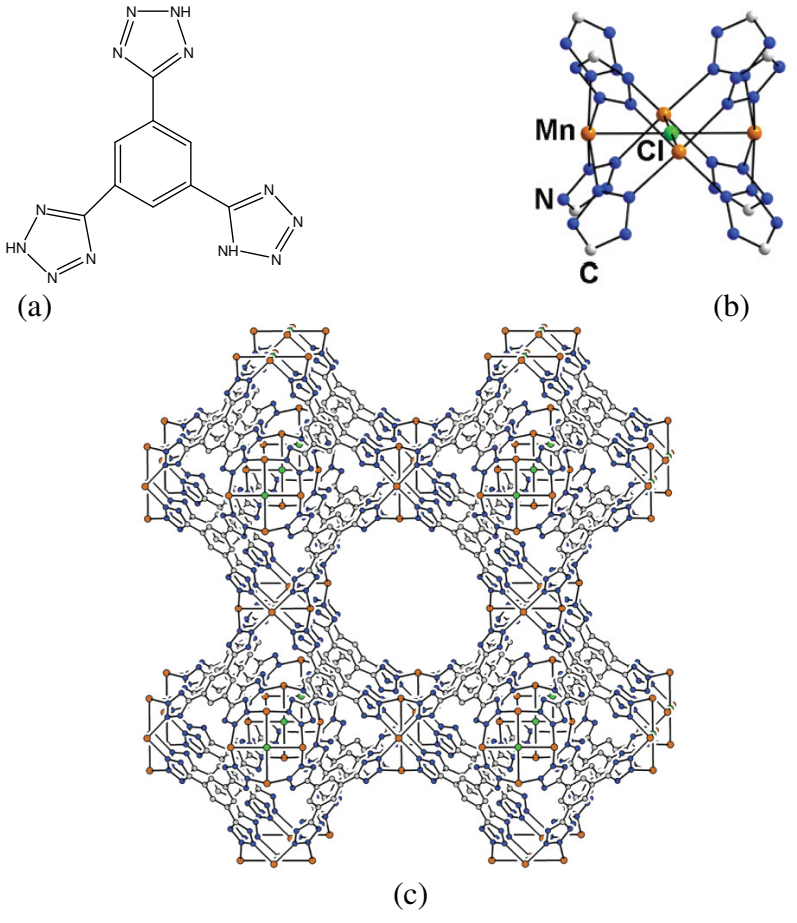

Figure 1.17 (a) Ligand 1,3,5-benzenetristetrazol-5-yl (H_3BTTP). (b) A square-planar Mn_4Cl cluster surrounded by eight tetrazolate rings (c) A cube of eight sodalite-cage like unit sharing square Mn_4Cl faces. Hydrogen atoms and solvent molecules are omitted for clarity. Selected interatomic distances (Å) and angles (°): Mn-Cl 2.736(1), Mn-N 2.227(3), Mn-Mn 3.869(2), Mn-Cl-Mn 90.0, N-Mn-N 87.6(1), 91.4(1), Mn-N-N 125.3(2). Taken from reference 61.

Despite the growing field of metal organic frameworks, a full knowledge of their potential remains unexplored. In contrast to well developed transition metal polymers we were interested in studying the main group elements. While many transition metal polymers are made by solvo or hydrothermal methods we were interested in a straight forward, high yielding method that would afford reproducible crystalline material for further investigation. In addition, we proposed studying bimetallic p/d block polymers that have potential in a multitude of unharnessed applications, as well as being of fundamental scientific interest and importance. This dissertation will present our efforts in that direction.

In Chapter 2 of this doctoral thesis, we document the use of pyrazine and pyrazine-2-carboxylic acid as molecular spacers in conjunction with metallic salts of selected group 13 elements (Ga, In and Tl) for the synthesis of 1D and 2D MOFs. This goal was achieved using short reaction times, "green solvents" and temperatures not exceeding the boiling point of the corresponding solvent, affording high yields of reproducible crystalline material.

Chapter 3 deals with the use of bipodal heteroelemental ligands containing nitrogen and sulfur atoms for the synthesis of MOFs. In particular we were interested in the synthesis of copper metal organic frameworks as a possible route to obtain synthetic multidimensional systems similar to the ones present in biological copper containing systems.

Related to carboxylic acids are phosphonic acids. Chapters 4-6 report our studies in the area of metal phosphonates. For example, in chapter 4, the use of 2-pyridylphosphonic acid derivatives afforded a series of Al/Ga phosphonate cages that show structural topology reminiscent of aluminum zeolites and related to methyl aluminoxane (MAO).

Chapter 5 explores the use of aminomethyl phosphonic acid (ampa) as a bifunctional organic spacer in reaction with metal salts of Zn, Cd, Hg, Pb, Ag and Cu for the synthesis of metal organophosphonates. This chapter also reports the synthesis of a bimetallic metal organic framework (Cu/Ag).

Chapter 6 reports the versatility of 5-pyrimidine phosphonic acid as an organic ligand for the synthesis of novel coordination polymers having Zn, Cd, Cu or Ag as metallic centers. The use of this organic spacer led us to the synthesis of Cu/Ag bimetallic frameworks as well.

This research gave us the opportunity to study the flexibility of the selected organic ligands in conjunction with the specific electronic and steric requirements of the chosen metallic centers for the synthesis of novel metal organic frameworks. At the same time these experiments will give us insights into the specific reaction conditions required for the particular formation of the corresponding MOFs.

Chapter 2

Group 13 metal organic frameworks with pyrazine and pyrazine-2-carboxylic acid as the spacer molecules

2.1 Introduction

In contrast to the plethora of work performed with transition elements,[3] main group element organic frameworks have been largely neglected. Nevertheless a handful of examples have been reported.[62] To address the paucity in this area we wished to explore using the triel elements to form extended networks. We anticipated that employing the triel elements would lead to MOFs with unique characteristics due the difference in their main oxidation states (+1 or +3) compared to common transition metals oxidation states (usually +2 or +3).[62] This difference in oxidation state can give an increase in the polarization power of the metallic center giving structures with relatively strong coordination bonds.[62] Moreover, we wished to explore whether using the lighter and cheaper group 13 elements would allow us to prepare materials for gas storage studies.

2.1.1 Aluminum metal organic frameworks

Although examples in this field are limited, Ferey *et al.* reported an aluminum metal organic framework, $Al(OH)[O_2C\text{-}C_6H_4\text{-}CO_2].[HO_2C\text{-}C_6H_4\text{-}CO_2H]_{0.70}$, synthesized from the hydrothermal reaction of aluminum(III) nitrate, 1,4-benzenedicarboxylic acid (BDC) and HF in water.[63] The 3D nanoporous metal organic framework was formed from infinite trans corner sharing octahedral chain units of $AlO_4(OH)_2$ which are linked to each other through the organic spacer. Initially the pores of the framework are filled with unreacted BDC molecules which are removed upon heating at temperatures between 300-320^oC leaving the structural pores open to adsorption. The framework has a hydrogen gas uptake of 3.8% wt at 77 K.[63]

2.1.2 Gallium metal organic frameworks

For gallium, the main approach for the synthesis of extended frameworks has been through reacting gallium(III) nitrate,[64] gallium(III) oxohydroxide[65] or gallium(III) sulfate[66] with phosphoric acid derivatives to afford gallium phosphates. An example of this strategy

was reported in 1994 with the synthesis of $[C_5H_5NH][CoGa_2P_3O_{12}(H_2O)_2]$[67] which was synthesized by the reaction of Ga_2O_3, CoO and $Si(OEt)_4$ in 1-butanol with addition of orthophosphoric acid. The resultant mixture was heated at 180°C for 7 days in a Teflon-lined stainless steel autoclave. The synthesized framework contains regular MO_4 (M = Co or Ga) and PO_4 tetrahedra with fully shared vertices. These tetrahedral units are linked in an alternating manner to give an open three dimensional framework consisting of four-, six- and ten-membered rings containing Ga, Co and P atoms.[67]

Stork *et al.* used a different approach using dipirrinato spacers to synthesize gallium-silver MOFs.[68] The procedure to obtain these frameworks began with the coordination of the dipyrrinato ligand to gallium through reaction of gallium(III) nitrate and tris-5-(4-pyridyl)dipyrrinato. Further reaction of tris(5-(4-pyridyl)dipyrrinato)gallium(III) with a benzene solution of silver salts ($AgCF_3CO_2$, $AgPF_6$, $AgSF_6$) yielded a series of different heterometallic tridimensional frameworks that display very interesting luminescent properties.[68]

2.1.3 Indium metal organic frameworks

A noteworthy example using indium atoms as building blocks for the synthesis of extended frameworks involved ortho-phenyleneindium bromide complexes as electrophilic spacer,[69] for reaction with pyrazine, which afforded molecular chains as depicted in Figure 2.1.

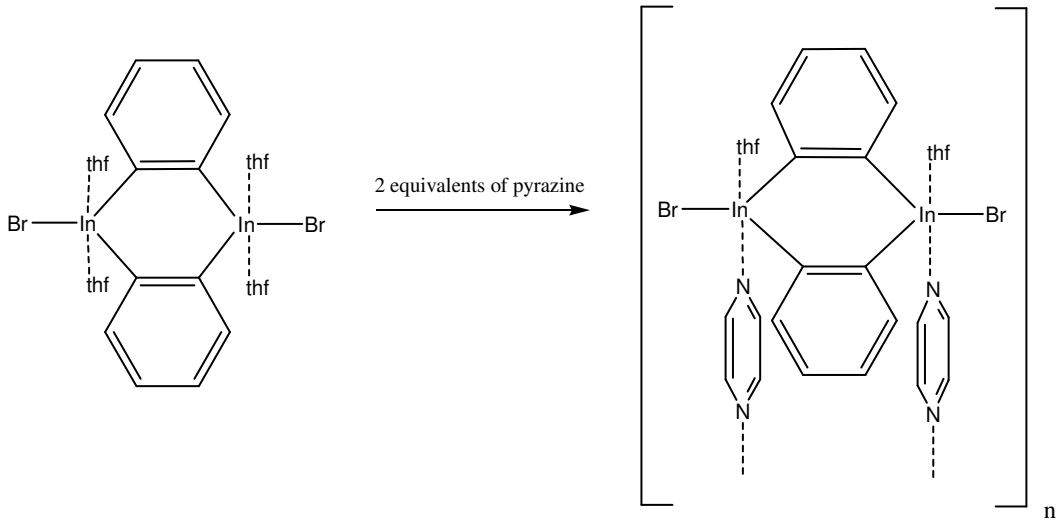

Figure 2.1 Ortho-phenyleneindium complexes used for the construction of molecular chains. Adapted from reference 69.

Other examples of indium polymers involve the use of functionalized carboxylates as spacer molecules. The reaction of 1,4-benzenedicarboxylic (BDC) acid with $InCl_3$ in the presence of triethylamine under hydrothermal conditions afforded an extended framework, $In_2(OH)_3(BDC)_{1.5}$. Each indium atom is found in an octahedral environment coordinated by three μ2 OH groups and three oxygen atoms from three different BDC ligands, giving rise to what can be considered an infinite six-membered ring containing sheet of composition $[In_2(OH)_3]_\infty^{3+}$(See Figure 2.2).[70] $In_2(OH)_3(BDC)_{1.5}$ was tested for catalytic activity in the hydrogenation of nitroaromatics and showed very promising results at low metal/substrate ratios representing a good alternative heterogenous catalyst for this type of reaction.

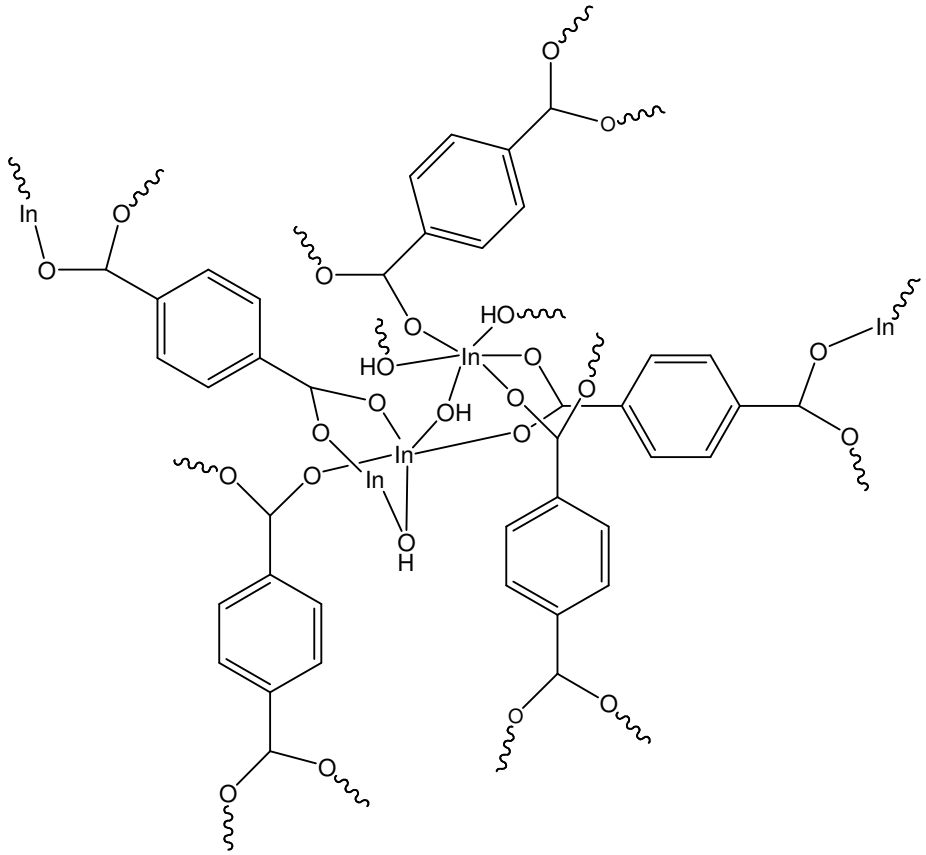

Figure 2.2 Representation of the hybrid polymer $In_2(OH)_3(BDC)_{1.5}$. Adapted from reference 70.

In an effort to study the effects of the presence of other ligands in indium carboxylate MOFs, Gomez-Lor *et al.*[71] selected o-phenanthroline (phen) and 2,2'-pyridyl (2,2'-bipy) as auxiliary organic spacers. These ligands can add interesting electronic properties to the

frameworks.[72] The product from the reactions of $InCl_3$, benzenedi- and benzenetri-carboxylic acids (1,4-benzendicarboxylic acid, H_2BDC and 1,3,5-benzentricarboxylic, H_3BTC) in the presence of additional ligands, 2,2'-bipy and phen, yielded MOFs containing indium atoms as interconnected through organic spacers: $In(BDC)_{1.5}$(2,2'-bipy), **(a)**, $In(OH)_2(BDC)_2(phen)_2$, **(b)**, In(BTC)(H_2O)(2,2'-bipy), **(c)**, and In(BTC)(H_2O)(phen), **(d)** (See Figure 2.3). Frameworks **(a)**-**(d)** were stable in water and organic solvents and were tested for their activity in the selective acetalization of aldehydes.[71] All showed catalytic activity with the exception of framework **(a)**. The lack of activity of this framework was attributed to the hindered accessibility of the reactants to the indium center due its eight coordination environment.[71]

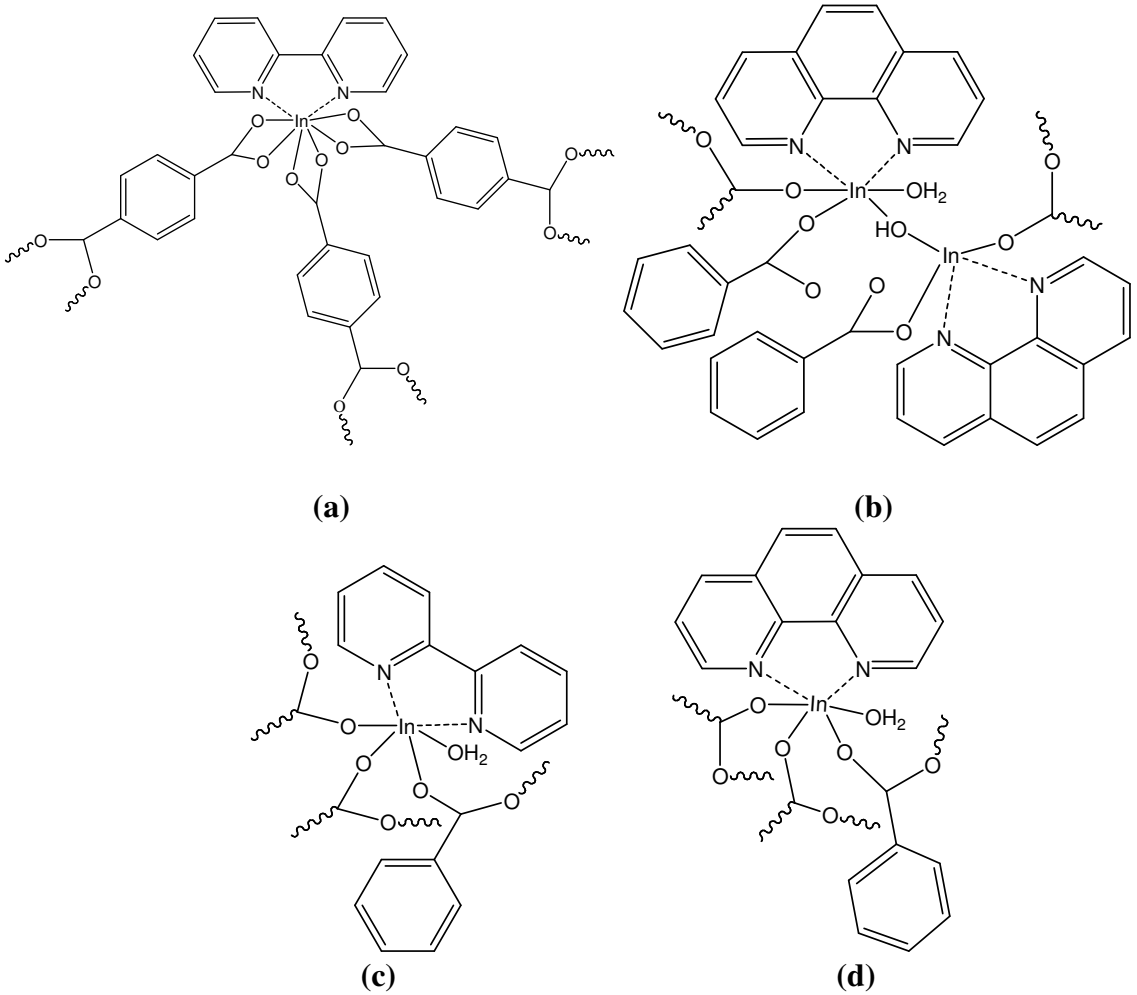

Figure 2.3 Representation of the asymmetric units of **(a)**-**(d)**. Notice the eight coordination around the indium atom in **a** and the six coordinating environment around the same atom in structures **b** to **d**. Adapted from reference 71.

A disadvantage associated with the isolation of these group 13 frameworks is the requirement of long reaction times, high temperatures and unpredictability of the product.[62] In the following section we will detail facile, reproducible syntheses of Ga, In and Tl MOFs using pyrazine and pyrazine-2-carboxylic acid as organic spacers. These bifunctional molecules were selected because they are commercially available, crystalline and have good solubility in readily available 'green' solvents such as ethanol and water. Furthermore, carboxylic derivatives of the pyrazine molecule are useful and have an additional coordination site and are able to promote hydrogen bonding that is often crucial for the growth of the framework.[73]

2.2 Results and discussion

The reaction of gallium(III) chloride or bromide with 1.2 equiv. of pyrazine affords a one-dimensional polymeric structure, Scheme 2.1. Following work-up of the reaction in diethyl ether, colorless crystals of compounds **1** and **2** were isolated in almost quantitative yield.

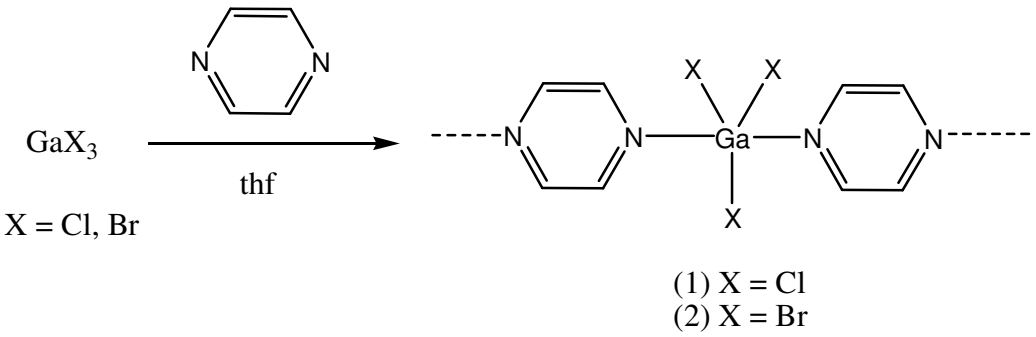

Scheme 2.1 Gallium halide-pyrazine polymers.

In the course of our experimental investigations numerous solvent systems were examined but it was found that running the reaction in solvents other than tetrahydrofuran or diethyl ether, for example, ethanol or water, leads to formation of insoluble gallium oxide or hydroxide. Compounds **1** and **2** are unstable to air. On exposure to ambient conditions, compound **1** decomposes to $[GaCl_4]^-[C_4H_4N_2H]^+$(determined through X-ray structure

analysis). However, it is indefinitely stable in the solid state under nitrogen. Compound **1** is significantly more thermally stable than compound **2** (m.p. for compound **1**: 178-180^{o}C, m.p. for compound **2**: 88-90^{o}C). This instability is presumably due to the longer and weaker gallium bromide bond. Attempts to create multi-dimensional chains through exchange of the spacer for pyrazine derivatives have to date been unsuccessful as polymerization of the solvent (thf) is observed for pyrazine-2-carboxylic acid (pyzca) and pyrazine-2,3-carboxylic acid. Small chains can be isolated when the spacer 4,4'-bipyridine is used. However, polymer termination occurs due to protonation of the heterocyclic nitrogen atom that presumably arises from the solvent.

Compound **1** crystallizes in the monoclinic space group, C2/*c* and is isostructural with the bromide analogue. Each gallium center is coordinated to three halide atoms and the polymer is linked by bridging pyrazine molecules. The geometry around the gallium center can be described as a slightly distorted trigonal bipyramidal (See Figure 2.4). This geometry is not an unusual coordination geometry for group 13 elements and is well documented for both polymers of both aluminum and gallium.[74] The bond lengths and angles in compounds **1** and **2** show good comparison to similar geometrical systems.[74,75]

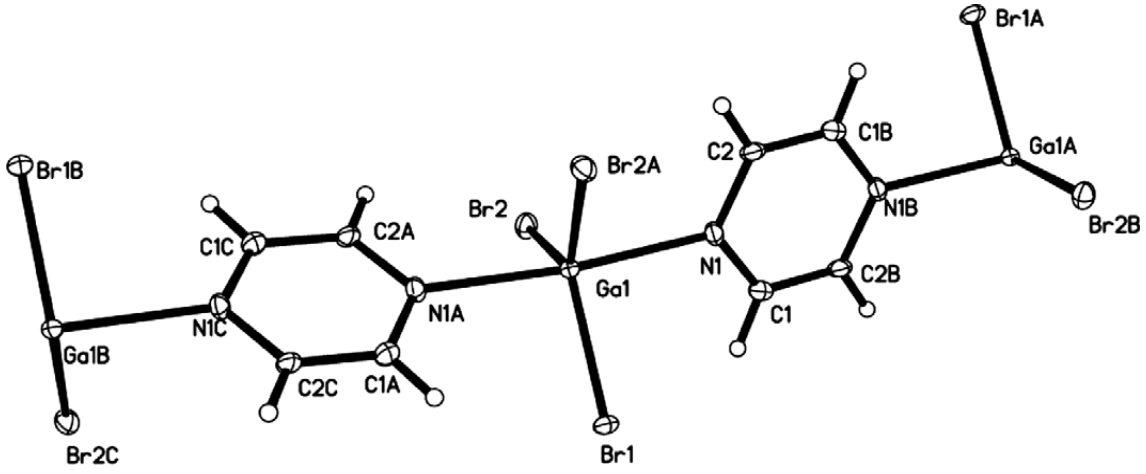

Figure 2.4 Thermal ellipsoid plot of compound **2**, thermal ellipsoids shown at 50% probability level.

Indium and thallium proved more robust for polymer synthesis and the reactions can be performed in aqueous conditions without protonation of the ligand and hydroxide formation. The reaction of an aqueous ethanol solution of $InCl_3.4H_2O$ with pyrazine (pyz) at 70^{o}C for 24 h, is a moderate yielding facile reaction (36%) affording $[InCl_3(pyz)]_n$ compound

3 which crystallizes as a two-dimensional polymeric material. The solid-state structure of **3** (Figure 2.5) revealed a six-coordinated indium center and a polymeric structure interlinked through pyrazine molecules which is structurally similar to that observed for gallium.

Compound **3** crystallizes in the tetragonal space group, P4(2)/*mnm*. The asymmetric unit consists of one indium center, two halves of bridging pyrazine molecules and two terminal chloride ions. One of the bridging pyrazine molecules is disordered over two symmetry equivalent positions. Because of the disorder associated with this pyrazine, the structure was refined with no hydrogen atoms on the carbon atom, C(2). The geometry of both orientations is shown in Figure 2.5. Each In(III) center is coordinated to three chlorine atoms and three nitrogen atoms. The coordination geometry around each indium atom can be described as a slightly distorted octahedron.

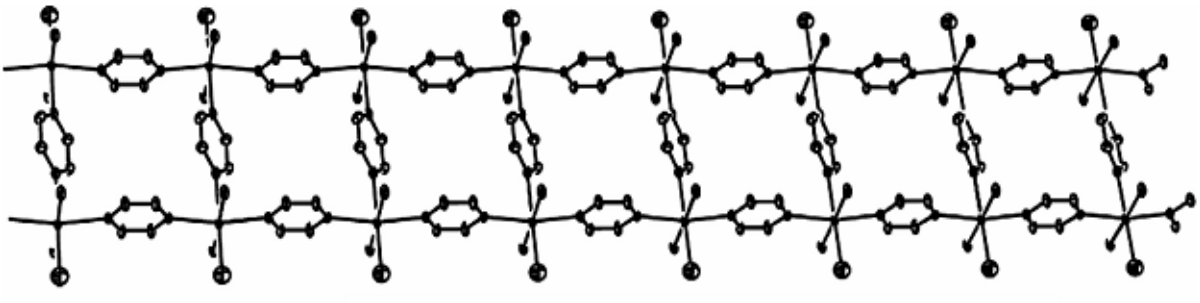

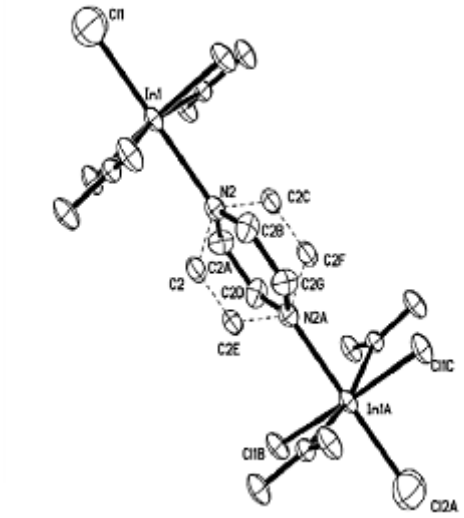

In(1)-N(1)	2.372(9)
In(1)-N(2)	2.327(14)
In(1)-Cl(1)	2.417(3)
In(1)-Cl(2)	2.397(10)
In(1)-In(1A)	7.503
N(1)-In(1)-Cl(1)	89.869(11)
N(1)-In(1)-Cl(2)	95.7(2)
N(2)-In(1)-Cl(2)	180.0
Cl(1)-In(1)-Cl(2)	91.32(9)

Figure 2.5 Crystal structure of compound **3** shown with selected bond lengths (Å) and angles (^{o}). Thermal ellipsoids at 30% probability level, hydrogen atoms are omitted for clarity.

The In-Cl distances are within the expected range, however the In-N distance of 2.372(9)Å is shorter than the distances of 2.528(4)-2.540(4)Å that are found in the related *ortho*-phenyleneindium bromide complexes with pyrazine and thf.[69] This shortening of the bond is presumably due to packing arrangement of the octahedral geometry. The rectangular distance between the chains is 6.99 by 7.50Å (Scheme 2.2).

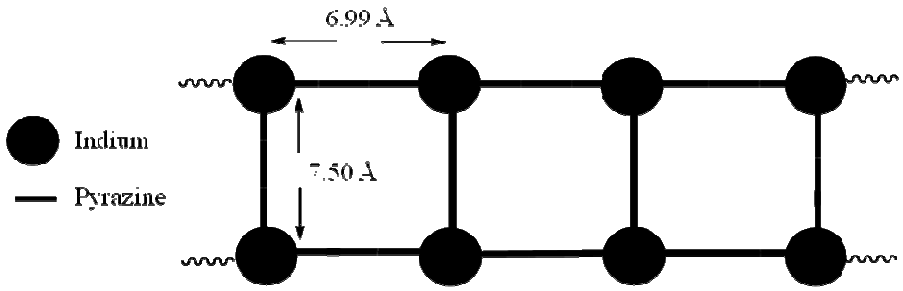

Scheme 2.2 Distances between the chains in compound **3**.

The original crystalline material that the X-ray data were collected on was obtained from a reaction mixture of indium(III) chloride and indium(III) nitrate. However further experimental work has shown that compound **3** can also be isolated directly from the reaction of indium(III) chloride with pyrazine under similar reaction conditions.

To extend further the series of indium polymers, the reaction of indium(III) bromide with 1.2 equivalents of pyrazine was performed in ethanol and afforded a one-dimensional polymer, **4** (see Figure 2.6).

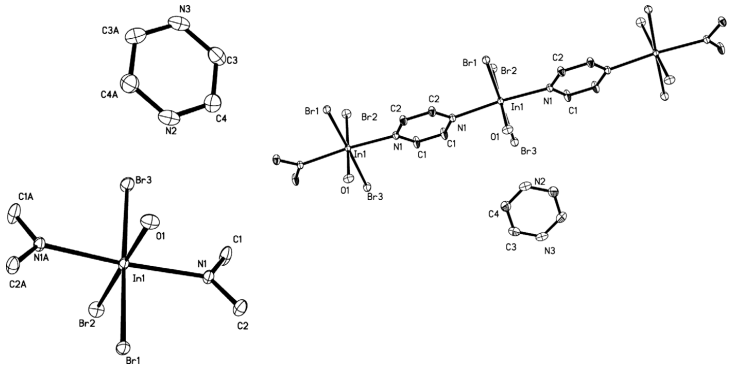

Figure 2.6 Crystal structure of asymmetric unit (left) and polymer of compound **4** (right). Thermal ellipsoids shown at 30% probability level, hydrogen atoms are omitted for clarity.

The solid-state analysis of **4** revealed a free molecule of pyrazine exists in the lattice. The molecule of pyrazine is believed to occur due to recrystallization of the initial reaction product from a mixture of ethanol and water and also explains the water molecule coordinated to the indium center. Evidence to support this can be obtained from compound **3**,[76] (a 2D polymer) which features an interconnecting ladder type structure, therefore it is presumable that without a hot water recrystallization the isostructural 2D ladder polymer, similar to **3**, initially forms but on recrystallization a halide bond and a pyrazine molecule are hydrolyzed affording a 1D polymeric material.

To examine whether deviations from the ladder type structure could be obtained, pyrazine was exchanged for pyrimidine. It was anticipated that a polymeric material with a zigzag motif would result (Scheme 2.3). Despite our best efforts, a polymeric material could not be isolated. Instead a monomer was formed due to chain termination through protonation of the heterocyclic nitrogen atom (See scheme 2.3).

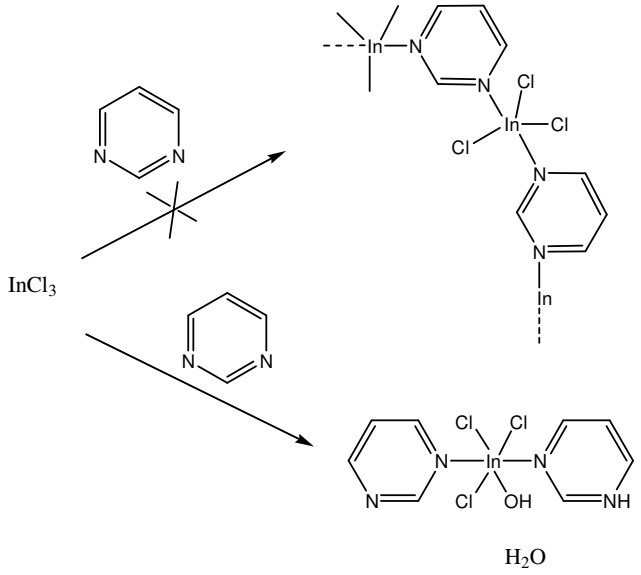

Scheme 2.3 Attempts to achieve derivatives from a linear ladder type structure, led to monomeric indium complexes.

Exchange of the pyrazine spacer for pyrazine-2-carboxylic acid (pyzca) upon reaction with indium(III) chloride and indium(III) nitrate in methanol affords compound **5**, which was isolated as X-ray quality single colorless crystals from methanol. The solid-state structure of **5** is shown in Figure 2.7.

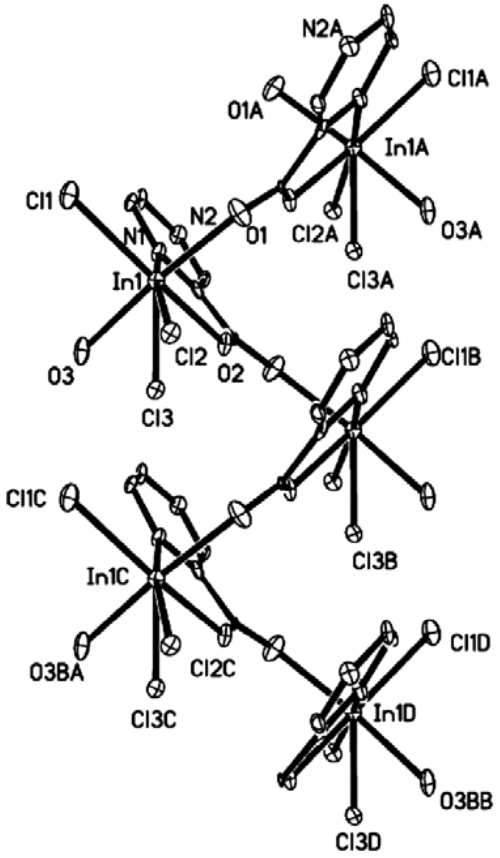

In(1)-O(1)	2.186(10)
In(1)-O(2)	2.159(8)
In(1)-O(3)	2.167(11)
In(1)-Cl(1)	2.445(4)
In(1)-Cl(2)	2.388(3)
In(1)-N(1)	2.318(10)
O(3)-In(1)-O(1)	174.0(4)
O(1)-In(1)-N(1)	90.8(4)
N(1)-In(1)-Cl(2)	166.8(3)
O(3)-In(1)-Cl(1)	90.8(3)
N(1)-In(1)-Cl(1)	89.9(3)

Figure 2.7 Solid state structure of compound **5** shown with selected bond lengths (Å) and angles (°). Thermal ellipsoids at 30% probability level, hydrogen atoms are omitted for clarity.

Each indium center is coordinated to three chlorine atoms, one nitrogen atom from the pyrazine spacer and three oxygen atoms. The oxygen atom (OH_2) coordinated to the indium center arises from the aqueous reaction medium and reaction work-up. It aids in the formation of a framework structure through hydrogen bonding. A seven-coordinated indium atom affords distorted pentagonal bipyramidal geometry. The high coordination number at the indium center is not a new phenomenon and has been previously observed in an indium three dimensional oxalate polymer.[77] Each indium center is linked by a bridged oxygen atom resulting in an infinite 'zigzag' polymeric structure. The approximate distance between the zigzag chains is 6.02Å (i.e. from C(l1A)-C(l1B), or O(3)-O(3BA). The average In-O distance is 2.171Å and is comparable to 2.154Å as observed in similar indium-carboxylate systems.[78]

The infrared spectrum of **5** reveals a broad peak centered at 3413 cm^{-1} attributed to the symmetric and asymmetric stretch of the hydroxy group. At 1067 cm^{-1} the bending mode of the OH group is observed and at 1613, 1578, and 1383 cm^{-1} frequencies that correspond to υ asym, υ sym (CO_2H).[78]

From the reaction of $InBr_3$ and pyrazine-2-carboxylic acid in ethanol, single crystals of compound **6** were isolated. Their X-ray analysis revealed the formation of a one dimensional zigzag structure. This structure is similar to the earlier reported zigzag $[InCl_3(pyzca)]_n$ polymer (See scheme 2.4).[76]

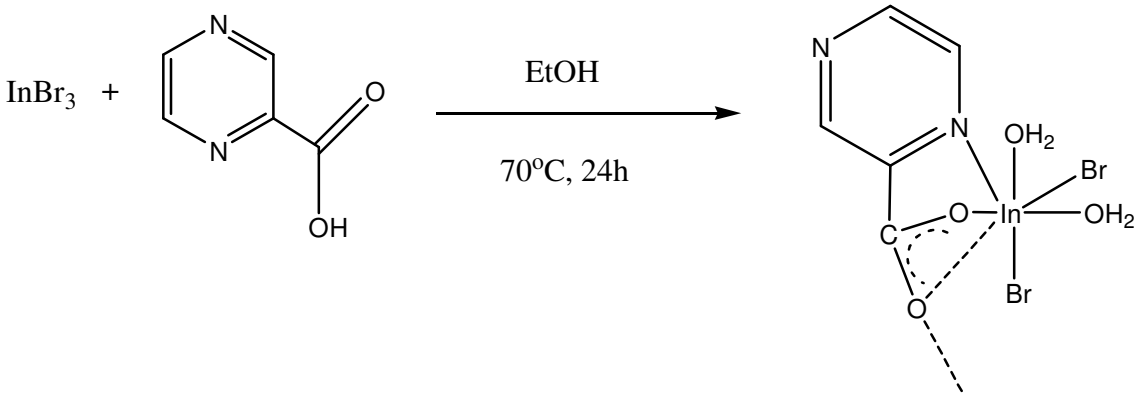

Scheme 2.4 Formation of the zigzag indium polymer, compound **6**.

The difference between polymers **5** and **6** from the reaction of $InCl_3$ and $InBr_3$ with pyrazine carboxylic acid is the hydrolysis of one of the bromide ligands. The hydrolysis can be attributed to the weaker, more reactive In-Br bond compared to the In-Cl bond. Each indium center is linked through one of the oxygen atoms of the carboxyl group, resulting in an infinite 'zigzag' polymeric structure. The similar bond lengths of the carboxylic group, from C(5) to O(1), 1.249(13)Å and O(2), 1.239(12)Å, suggest single bonds for each. The charge on the ligand (-1), coupled with the two bromide ligands (-2), attached to the indium center lead us to believe that the oxygen atoms are coordinated water molecules and is reinforced by the long In(1)-O(3) distance of 2.547(10)Å. As in polymer **5** each indium atom has a coordination number of seven, giving rise to distorted pentagonal bipyramidal geometry which is an example of the high coordination geometries previously observed in indium polymers.[79] The approximate distance between the zigzag chains is ~6.24Å (i.e. from bromide to bromide). The average In-O distance of 2.171(7)Å is comparable to 2.154(2)Å that is observed in similar indium-carboxylate systems.[80] Adjacent indium centers are

separated by a distance of approximately 5.74Å. This indium-indium separation is significantly shorter than the approximate 8.0Å distance reported by You and coworkers. [81] Their indium(III) polymer with pyrazine-2,3-dicarboxylic acid as the spacer,[81] reinforces the fact that small spacer changes can lead to large structural changes in the polymer motif. The infrared spectra of **6** reveals a broad peak centered at 3355 cm^{-1} attributed to the symmetric and asymmetric stretch of the coordinated H_2O molecule and at 2924, 1416, and 1261 cm^{-1} frequencies that correspond to υ asym, υ sym (CO_2).[80]

In the course of preparing these compounds various solvent systems were investigated. $[InCl_3(dmso)_2(pyz)]_2$, compound **7** (Figure 2.8) was isolated from the reaction of $InCl_3.4H_2O$ with pyrazine in DMSO (dimethylsulfoxide).

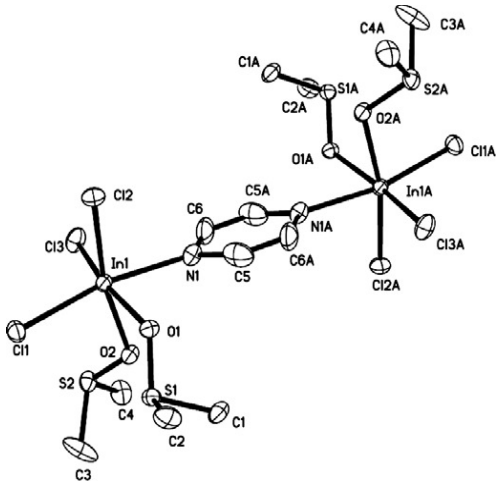

Figure 2.8 Solid state structure of compound **7**, thermal ellipsoids are at 30% probability level, hydrogen atoms are removed for clarity.

The isolation of compound **7** reveals that in order to obtain a polymeric framework, coordinating solvents must be avoided to prevent blocking potential coordination sites at the metal center. Compound **7** is a dimeric In(III) complex that has a slightly distorted octahedral geometry around both indiums that are linked by a molecule of pyrazine. Each indium center also has two molecules of DMSO coordinated. No noteworthy discrepancies in bond lengths or angles are observed. Compound **7** has a lower melting point than the preceding indium polymers attributed to DMSO coordination.

Continuing with our desire to explore main group element organic frameworks, the reaction of thallium(III) chloride tetrahydrate with pyrazine in ethanol was performed. Compound **8**, a one-dimensional polymer was as predicted by Walton in 1967.[82] Although

thallium(III) one-dimensional polymers are well-known,[83] structural characterization of thallium with pyrazine and its derivatives are uncommon. In this framework, the thallium center has a coordination number of six and distorted octahedral geometry is observed (see Figure 2.9).

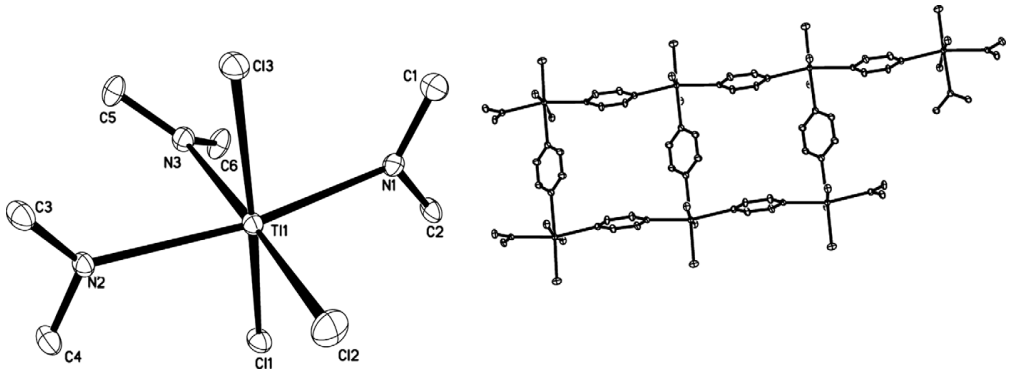

Figure 2.9 Solid state structure for the asymmetric unit and the polymeric structure of compound **8**. Hydrogen atoms are omitted for clarity. Thermal ellipsoids are at 30% probability level.

The average Tl-Cl bond of 2.45Å compares well with other Tl(III) chloride complexes in which thallium has an octahedral environment.[84] Deviation from a linear angle is greater than has been observed in reported Tl(III) coordination complexes. For example, mer-trichloro tris(pyridine) thallium(III), has a Cl-Tl-N angle of 174.27(3)^{o} and mer-trichloro tris(n-methyl imidazole) thallium(III) has a Cl-Tl-Cl angle at 174.02(1)^{o}.[84] This geometrical distortion can be attributed to the rigidity of the framework and the steric constraints placed on the thallium center. Acquisition of NMR data for compound **8** was attempted and the proton peaks for the pyrazine were recorded at 8.67ppm. Since uncoordinated pyrazine peaks appear at 8.62 ppm it was unclear whether D_2O was displacing the pyrazine from the thallium center. A similar result was obtained in dimethylsulfoxide; however this might be expected as thallium DMSO complexes have been previously reported.[85] Attempts in other solvents failed due to limited solubility of the polymer.

2.3 Conclusions

A series of one-dimensional polymers featuring the triel elements were prepared and characterized. Stability of the polymers increases descending group 13 and decreases when the group 13 bromide precursor is employed. The resultant structures also provide an interesting comparison of how changing the functionality of the spacer and the reaction conditions can direct the framework motif. A major advantage of these syntheses is that they can be performed at room temperature or with gentle heat. These mild conditions can be contrasted with the usual hydrothermal methods currently employed. At the same time, this methodology allowed the manipulation of the size of the pores of the synthesized frameworks by the corresponding exchange of metal centers with increasing radii. Compounds **1**-**8** are of particular interest for their potential as pre-constructed building blocks for further multi-dimensional polymers through displacement of the exo-halides. Such an approach would allow the introduction of groups such as cyanide that can act as bidentate ligands and allow magnetic communication between metal centers, Scheme 2.5.

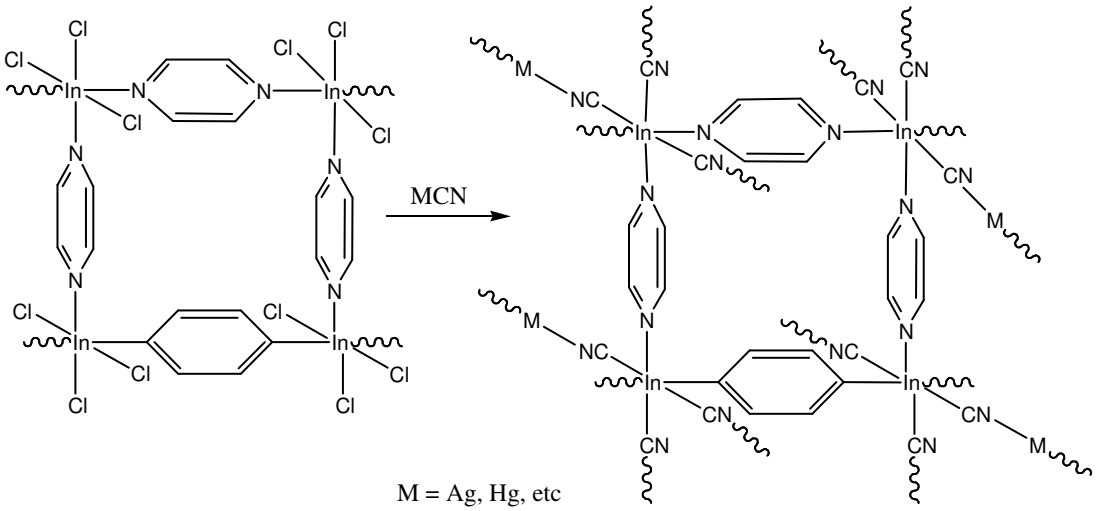

Scheme 2.5 One potential example for the use of the synthesized In-polymers for the construction of multidimensional polymers through exo-halide displacement. Note that depending of the nature of the metal center (M) it can be possible to synthesize homo- and heterometallic MOFs.

2.4 Experimental

Crystal data for all compounds in chapters **2**-**6** data were collected with a Bruker SMART 1000 diffractometer using graphite monochromated molybdenum radiation (λ = 0.7107 Å). The data were corrected for absorption. Structures were solved by direct methods using the SHELXS-97 program and refined via full-matrix least squares.[86] Crystal data for compounds **1**-**8** compounds is given in Tables 2.1 and 2.2 at the end of this chapter.

All reagents were purchased from Aldrich and used without further purification. Tetrahydrofuran HPLC grade was used as received. Grease free (i.e. Teflon sealed) Schlenk flasks were used to allow heating of the solutions without the use of a reflux condenser and to avoid grease contamination.

2.4.1 Preparation of compound 1 and 2

$GaCl_3$ (0.3 g, 1.7 mmol), pyrazine (0.16 g, 1.7 mmol) were added together under a stream of nitrogen. Tetrahydrofuran (from the bottle) was added directly to the Schlenk flask, and a yellow colored solution was observed. The flask was sealed and stirred for 16 h after which time the solvent was removed in vacuo and the powdery solid extracted into diethyl ether. After filtration under anaerobic conditions and storage at room temperature for 24 h, colorless needles of **1** were isolated. Yield: 87% (based on $GaCl_3$), m.p. 178-180^oC, decomposed, some sublimation observed immediately before decomposition, IR (KBr pellet, υ cm^{-1}): 3119(w), 3098(m), 3064(m), 2639(m), 2545(m), 1430(m), 1410(m). ^1H NMR ($CDCl_3$, 25^oC) pyrazine protons appear at 9.1 ppm (singlet). The synthesis of compound **2** was performed in an identical manner to **1**. Yield: 85% (based on $GaBr_3$), m.p. 88-90^oC. Similar results for **1** and **2** were recorded in the IR and NMR experiments.

2.4.2 Synthesis of compound 3

An ethanol solution (5 mL) of pyrazine (0.04 g, 0.50 mmol), indium(III) nitrate pentahydrate (0.20 g, 0.51 mmol) and indium(III) chloride tetrahydrate (0.15 g, 0.51 mmol) were stirred at 70 ^oC in a grease free Schlenk flask for 24 h. After filtering the solution to remove any solid particles, the clear solution was stored at room temperature. After 2 days, a

white crystalline material was isolated that was suitable for single crystal X-ray analysis. Yield: 36% (based on $InCl_3 \cdot 4H_2O$), m.p. >250°C. IR (KBr pellets, υ cm^{-1}); 3576 (w), 1603(m), 1495(m), 1418(m), 1157(m), 118(m), 1054(m), 618(m). Compound **3** can also be prepared reacting pyrazine (0.04 g, 0.50 mmol) and indium(III) chloride tetrahydrate(0.22 g, 0.75 mmol) in ethanol at 70°C for 3 days in a grease free Schlenk tube. After filtration and storage at room temperature for 2 days, white crystalline material can be isolated.

2.4.3 Synthesis of compound 4

$InBr_3$ (0.3 g, 0.85 mmol) and 0.068 g (0.85 mmol) of pyrazine were dissolved in 5 mL of ethanol and placed in a grease free Schlenk flask. The solution was stirred at 65°C for one day after which time the reaction mixture was filtered and transferred to a beaker for crystallization. After 3 days, crystalline material was isolated, however the crystals exhibited twinning problems. The solid was redissolved in hot water and stored at room temperature overnight. Suitable crystals for single crystal X-ray diffraction were isolated from this solution. Yield: 67% (based on $InBr_3$). The product decomposes at 150°C to a brown solid. IR (KBr pellets, υ cm^{-1}); 3412(w), 1597(m), 1495(m), 1396(m), 1151(m), 1111(m), 1002(m), 614(m).

2.4.4 Synthesis of compound 5

A methanol solution (5 mL) of indium(III) nitrate (0.31 g, 0.8 mmol), pyrazine-2-carboxylic acid (0.10 g, 0.8 mmol) and indium(III) chloride (0.24 g, 0.8 mmol) was stirred and heated in a grease free Schlenk for 1 day at 65°C. After 1 day, the reaction mixture was filtered and transferred to a beaker for further crystallization. The clear reaction mixture yielded white crystals suitable for X-ray diffraction. Yield: 42% (based on $InCl_3.4H_2O$), m.p. >250°C, the sample shows an evolution of a gas in the interval 100-105°C (H_2O). The sample did not melt at 250°C. IR (KBr pellets, υ cm^{-1}); 3413(s), 1067(m), 1613(s), 1578(m), 1383(m), 784(m), 738(m), 709(m), 568(m).

2.4.5 Synthesis of compound 6

$InBr_3$ (0.3 g, 0.85 mmol) and pyzca (0.126 g, 1.01 mmol) were dissolved in approximately 5 mL of ethanol placed in a Teflon-sealed flask and stirred at 70 ^oC. After 24h, the clear colored reaction mixture was transferred to a beaker where upon standing at room temperature for 3 days afforded X-ray quality crystals of **6**. Yield: 61% (based on $InBr_3$), m.p. >250 ^oC, the sample shows an evolution of a gas in the interval 100-105^oC (H_2O), IR: (KBr pellet, υ cm^{-1}) 3355(s), 3101(s), 3067(m), 2924(s), 1625(m), 1501(m), 1416(s), 1302(m), 1261(s), 1178(m), 1139(m), 1139(m), 1044(m), 1029(m), 863(m), 840(m). Insolubility of the crystals in deuterated solvents prevented acquisition of the NMR data.

2.4.6 Synthesis of compound 7

An aqueous solution of DMSO (dimethyl sulfoxide) (5 mL), pyrazine (0.04 g, 0.50 mmol), indium(III) chloride tetrahydrate (0.22 g, 0.75 mmol) were stirred at room temperature in an open beaker for 24 h. The solution was filtered to remove any insoluble material. After storage at room temperature for 1 day suitable for X-ray diffraction white crystalline material was obtained. Yield: 49% (based on $InCl_3 \cdot 4H_2O$), m.p. 137-138^oC. IR (KBr pellets, υ cm^{-1}); 3569(w), 3036(m), 2999(m), 2932(m), 2918(m), 1409(s), 1316(m), 1296(s), 1036(s), 988(s), 951(m).

2.4.7 Synthesis of compound 8

In a Teflon-sealed flask pyrazine (0.106 g, 1.32 mmol) and $TlCl_3.4H_2O$ (0.4 g, 1.1 mmol) were dissolved in ethanol (5 mL). The reaction mixture was gently heated to 60^oC and stirred overnight. The clear solution was transferred to an open beaker. Storage at room temperature for 3 days afforded crystalline material of **8** suitable for X-ray diffraction. Yield: 78% (based on $TlCl_3 \cdot 4H_2O$). The product decomposes at 130^oC. IR (KBr pellet, υ cm^{-1}) 3426(w), 2924(m), 1416(m), 1261(m), 1164(m), 1119(m), 818(m), 448(m).

Table 2.1 Crystal data of compounds **1**-**4**

Compound	**1**	**2**	**3**	**4**
Chemical formula	$C_4H_4Cl_3GaN_2$	$C_4H_4Br_3GaN_2$	$C_6H_6Cl_3InN_3$	$C_8H_8Br_3InN_4O$
Formula weight	256.16	389.54	341.31	530.73
Crystal system	Monoclinic	Monoclinic	Tetragonal	Orthorhombic
Space group	C2/*c*	C2/*c*	P4(2)/*mnm*	C*mcm*
T (K)	293	293	90.2	293
a (Å)	11.198(3)	11.3941(16)	11.8467(8)	14.2231(9)
b (Å)	6.3613(14)	6.7356(10)	11.8467(8)	7.5198(5)
c (Å)	11.648(3)	11.9568(18)	7.5032(10)	13.3712(9)
a (^{o})	90	90	90	90
b (^{o})	102.061(3)	102.903(2)	90	90
c (^{o})	90	90	90	90
V (Å^3)	811.4(4)	894.5	1053.03(17)	1430.12(16)
Z	4	4	4	4
Reflections collected	3209	1712	2436	6685
Independent reflections	738	775	678	1400
Unique data (Rint)	0.0270	0.0560	0.0514	0.0299
R indices (all data)	R_1 = 0.0171, wR_2 = 0.0415	R_1 = 0.0637, wR_2 = 0.152	R_1=0.0642, wR_2 = 0.1699	R_1 = 0.0325, wR_2 = 0.0666
Final R indices [I > 2r(I)]	R_1 = 0.0163, wR_2 = 0.0407	R_1 = 0.0587, wR_2 = 0.1452	R_1=0.0525, wR_2 = 0.1591	R_1 = 0.0235, wR_2 = 0.0573

Table 2.2 Crystal data of compounds **5-8**

Compound	**5**	**6**	**7**	**8**
Chemical formula	$C_5H_6Cl_3InN_2O_3$	$C_5H_6NBr_2InN_2O_4$	$C_{12}H_{28}Cl_6In_2N_2O_4S_4$	$C_6H_6Cl_3N_3Tl$
Formula weight	360.26	432.76	834.94	430.86
Crystal system	Orthorhombic	Orthorhombic	Monoclinic	Monoclinic
Space group	P2(1)2(1)2(1)	P2(1)2(1)2(1)	P21/*n*	P2(1)/*n*
T (K)	90.2	293	90.2	293
a (Å)	6.0291(7)	6.2377(10)	7.1036(7)	7.6902(15)
b (Å)	11.1140(14)	11.2205(19)	15.1089(14)	11.742(2)
c (Å)	13.8525(17)	14.082(2)	13.5193(13)	11.651(2)
a (^{o})	90	90	90	90
b (^{o})	90	90	94.613(2)	92.815(3)
c (^{o})	90	90	90	90
V (Å^3)	928.2	985.6(3)	1446.3(2)	1050.8(4)
Z	4	4	2	4
Reflections collected	7138	8293	8268	5329
Independent reflections	1675	1780	2612	2068
Unique data (Rint)	0.0411	0.0325	0.0395	0.0308
R indices (all data)	R_1=0.0682, wR_2 = 0.1861	R_1 = 0.0430, wR_2 = 0.1094	R_1=0.0458, wR_2 = 0.1030	R_1 = 0.0339, wR_2 = 0.0564
Final R indices [$I > 2\sigma(I)$]	R_1=0.0646, wR_2 = 0.1799	R_1 = 0.0397, wR_2 = 0.1070	R_1=0.0372, wR_2 = 0.0975	R_1 = 0.0254, wR_2 = 0.0519

Chapter 3

Copper halide clusters and polymers supported by bipodal heteroelemental ligands

3.1 Introduction

Sulfur containing ligands that are derivatives of heterocyclic thiones are of biological interest as the active site in many proteins involves sulfur/nitrogen coordination.[87] Among these proteins it is noteworthy to mention two examples: azurin and cytochrome *c* oxidase. Azurin belongs to a class of mononuclear copper proteins that contain the so-called blue copper site (cupredoxin).[88] These proteins are involved in electron transport processes in the denitrifying chains of certain bacteria such as Alcaligenes xylosoxidans.[89] In the protein azurin, copper ions are strongly coordinated by three ligands in a plane: the sulfur atom of a cysteine, (Cys 112), and the two nitrogen atoms of two histidines, (His 46 and His 117) (See Figure 3.1).[89]

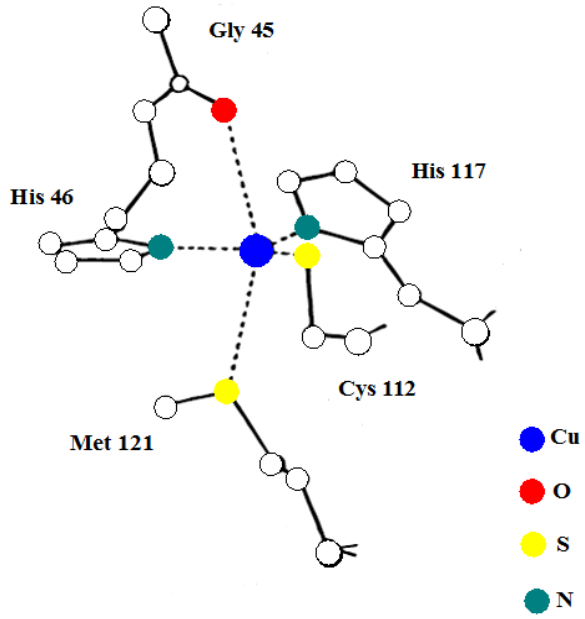

Figure 3.1 Active site of azurin, showing the ligands coordinated to the copper atom.

This strong N_2S donor set is a common characteristic in all members of the blue copper protein family.[90] The highly covalent nature of the copper-sulfur bond gives blue

copper proteins unique spectroscopic properties such as an intense absorption near 600 nm arising from a (Cys)S → Cu(II) charge transfer.[90] It is also possible to notice the presence of two weaker axial interactions, one from the sulfur atom of a methionine, (Met 121), and the other from the carbonyl oxygen of a glycine residue (Gly 45) which has an electrostatic nature.[91]

Meanwhile, cytochrome *c* oxidase belongs to the so-called purple copper centers which are characterized by an intense purple color due to strong absorptions around 480, 530 and 800 nm.[92] Cytochrome *c* oxidase is involved in food oxidation processes catalyzing electron transfer to molecular oxygen.[93] In this case, the purple copper center is formed by a dithiolate-bridged copper center in which two copper atoms are found in distorted tetrahedral sites (See Figure 3.2).[94]

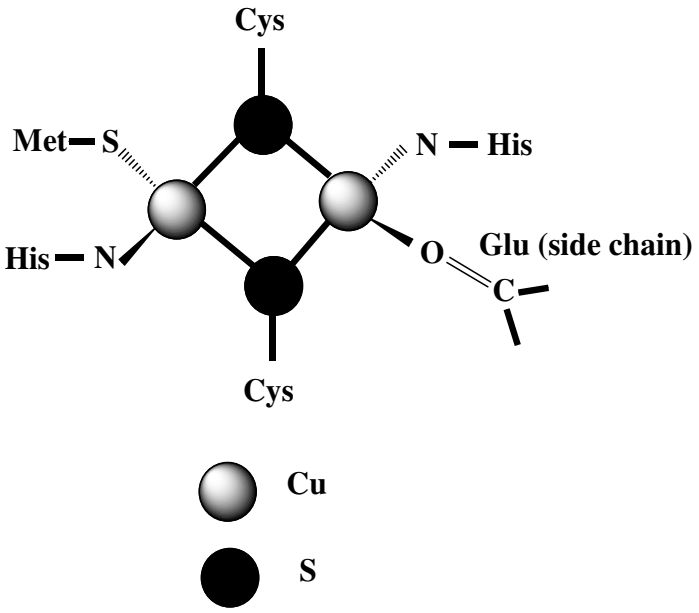

Figure 3.2 Cu_A site in cytochrome *c* oxidase. Taken from reference 94.

Based on these biological examples, research has been directed towards the reproduction of similar building blocks containing copper for the construction of novel artificial architectures displaying interesting electronic features.[95] In particular heteroelemental donor ligands containing nitrogen and sulfur have found useful applications for the coordination of copper(I) and copper(II).[96, 97] For example when copper(I) halides are

combined with monodentate ligands it is possible to synthesize a variety of oligomeric structures as depicted in Figure 3.3.[98]

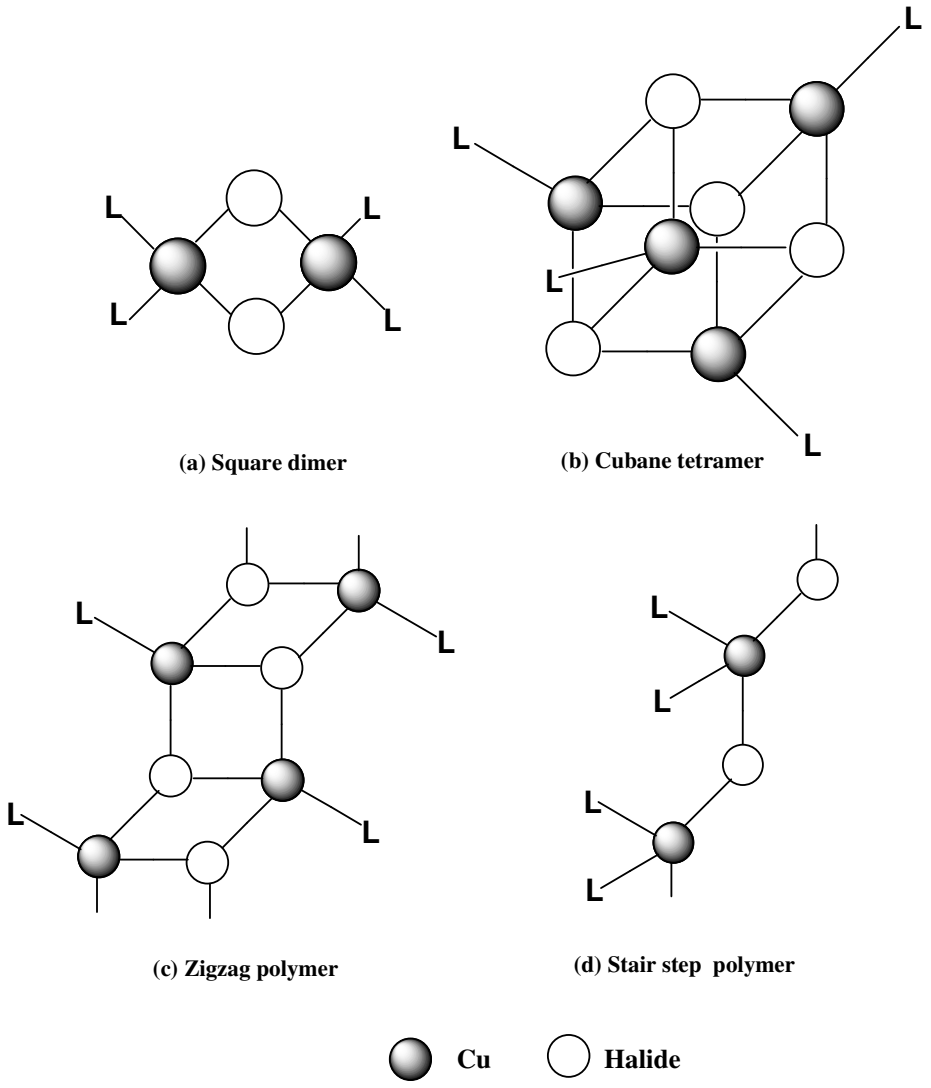

Figure 3.3 Geometrical arrangements found when copper(I) halides are combined with a monodentate ligand (L). Taken from reference 98.

Given the potential in this area, we chose to prepare a series of flexible dipodal ligands that possess both nitrogen and sulfur atoms for metal coordination. $(PyS)_2CH_2$ (Py = pyridyl, C_5H_4N), $(PymS)_2CH_2$ and $(PymS)_2$ (Pym = $C_4H_3N_2$), (See Figure 3.4) were prepared to explore their reactivity with various copper precursors and to determine whether these ligands would lead to the formation of monomers, cubane clusters or polymeric structures.[99-103]

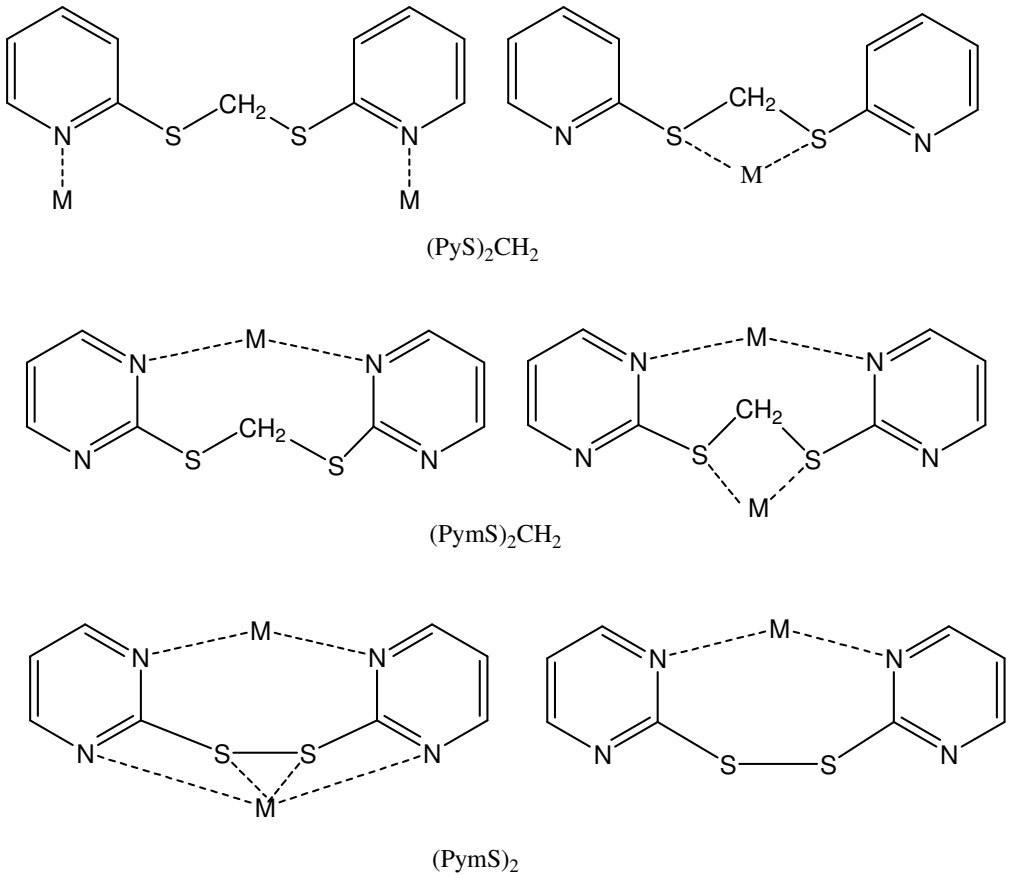

Figure 3.4 Coordination modes of $(PyS)_2CH_2$, $(PymS)_2CH_2$ and $(PymS)_2$

In free bis(pyridylthio)methane, $(PyS)_2CH_2$, the two aromatic ligands are essentially planar and they adopt a *transoid* configuration that minimizes unfavourable electronic interactions between the lone pairs of the sulfur and the nitrogens.[104] On coordination to metal centers the molecule is able to rotate. It is this rotation that allows the molecule to open up for bridged coordination or wrap around a metal center and use its multiple donor atoms for coordination. The multiple coordination sites allow these ligands to have a plethora of coordination modes that can lead to several structural outcomes, Figure 3.4.

To this end we wished to investigate the coordination potential of the aforementioned ligands with a series of copper precursors. Moreover, we were particularly interested in using copper cyanide and thiocyanide precursors for cluster or framework syntheses. These ambidentate ligands behave as pseudo halides that can coordinate end on, or end-to-end. Unlike their halide counterparts they have been less utilized for creating infinite polymeric

chains, but can afford frameworks that display various degrees of interpenetration.[105] Traditionally, the synthesis of copper polymers has involved high temperatures as it was believed this was required to form metastable phases that would not be accessible at lower temperatures.[106] For example, the reaction of CuSCN with 1,2-bis(4-pyridyl)bipyridylethane (bpa), to form the infinite polymer $[Cu(SCN)_2bpa]_\infty$, involves vacuum synthesis at 180°C.[107] On the other hand, slow diffusion or co-crystallization techniques have yielded polymeric chains but usually in low yields.[108,109] Instead of these typical methods, we wished to utilize synthetic routes that employ mild conditions and result in air stable products that can be isolated in moderate yields, thus allowing exploration of their further chemistry. Experimentally it was determined that reaction of the copper precursor and ligand in acetonitrile, followed by overnight heating to 70-100°C, afforded a series of copper complexes that vary structurally depending on the copper precursor selected.

3.2 Results and discussion

The reaction of bis(pyrimidylthio)methane with $CuCl_2$ afforded teal, paramagnetic crystals of the complex $[(PymS)_2CH_2CuCl_2]_\infty$, **9**, as shown in Scheme 3.1.

Attempts using tetrahydrofuran, benzonitrile, ethanol, water or toluene were all unsuccessful and no coordination of the ligand to the metal was observed. For all reactions, acetonitrile was used as the solvent.

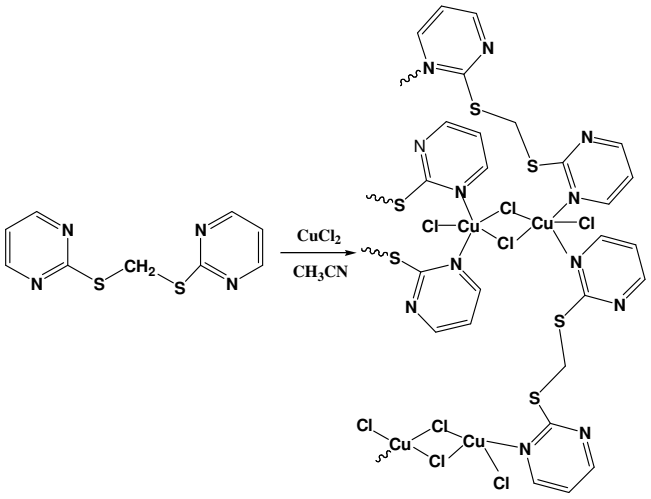

Scheme 3.1 Synthesis of **9**, $[(PymS)_2CH_2CuCl_2]_\infty$.

The overall structural motif of **9** can be described as two dimensional sheet with the interchain linkage provided by the organic ligand. The X-ray crystal structure of **9** is exhibited in Figure 3.5.

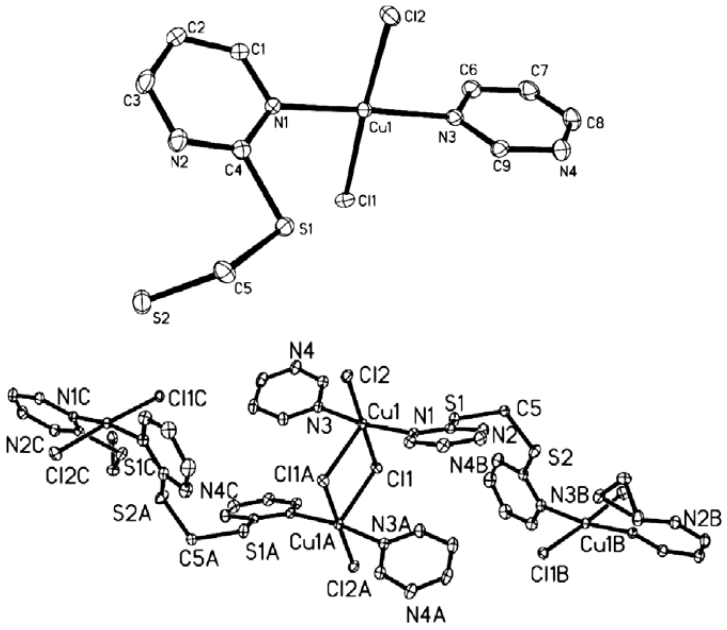

Figure 3.5 Top, diagram of the asymmetric crystallographic unit and the polymeric structural motif of **9**. Below, thermal ellipsoids shown at 30% probability level, hydrogen atoms are omitted for clarity. Selected bond lengths (Å) and angles (°): Cu(1)-N(1) 2.049(2), Cl(1)-Cu(1)-N(1) 93.04(6), N(3)-Cu(1)-Cl(2) 88.11(7), Cl(1)-Cu(1)-Cl(1A) 85.97(3).

The geometry around each copper atom is five coordinate corresponding to distorted trigonal bipyrimidal geometry. As can be seen in Figure 3.5 each ligand bridges the copper centers. Every copper atom is coordinated to two nitrogen atoms, N(1) and N(3), from pyrimidine groups provided by two different ligand molecules. Making up the remaining two coordination sites on copper are two chloride atoms, Cl(1) bridges two copper centers (μ2) while the other chlorine atom remains terminal. The Cu-Cl bond lengths vary only slightly. The terminal chloride has a Cu-Cl distance of 2.2468(8)Å compared to the bridged Cu-Cl distance of 2.2822(7)Å. Compound **9** can be compared to a previously reported structure [$CuCl_2$(μ-dpds)] (dpds = dipyridyl disulfide) (**A**), Figure 3.6, that was isolated from the similar reaction of bis(2-pyridylthio)methane with $CuCl_2$.[110]

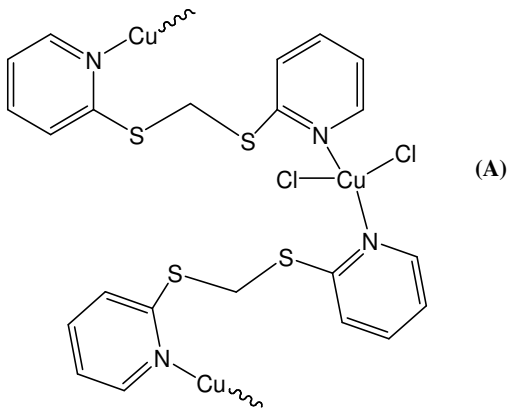

Figure 3.6 Structurally similar molecule to **9**, from the reaction of $CuCl_2$ with bis(2-pyridylthio)methane.

Comparison of the structures of $[CuCl_2(\mu\text{-dpds})]$, **(A)**, with $[(PymS)_2CH_2Cu(\mu Cl)Cl]_\infty$, **9**, reveals that distinct structural differences arise from the different experimental procedures. $[CuCl_2(\mu\text{-dpds})]$ (**A**), was formed from the slow diffusion of a methanol solution of copper(II) chloride and the ligand, while **9** was prepared from the reaction of copper(II) chloride and the ligand in acetonitrile with heating at ~100°C. The main difference between the two structures is that in (**A**) the chloride atoms do not bridge, instead they retain their trans-terminal geometry yielding an infinite helical chain. The bridging halides in complex **9** help minimize the distance between the pyridyl layers, by constraining the geometry. The Pym-Pym distance is approximately 3.7Å (between corresponding aromatic carbons), which is relatively short and so should allow π-π stacking.[111] However, the arrangement of the pyrimidyl rings is slightly twisted, preventing this phenomena.

Polymer **9** is soluble in common organic solvents and is relatively thermally stable, melting to a green liquid at 150-152°C. Luminescence measurements were attempted in acetonitrile at room temperature, but no meaningful data could be obtained.

In an attempt to further develop polymeric networks, the reaction of $(PyS)_2CH_2$ with CuCN was performed, Scheme 3.2.

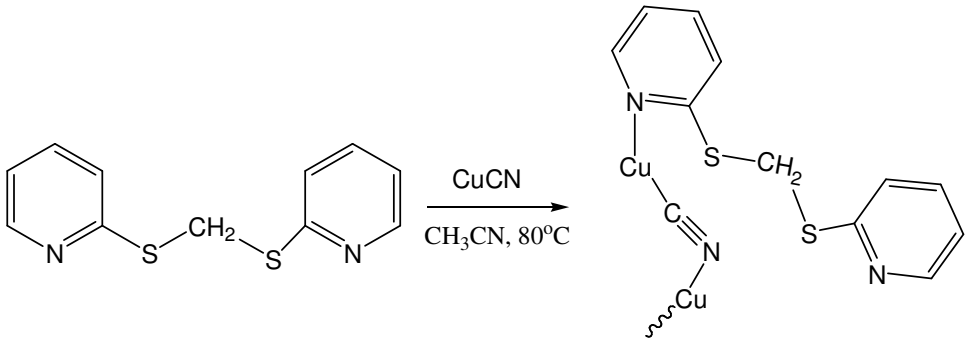

Scheme 3.2 Synthesis of **10**, $[(PyS)_2CH_2CuCN]_\infty$.

CuCN has limited solubility in acetonitrile, but the reaction proceeds as a suspension. The lower yield of the product (39%) is due to the lower solubility of the metal salt. Colorless crystals of **10** (Figure 3.7) were isolated at room temperature and crystallize in the orthorhombic, chiral space group, P2(1)2(1)2(1).

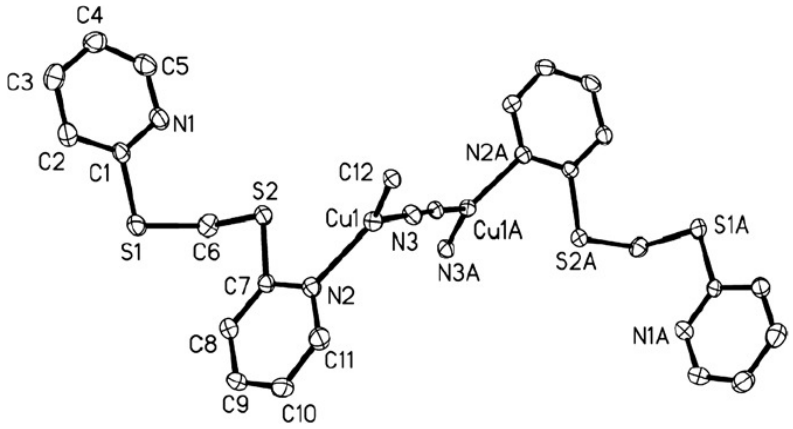

Figure 3.7 Crystallographic analysis of **10**, $[CuCN(PyS)_2CH_2]_\infty$. Thermal ellipsoids are shown at 30% probability level with hydrogen atoms omitted for clarity. Selected bond lengths (Å) and angles (°) of **10**: Cu(1)-N(2) 2.034(2), Cu(1)-C(12) 1.872(3), C(12)-N(3) 1.154(3), N(2)-Cu(1)-C(12) 120.93(10), N(3)-C(12)-Cu(1) 174.9(2), Cu(1)-Cu(1A) 4.933.

Solid-state X-ray analysis revealed the ambidentate CN ligand bridges each copper center. Each copper atom is also coordinated to a nitrogen atom from the pyridyl group in bis(bipyridylthio)methane. Overall, each copper center has two cyanide groups that along with the N atom give rise to a distorted trigonal planar geometry. The C-N distance of 1.154(3)Å is typical of the CN triple bond in cyanide.[112] The distance between Cu centers is approximately 4.9Å. The geometry around the Cu(1)-C(12)-N(3) ligand is close to linear,

with an angle of 174.9(2)°. Infrared spectroscopy exhibited a distinctive CN stretch at 2361 cm^{-1} that is within the range expected for a bridged CN ligand.[112,113] Proton NMR on **10** showed the proton signals shifted downfield when compared with the free ligand.[113] This downfield shift was observed in the spectra of complexes **10**-**13** suggesting that the structure is retained in solution when the crystalline material is redissolved. Bond lengths and angles of **10** show good agreement with other Py-CuCN complexes. For example, $(CuCN)_2[CuCN]_2(\mu$-4,4'-bipy)] has a Cu-CN bond length of 1.862(3)Å and a Cu-N(Py) bond length of 2.069(2)Å.[114] Within the polymeric network of **10** the distance between the aromatic layers (i.e. from C(1)-C(1A) or S(1)-S(1A)) is approximately 8.7Å.[115]

Having successfully isolated polymeric chains from copper(II) chloride and copper(I) cyanide, we wished to extend the series and examine if polymeric chains would be isolated using copper(I) iodide. Using similar reaction conditions as were used for the formation of **9** and **10** $(PyS)_2CH_2$ and $(PymS)_2$ were reacted with CuI. Complexes **11** and **12** show structural similarity. Both feature the Cu_4I_4 core which can be described as a 'ladder type' arrangement that is well documented common for copper halides.[116] The four copper atoms and four iodine atoms form parallelograms, with Cu-Cu distances of 2.849(3)Å and 2.862(4)Å between the two copper atoms in **11** and 3.038(1) and 2.657(2)Å in **12** and are typical values for discrete Cu-I ladder structures (See Figure 3.8).[117a]

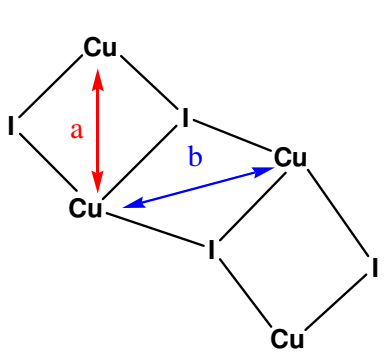

(11)

a = 2.862 (4)Å, b = 2.849(3)Å

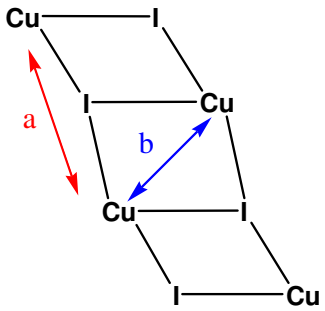

(12)

a = 3.038(1)Å, b = 2.657(2)Å

Figure 3.8 Representation of the CuI cores in **11** and **12** showing corresponding bond distances.

These Cu-Cu distances can be compared with the Cu-Cu separation in metallic copper of 2.556Å and the Van der Waals radius of copper at 2.80Å.[118] Complex **11** is analogous to the Cu(I) bromide compound isolated by Garcia-Martinez and co-workers[104] from the reaction of $(PyS)_2CH_2$ with Cu(I)Br which afforded a CuBr cluster. Unlike the copper cluster, $[Cu_4Br_4((PyS)_2CH_2)_2]$ complex **11** was the major reaction product and was isolated in 67% yield. Complex **11** crystallizes as yellow crystals in the triclinic space group Pī, while complex **12** crystallizes as yellow monoclinic crystals, space group, $P2_1/c$ (Figure 3.9).

Single crystal X-ray analysis of complex **11** reveals that two different bonding arrangements occur around the copper centers, but both adopt distorted tetrahedral geometries. Cu(1) is coordinated to the pyridyl nitrogen (N1) and two bridging iodides, I(1) and I(2). The second copper center, Cu(2), has coordination to a pyridyl nitrogen atom N(2), a sulfur atom from the ligand, S(1) and two bridging iodides, I(1) and I(2). Thus, the ligand bridges two copper centers. The iodide atoms bridge the copper atoms in μ3 and μ2 modes. The two copper centers have distorted tetrahedral geometry with angles ranging from 102.43(2)^o to 118.11(11)^o for Cu(1) and 100.48(12)^o to 116.68(4)^o around Cu(2). The Cu-I bridges are found to be slightly asymmetric, Cu(1)-I(1) 2.7257Å, Cu(1)-Cu(I2A) 2.6776(8) Å , but this is not uncommon for bridged halides and can be compared to $[Cu_4(L^1)_2I_4]$ (L^1 = bis(6-methyl-2-pyridyl methyl sulfide)) that has bond lengths of 2.586(1)-2.652(1)Å for the bridged iodides, a Cu-N distance of 2.031(3)Å and a Cu-S distance of 2.570(1)Å.[117b] Unlike the analogous bromide compound, complex **11** has no hydrogen bonding existing between the CH_2 group and the iodides.[104] The lack of hydrogen bonding is possibly due to the lower electronegativity of the iodine versus bromine and the larger size between the atoms. Therefore a polymeric chain of clusters does not form. Solution luminescent measurements in acetonitrile were performed on **11** and **12** but no luminescence was recorded, it is possible that low temperature solid-state measurements are required.

PymS-SPym was prepared serendipitously in high yield from the attempted synthesis of $(PymS)_3CH$ (see experimental section). Despite this not being the desired product, it could be reproducibly prepared in high yield and used for further reactions. The reaction of $(PymS)_2$ with CuI afforded yellow crystals of compound **12** in high yield.

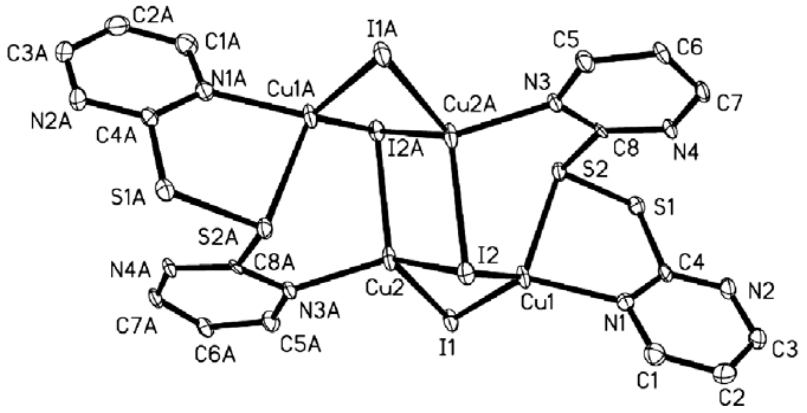

Figure 3.9 X-ray crystal structure of $[(PymS)_2Cu_2I_2]_2$, complex **12**, thermal ellipsoids at 30% probability level. Hydrogen atoms are omitted for clarity. Key bond lengths (Å) and angles (^{o}): Cu(1)-N(1) 2.053(7), Cu(2)-N(3) 2.061(7), Cu(1)-S(2) 2.421(2), Cu(1)-I(1) 2.5612(11), N(1)-Cu(1)-I(2) 114.1(2), I(1)-Cu(1)-S(2) 106.20(6), N(1)-Cu(1)-Cu(2) 172.1(2), N(1)-Cu(1)-S(2) 85.97(19).

The solid-state analysis of **12** reveals a dimeric structure that features a tetrameric core of copper atoms (Figure 3.9). Each ligand chelates one copper atom through S(1) and N(1) atoms and coordinates to another Cu(2) through another nitrogen atom, thus bridging the two metal atoms in **12**. An average Cu-S bond is reported to be around 2.67Å,[119] the Cu-S distance of 2.421(2)Å is significantly shorter than this distance, and is attributed to the steric constraints of the ligand. It is noteworthy to mention that complex **12** appears to be thermally robust in the solid-state and in solution. However, attempts to use the related system, PyS-SPy, for framework synthesis resulted in cleavage of the S-C aromatic bond and formation of elemental sulfur.

Continuing with our studies of the coordinating abilities of the synthesized ligands, the reaction of CuCN with $(PymS)_2$ was performed, however no crystalline product could be isolated. Exchange of copper cyanide for copper thiocyanate, afforded colorless crystals of an infinite two dimensional polymeric material **13**, Scheme 3.4 and Figure 3.10. Use of copper(I) thiocyanate has not been well explored for use in metal organic framework construction, in part because of its limited solubility in organic solvents.[120]

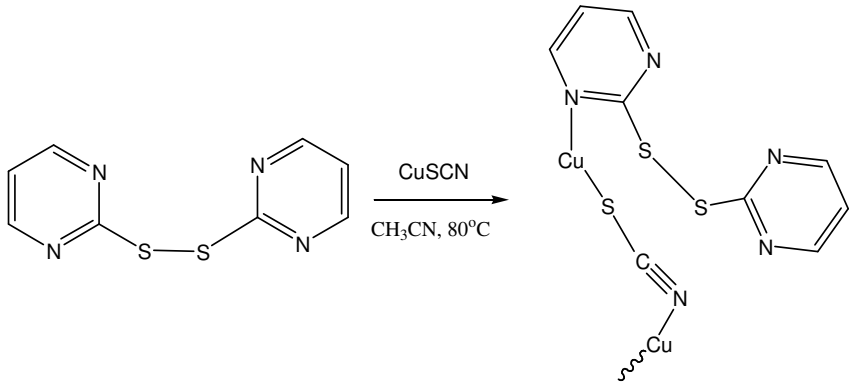

Scheme 3.3 Synthesis of **13** from the reaction of $(PymS)_2$ with CuSCN.

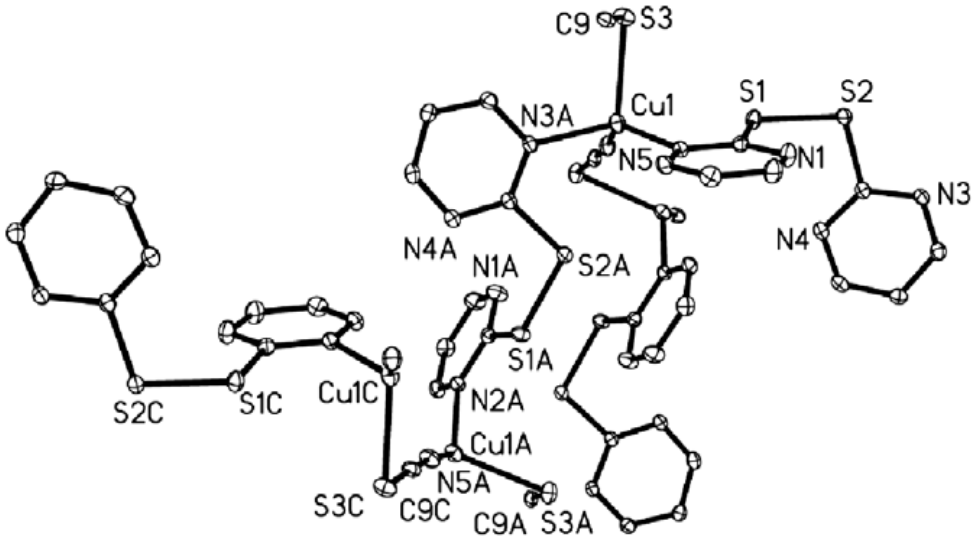

Figure 3.10 Crystal structure of the polymeric network $[(PymS)_2CuSCN]_\infty$, **13**. Thermal ellipsoids at 30% probability level and hydrogen atoms are omitted for clarity. Selected bond lengths (Å) and angles (°): Cu(1)-N(3) 2.1580(19), Cu(1)-S(3) 2.3957(7), Cu(1)-N(2) 2.036(2), Cu(1)-N(5) 1.918(2), S(1)-C(1) 1.785(2), S(3)-C(9) 1.656(3), N(2)-Cu(1)-S(3) 96.95(6), N(5)-Cu(1)-S(3) 115.80(7), N(2)-Cu(1)-N(3) 105.77(8).

We were drawn to the precursor, CuSCN, given our success with copper cyanide, and because this copper salt exists as polymeric $[Cu(SCN)]_\infty$.[121] Additionally, CN and SCN ligands can act as a bridge between metal centers thus promoting magnetic communication.[107]

Polymer **13** crystallizes in the monoclinic space group $P2_1/c$ and the X-ray analysis shows that each copper is tetrahedrally coordinated to two nitrogen atoms from two different ligands and to sulfur and nitrogen from the thiocyanate group. The geometry around the

thiocyanate group is nearly linear, with an S-C-N angle of 178.3(2)^{o}, and a Cu-Cu separation of ~5.6Å. The bond lengths and angles in **13** compare well with $[Cu(SCN)(pyz)]_{\infty}$, that has Cu-S and Cu-N bonds of 2.349(2)Å and 1.940(4)Å,[122] respectively. Infrared spectroscopy of polymer **13** exhibited CN stretches at 2110 and 2066 and at 767cm^{-1}, associated with the S-C stretch and these values compare well with other reported polymeric structures.[123]

3.3 Conclusions

We have shown that copper(II) chloride, copper(I) iodide and the copper pseudo halides, CuCN and CuSCN, can be used in conjunction with flexible heteroelemental organic linkers to form clusters or polymers that can incorporate the anion into the framework. This type of preparation is a versatile useful approach for the construction of neutral polymeric frameworks that present the copper atom in a variety of geometrical arrangements. Furthermore, they offer potential for further reactions and framework growth, because of the availability of uncoordinated donor atoms present in the used ligands and could lead to the synthesis of heterometallic MOFs.

The isolation of clusters or polymers was attributed to the geometric requirements of the ligands, the electronic requirements of the copper atom as well as the specific size and coordination modes of the selected metal precursors. For example, when CuI was used we were only able to isolate clusters containing the Cu_4I_4 core due the larger size of the iodine atom compared to the chlorine atom or the coordinating atoms in the CN and SCN species. At the same time, the relative weakness of the CuI bond prevents the participation of the iodine atom in further multicentric bonds avoiding the formation of polymeric species. The Cu_4I_4 core displays distance between copper atoms which are characteristic of possible cuprophilic interaction. Unfortunately we were not able to confirm the presence of this class of interaction in the luminescent experiments at room temperature or in the solid state.

Our studies using CuCN and CuSCN have shown the viability of using pseudo halides for neutral polymer assembly, since anion incorporation is probable and promotes magnetic communication between metal centers.

The synthesized polymers and clusters were obtained in moderate to good yields by solvothermal synthesis in reaction times of 24 hours at most[106-107] due, in some cases, to the low solubility of the chosen metal precursor. It is predicted that the use of different derivatives of 2-mercaptopyridine and 2-mercaptopyrimidine having a different number of nitrogen atoms in the heterocyclic aromatic ring could lead to the synthesis of novel ligands with different coordination modes that can give us the possibility of constructing new structural motifs.

3.4 Experimental

All chemicals were purchased from Aldrich or Acros and used as received. The synthesis of $(PyS)_2CH_2$[124] and $(PymS)_2CH_2$[125] were performed according to the published procedure. $(PymS)_2$ was prepared through modification of the literature procedure as follows: 2-mercaptopyridine (1.68g, 15 mmol) was added to a stirred solution of potassium hydroxide (0.84g, 15 mmol) in ethanol (60 mL). The reaction mixture was warmed to reflux and then bromoform (1.3 mL, 15 mmol) was added drop-wise. The resultant mixture was refluxed for 24h. After adding water (90 mL), the reaction mixture was left to stand overnight. The yellow precipitate was filtered off and washed with cold ethanol and cold water giving a brown solid that was recrystallized from hot ethanol and water.

Melting points were preformed on a Meltemp apparatus under ambient conditions. In a typical experiment, the ligand and copper salt in a 1:1 mol ratio were dissolved in acetonitrile and heated to between 80 and 90^oC for 12 h. Grease free Teflon sealed Schlenk flasks were employed to avoid grease contamination and to allow heating of a sealed system. All crystals were obtained from slow evaporation of the solution at room temperature.

3.4.1. Synthesis of compound 9

In a grease free Schlenk flask, 5 mL of acetonitrile, $CuCl_2.2H_2O$ (0.04 g, 0.23 mmol) and $(PymS)_2CH_2$ (0.05 g, 0.23 mmol) were added together. The reaction mixture was heated at ~100^oC. After 14 h, the green colored reaction mixture was gravity filtered to remove insoluble impurities. The solution was kept at room temperature for 2 days, during which time large, teal green colored crystals, suitable for single crystal analysis were isolated. The product decomposes at 150-152^oC. Yield: 0.045 g (51% based on $CuCl_2{\cdot}2H_2O$), IR (KBr pellet, υ cm^{-1}): 2956(s), 2923(s), 2855(s), 1614(m), 1578(m), 1461(m), 1449(m), 1386(m), 1181(m), 817(m), UV-Vis (CH_3CN): λ max (nm) = 254, 311, 462.

3.4.2. Synthesis of compound 10

In a grease free Schlenk flask, 5 mL of acetonitrile, CuCN (0.035 g, 0.39 mmol) and $(PyS)_2CH_2$ (0.1 g, 0.39 mmol) were added together. The reaction mixture was stirred at 80-100^oC for 14 h. After cooling to room temperature the colorless solution was gravity filtered to remove insoluble particles. The solution was stored overnight at room temperature,

yielding colorless single crystals of **10**, m.p. 72-74°C, yield: 0.049 g (39% based on CuCN), IR (KBr pellet, υ cm^{-1}): 2361(s), 1578(s), 1554(s), 1465(m), 1455(m), 1411(m), 1337(m), 1285(m), 1214(m), 1143(m), 1123(m), 1040(m), 986(m), 755(m), 740(m), 714(m), ^{1}H NMR (300 MHz, CD_3CN, 25°C): 5.01 (s, 2H), 7.13 (t, 2H), 7.26 (d, 2H), 7.62 (t, 2H), 8.49 (d, 2H). UV–Vis (CH_3CN): λ max (nm) = 250, 290.

3.4.3. Synthesis of compound 11

CuI (0.02 g, 0.12 mmol) and $(PyS)_2CH_2$ (0.03 g, 0.12 mmol) were dissolved in ~5 mL of acetonitrile. The solution was stirred for 14 h at 80-90 °C. Following filtration, storage of the solution at room temperature afforded pale yellow crystals of **11** suitable for X-ray diffraction. The product decomposes at 145-147°C. Yield: 0.30 g (67% based on CuI), IR (KBr pellet, υ cm^{-1}): 2960(s), 2927(s), 2854(m), 1449(m), 1413(m), 1373(m), 1260(m), 797(s), 765(s), 749(m), ^{1}H NMR (300 MHz, CD_3CN, 25°C): 5.02 (s, 2H), 7.14 (t, 2H), 7.28 (d, 2H), 7.63 (t, 2H), 8.49 (d, 2H). UV-Vis (CH_3CN): λ max (nm): 209, 245, 360.

3.4.4. Synthesis of compound 12

CuI (0.1 g, 0.52 mmol) and $(PymS)_2$ (0.18 g, 0.52 mmol) were dissolved in 5 mL CH_3CN and heated to 70-80°C for 14 h. After filtration of the yellow solution and storage at room temperature for 5 days, suitable X-ray quality yellow crystals of compound **12** were isolated, m.p. 175-177°C, yield: 0.34 g (50% based on CuI) IR (KBr pellet, υ cm^{-1}): 2359(s), 1640(s), 1425(m), 1376(m), 1196(m), 1167(m), 822(m), 804(s), 774(m), 766(m), 744(m), 629(m), 448(m), ^{1}H NMR (300 MHz, CD_3CN, 25°C): 7.25 (t, 2H), 8.61 (d, 4H). UV-Vis (CH_3CN): λ max (nm) = 209, 242, 359.

3.4.5. Synthesis of compound 13

Acetonitrile (5 mL), CuSCN (0.04 g, 0.29 mmol) and $(PymS)_2$ (0.1 g, 0.29 mmol) were added together in a grease free Schlenk flask. The reaction mixture was stirred for 14 h at 90-100°C. The colorless solution was gradually filtered by gravity to remove a cloudy precipitate. Slow evaporation of the colorless solution at room temperature afforded colorless crystals of **13**, m.p. 112-115°C, yield: 0.037 g (30% with respect to CuSCN), IR (KBr pellet, υ cm^{-1}): 2110(s), 2066(s), 1550(m), 1427(m), 1375(m), 1196(m), 1169(m), 817(m), 767(w),

743(m), 629(m), ^{1}H NMR (300 MHz, CD_3CN, 25^{o}C): 6.91 (t, 2H), 6.94 (t, 2H), 8.10 (d, H), 8.30 (d, 4H). UV-Vis (CH_3CN): λ max = 236 nm.

Chapter 4

Metal organophosphonates

4.1 Introduction

Organic compounds containing the phosphorus atom constitute a very broad field with possibilities for research and applications.[126] As an example of this diversity, we can mention the organophosphorus-oxygen compounds which include: phosphates, phosphinates, phosphonates, phosphine oxides, phosphonic acids and phosphinic acids (Figure 4.1).[127]

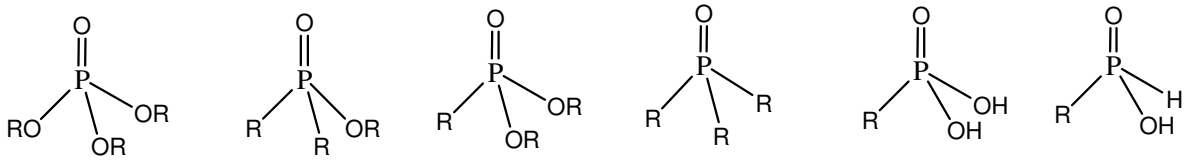

Figure 4.1 Some examples of organophosphorus-oxygen compounds.

Of relevance to our research field are phosphonic acids of the general formula $RP(O)(OH)_2$. Clearfield *et al.*[128,129] pioneered the use of phosphonic acids for the synthesis of Ti(IV) and Zr(IV) metal organophosphonates which are classified as hybrid compounds (organic-inorganic compounds).[130] A great number of studies have been directed to the synthesis of metal phosphonates using divalent (Mg, Zn, Ni, Co, Mn, Cu, Cd)[131-133] and trivalent metals (Mn, Al) formed from the reaction of phosphonic acid and a metal salt.[134,135] The structures of M^{II} phosphonates usually have two of the oxygen atoms chelating a metal center and also bridging across to an adjacent metal cation. The open coordination sites are usually completed by water molecules.[136] For M^{III} phosphonates, the metal center is usually coordinated with oxygens from different phosphonate moieties and its coordination sphere is completed with solvent molecules.[137] In the case of M^{IV} phosphonates, the coordination sphere around each metal center is octahedral and is built up only with phosphonate groups,[138] depending of whether the phosphonic acid remains singly protonated or doubly deprotonated (See Figure 4.2).[139-141]

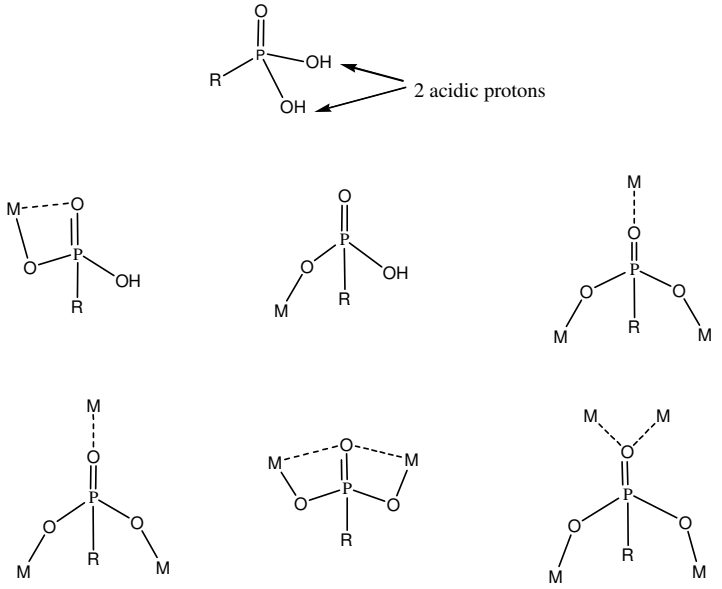

Figure 4.2 Representation of the possible coordination modes of phosphonic acids to metallic centers. Adapted from references 139-141.

Phosphonic acids have proved very versatile for phosphonate framework synthesis because of the great variety of secondary functional groups that can be introduced in the phosphonate moiety such as alkyl and aryl groups, e.g. $-NH_2$, $-CO_2H$ and $-SO_3H$.[142] The degree of chemical functionalization combined with the great availability of metallic salts has resulted in the synthesis of many microporous structures.[143]

Using similar strategies to those detailed in Chapter 1, metal phosphonates can be generated by a variety of methods including: hydrothermal synthesis, co-precipitation from a solution of the appropriate metallic salt with the required phosphonic acid and using soluble organometallic precursors.[144] In general, metal organophosphonates are air stable with exception of the Cr(II) derivatives and in the case of Fe(II) phosphonates which are stable once formed.[145]

4.2 Synthesis of phosphonic acids

Phosphonic acids are derived from phosphonates, $RP(O)(OR)_2$, and can be synthesized by the Michaelis-Arbuzov reaction[146] which involves the reaction of an P(III) ester with alkyl halides (Scheme 4.1).

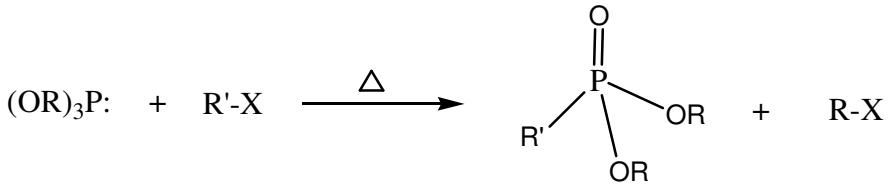

R = alkyl, aryl, etc
R' = alkyl, aryl, etc
X = halogen

Scheme 4.1 Synthesis of phosphonates through the Michaelis Arbuzov rearrangement.[146]

When R' = R, the process consists of an isomerization of the phosphite, $(OR)_3P$ and involves shell expansion of the phosphorus atom from eight to ten electrons associated with the availability of low energy 3d orbitals as a result a dπ-pπ bonding between the phosphorus and oxygen atoms.[147] Usually any halide capable of reacting with nucleophiles by a S_N2 mechanism is suitable for the reaction. In the case of the phosphorus reagent, it is possible to use practically any class of R group attached to the phosphite: alkoxy, aryloxy, alkyl or aryl.[147] The phosphonates obtained by this method are usually hydrolyzed or deprotected using trimethylbromosilane, (TMSBr) (McKenna's protocol),[148] in order to get the desired phosphonic acid. HCl hydrolysis can be also employed to obtain the corresponding phosphonic acid (Scheme 4.2).[129]

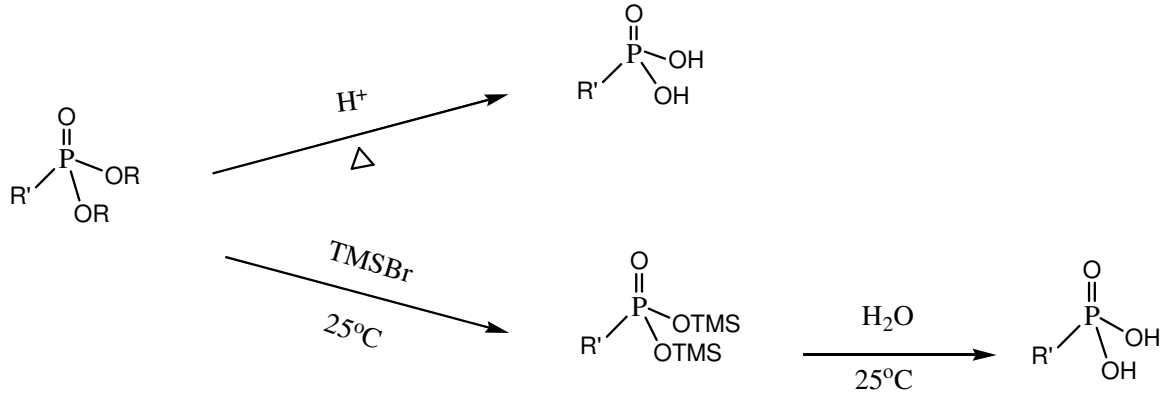

Scheme 4.2 Synthesis of phosphonic acids through hydrolysis or by deprotection with TMSBr. Adapted from references 129 and 148.

For the synthesis of aryl phosphonates, the Hirao coupling[149] has been widely used. The Hirao coupling employs transition metals to promote the formation of phosphorus-carbon bonds by the reaction of dialkylphosphites with aromatic halides. Initially, this

coupling reaction was performed in the presence of a base, using a palladium catalyst.[149,150] Today it is possible to replace palladium by other less expensive metals such as Ni and Cu (Scheme 4.3).[151-153]

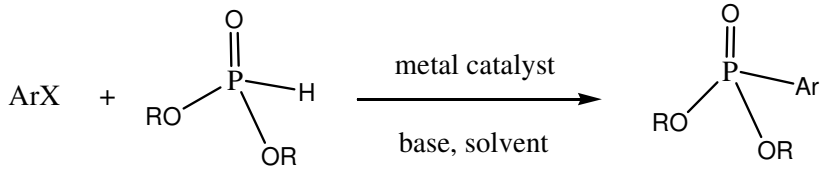

Scheme 4.3 Hirao coupling. ArX = aryl halide, R = alkyl, aryl.[149-153]

The numerous coordination modes of phosphonic acids, their more acidic nature than carboxylic acids[154] and the possibility of introducing secondary functional groups makes them desirable spacers to tailor frameworks for specific applications.[146] Based on our success using pyrazine and pyrazine carboxylic acid with group 13 elements, we wished to explore their potential as linkers for the construction of main group phosphonates and pursue the synthesis of bimetallic metal phosphonates. Figure 4.3 depicts a series of phosphonic acids that were prepared for study.

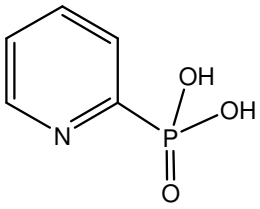

2-pyridylphosphonic acid

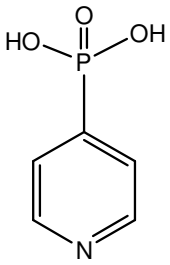

4-pyridylphosphonic acid

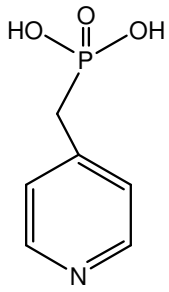

4-pyridylmethylphosphonic acid

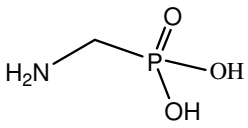

aminomethylphosphonic acid

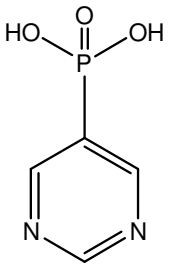

5-pyrimidylphosphonic acid

Figure 4.3 Selected phosphonic acid ligands used for the synthesis of MOFs detailed in Chapters 4 to 6.

The following chapters will deal with the use of these selected phosphonic acids for the synthesis of molecular phosphonate cages and metal organophosphonate multidimensional frameworks.

4.3 Aluminum and gallium phosphonate cages

The reactivity of phosphoric acid with aluminum and gallium alkyls has been studied as early as 1975 by Cassidy *et al.*[155] who prepared a tetrameric complex of aluminum phosphate from the reaction of $AlCl_3$ with phosphoric acid in ethanol, that on heating readily decomposes to aluminum phosphate. Later work in this area was pioneered by Roesky[156] and Barron[157] and led to the formation of molecular phosphonate cages. Investigations of phosphonic acid derivatives of the *p* block elements have been more limited, and for the most part have used methyl or phenyl phosphonic acids with aluminum alkyls.[156-158] For example, Barron *et al.*[157a] explored the products formed from the hydrolysis of $Al(^tBu)_3$, in the presence of the hydrated salt $Al_2(SO_4)_3.14H_2O$ (Scheme 4.4). The oligomeric aluminum species obtained provided experimental evidence for the structural relationship between alkylalumoxanes and the mineral boehmite.[157c]

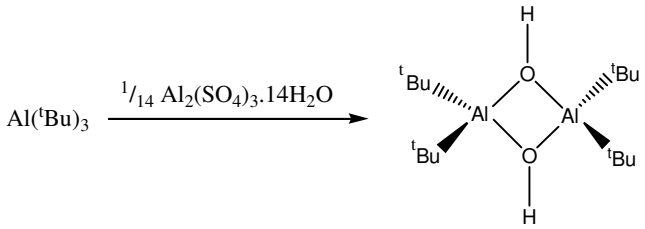

Scheme 4.4 Hydrolysis of $Al(^tBu)_3$ for the synthesis of dimeric alkylalumoxanes.[157a]

To date, most aluminum phosphonates have layered structures prepared from hydrothermal methods, under reflux, or by melting an alum salt together with a phosphonic acid.[158] Although hydrothermal methods give interesting products,[158,159] the isolated product is unpredictable, very sensitive to precise reaction conditions, reaction composition, and the exact method of crystallization is not clearly understood. Phosphonic acid derivatives make ideal candidates as spacers for metal phosphonates as they can incorporate virtually any organic group, are prepared by facile syntheses,[160] and when combined with a metal precursor, afford products that vary structurally from discrete molecules to multi-dimensional

polymers.[161] Much of the recent work has been driven by the fact that these compounds have potential as ion exchangers, in catalysis and as sensors.[162] The majority of work using pyridyl phosphonates has focused on tetravalent transition metal atoms.[163] We were interested in expanding the work of pyridyl phosphonic acids[164] to the main group elements to examine how structural motif would vary with the nature of the metal ions, solvent and temperature, and how these factors would affect the extent of phosphonic acid deprotonation that, in turn, would govern dimensionality of the product. To this end, we investigated the reactivity of aluminum(III) chloride and nitrate, gallium(III) chloride with 2- or 4-pyridyl phosphonic acids and $Ga(NO_3)_3$ with $4PyCH_2PO_3H_2$ employing room temperature syntheses.

4.3.1 Results and Discussion

In keeping with our earlier work,[165] we wished to perform reactions in aqueous solutions using mild conditions. An array of water-soluble precursors was investigated allowing reactions to be performed in open vials at ambient temperatures. Furthermore, hydrolysis of aluminum chloride and alkyls by hydrated salts is a mild widely used route for alumoxane synthesis.[157,166] It was anticipated that these hydrated salts might combine these factors and would favor either alumoxane or polymer isolation. Gallium precursors proved more troublesome, as $GaCl_3$ readily forms $Ga(OH)_3$ under aqueous conditions.[167,168] To slow the hydrolysis process down and give gallium a chance to complex with the ligand, the reactions were performed and worked up under inert conditions, although solvents were used undried, directly from the bottle.

4.3.1.1 Synthesis of complexes $[(2PyPOH)_4Al_4(OH_2)_{12}]Cl_8.6H_2O$ (14), $[(4PyPOH)_4Al_4(OH_2)_{12}]Cl_8.6H_2O$ (15) and $[(2PyPOH)_4Al_4(OH_2)_{12}](NO_3)_8.7H_2O$ (16)

Complexes **14** and **15** were isolated in moderate yield from the 1:1 reaction of $AlCl_3.6H_2O$ and 2-pyridyl phosphonic acid ($2PyPOH_2$) or 4-pyridyl phosphonic acid ($4PyPOH_2$) as shown in scheme 4.5.

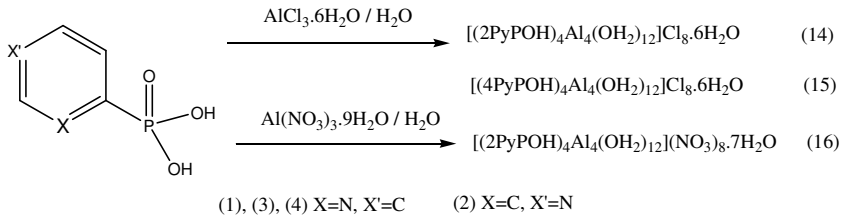

Scheme 4.5 Synthesis of complexes **14**-**16**

A general rule established for the synthesis of aluminophosphates is that increased temperature favors three-dimensional structures over layered materials.[169] Therefore, the isolation of **14**-**16** from a room temperature synthesis is not too surprising because the high charge density of Al^{3+} in solution drives the crystallization process. This high charge density leads to extensive hydrolytic processes and has often been used for the formation of oxy-hydroxy species containing from 13-30 aluminum centers.[170]

4.3.1.1.1 Crystal structures of complexes $[(2PyPOH)_4Al_4(OH_2)_{12}]Cl_8.6H_2O$, (14), $[(4PyPOH)_4Al_4(OH_2)_{12}]Cl_8.6H_2O$, (15) and $[(2PyPOH)_4Al_4(OH_2)_{12}](NO_3)_8.7H_2O$, (16)

Crystallographic analysis of complexes **14**-**16** revealed the formation of an interesting aluminum(III) phosphonate cluster as shown for **14** in Figure 4.4 (crystal data for all compounds is given in Table 4.3 at the end of this chapter).

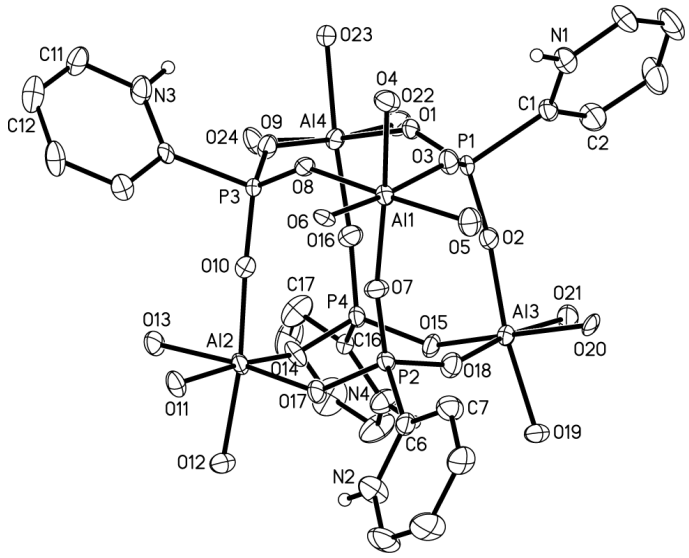

Figure 4.4 X-ray crystal structure of the cation of **14**, $[(2PyPOH)_4Al_4(OH_2)_{12}]^{8+}$. Thermal ellipsoids are shown at 50% probability level. Only the hydrogen atoms of the pyridyl groups are shown as circles of arbitrary size. Selected bond lengths (Å) and angles (°) around Al(2): Al(2)-O(13) 1.920(5), Al(2)-O(10) 8.863(5), P(3)-O(10) 1.491(5), O(10)-Al(2)-O12 173.2(2).

Complex **14** features four aluminum centers and four pyridyl phosphonate ligands in the asymmetric unit. All of the phosphonate groups are doubly deprotonated at oxygen but are protonated at the pyridyl nitrogen atom. Aluminum maximizes its coordination number

yielding coordinatively saturated metal centers with octahedral geometry made up by coordination to three μ^2 oxygens from the phosphonate group, each from different ligands and that interlink to other Al centers through these oxide bridges. The remaining three coordination sites are made up of water molecules. Eight displaced Cl^- ions are located around the cationic core. The net +8 charge is created by four Al^{3+} ions in addition to four protonated phosphonates each having a -1 charge. A large quantity of water molecules and chloride ions in the structure leads to strong hydrogen bonding. The chloride ions are located in close proximity to both bound and free water molecules due to hydrogen bonding. This hydrogen bonding is seen throughout the structure and allows the molecule to propagate into a chain of cyclic rings held in place by hydrogen bonds. These structures are particularly interesting as they have the potential to act as a template for the preparation of extended structures and because metal oxide/hydroxide structures are important to make controlled particles of a certain size and morphology.

Complexes **14**-**16** have a topology reminiscent of the alumoxane structures prepared by Roesky *et al*.[156–158] Like the alumoxanes, the structural motif of **14**-**16** can be considered as a distorted cubane type structure, with an $Al_4O_{12}P_4$ core made up of six $M_2O_4P_2$ rings. Alternate corners of the "cube" are made up of Al and P atoms that are linked by bridging oxygen atoms sitting between these corners and along the edge of the cube (Figure 4.5). This core atom arrangement resembles the secondary building units (D4R) found in zeolites[156a] and phosphonate molecular sieves, although in these the aluminum is most commonly three- or four coordinate.[171]

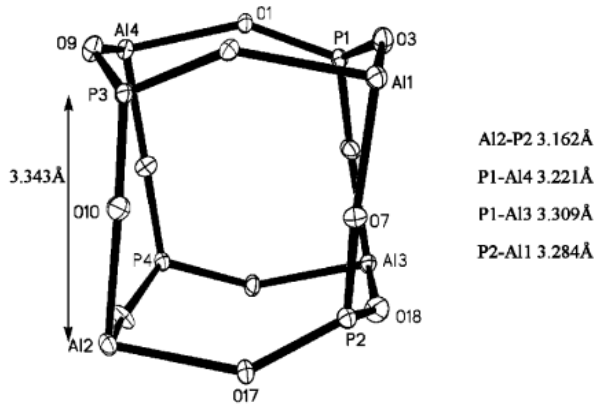

Figure 4.5 Diagram to show the overall geometry in **14**. Thermal ellipsoids are drawn at 30% probability level.

In an attempt to increase the number of Al atoms within the structure, $2PyPOH_2$ was replaced with $4PyPOH_2$, with the rationale being a larger bite angle would increase dimensionality through Al-N and Al-O, (phosphonate) coordination. However, the reaction of $4PyPOH_2$ with $AlCl_3.6H_2O$ yields essentially the same structure, Figure 4.6. The similarity of these two structures is attributed to protonation of the nitrogen under the employed reaction conditions. In contrast, the hydrothermal reactions of phenylphosphonic acid with $AlCl_3.6H_2O$ affords polymeric chains of octahedrally coordinated aluminum, with five of the six positions taken by oxygen atoms of the phosphonate group, and the sixth site being occupied by a water molecule.[172]

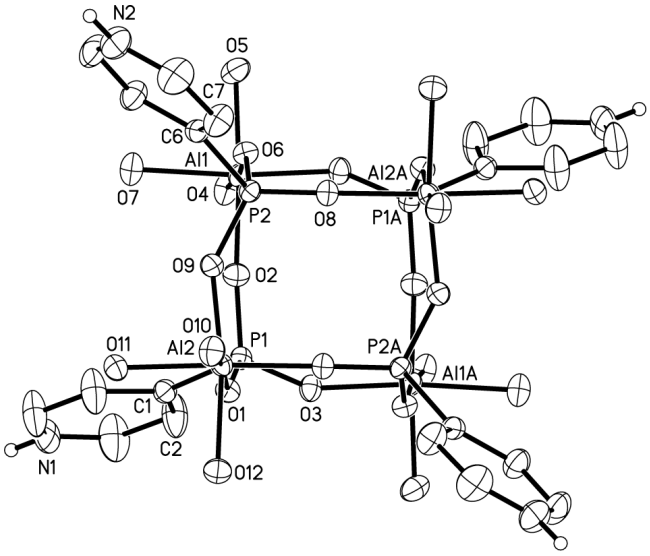

Figure 4.6 A drawing of the cation core of **15** as viewed down the 2-fold axis. Thermal ellipsoids are shown at the 50% probability level, only hydrogen atoms of the pyridine groups are shown. Selected bond lengths (Å) and angles (°) around Al(2): Al(2)-O(12) 1.9475(16), Al(2)-O(9) 1.8295(14), P(1)-O(1) 1.5168(14), O(12)-Al(2)-O(11) 86.32(7).

Complex **15** crystallized in the monoclinic space group P2/*n* with 2-fold crystallographic symmetry. Complexes **14** and **15** have comparable bond lengths and angles that correspond well to reported literature values.[173] As one would expect the Al-O bond lengths for water coordination are longer than for the bridged oxygen atoms. As in **14**. The similar P-O bond lengths along with charge balance, suggest a fully deprotonated phosphonate moiety.

Attempts were made to perform the reactions in basic *p*H conditions to prevent protonation of the pyridyl nitrogen, however these resulted in the isolation of an insoluble material that could not be used for further characterization.[174]

In order to check the generality of our synthesis, aluminum chloride was exchanged for aluminum(III) nitrate. The stoichiometric reaction of Al(III) nitrate with $2PyPOH_2$ resulted in the isolation of complex **16** in almost quantitative yield. Figure 4.7, shows the cationic component of cluster of **16**, viewed perpendicular to a pseudo 2-fold axis. It can be seen that the symmetry is broken primarily by the position of the pyridyl group based on N(3).
A comparison of the bond lengths and angles of **14**-**16** is given in table 4.1.

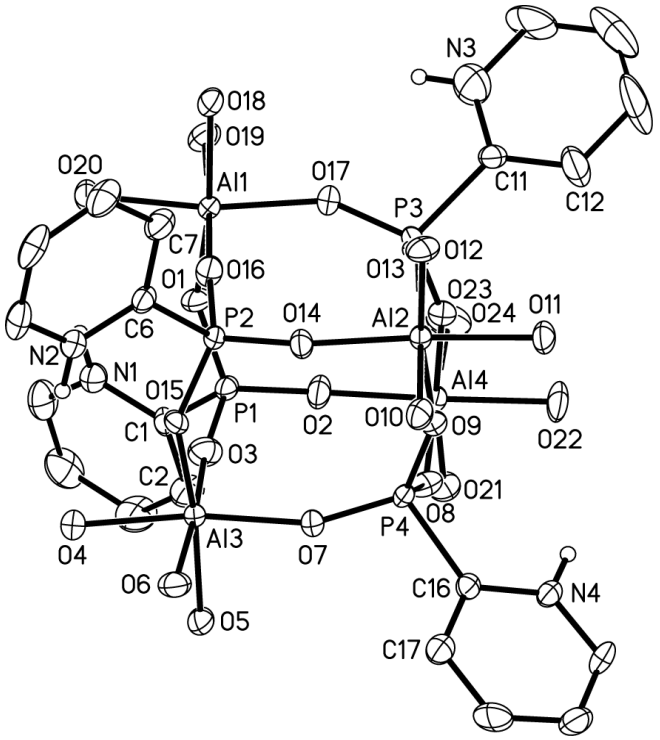

Figure 4.7 A view of the cation of the nitrate salt, **16**, with thermal ellipsoids drawn at the 50% probability level. Selected bond lengths (Å) and angles (°) around Al(3): Al(3)-O(7) 1.840(3), Al(3)-O(4) 1.917(3), P(1)-O(2) 1.510(3), O(5)-Al(3)-O(7) 87.60(13).

Further work attempted exchange of the aluminum halide precursor for aluminum triethoxide, however no suitable material for analysis could be isolated.

Table 4.1 Comparison of selected bond lengths and angles for complexes **14**-**16** (in each case the same bonds/ angles are compared)

Bond Length (Å) or Angle (°)	$[(2PyPOH)_4Al_4(OH_2)_{12}]C_8$.$6H_2O$, **14**	$[(4PyPOH)_4Al_4(OH_2)_{12}]Cl_8$.$6H_2O$, **15**	$[(2PyPOH)_4Al_4(OH_2)_{12}](NO_3)_8$.$7H_2O$, **16**
P-O	1.496(5)	1.5168(14)	1.503(3)
P-C	1.820(7)	1.8116(19)	1.823(4)
Al-O(oxo)	1.844(5)	1.8229(15)	1.858(3)
Al-O(water)	1.955(5)	1.9411(16)	1.945(3)
P—Al	3.184	3.316	3.207
O-P(1)-O	112.6(3)	113.41(8)	113.82(17)
O(oxo)-Al-O(oxo)	91.7(2)	92.70(6)	97.62(14)
$O(H_2O)$-Al- $O(H_2O)$	81.8(2)	87.71(7)	86.92(14)
$O(H_2O)$-Al- O(oxo)	90.5(2)	92.12(7)	86.92(14)

4.3.1.1.2 Spectroscopy and TGA analysis of $[(2PyPOH)_4Al_4(OH_2)_{12}]Cl_8.6H_2O$, (14), $[(4PyPOH)_4Al_4(OH_2)_{12}]Cl_8.6H_2O$, (15) and $[(2PyPOH)_4Al_4(OH_2)_{12}](NO_3)_8.7H_2O$, (16)

In D_2O solution, ^{31}P NMR spectra on complexes **14** and **15** exhibit single peaks at -6.2 and -0.17 ppm, respectively. Complex **16** exhibits two phosphorus signals in solution at -8.4 and -13.9 ppm. The single peaks displayed by **14** and **15** suggest that structural integrity is maintained in solution. Although complex **16** does not differ tremendously from these complexes, the two signals observed in the ^{31}P NMR suggest that in D_2O the cage dissociates, affording a mixture of species, which could also explain the complicated aromatic signals in the ^{1}H NMR spectra arising from free and complexed ligand. No noteworthy features are observed in the ^{1}H NMR of **14** and **15**. Infrared spectroscopy of **14**–**16** shows clear stretches associated with free water molecules, P-O stretches, and distinctive N-H stretches.

Complexes **14**-**16** are air and moisture stable and show good thermal stability, not melting at a temperature of 250°C; however on heating, visibly some mass loss is observed. TGA measurements on **14** revealed a mass loss of 48.5% on heating from 25-400°C that corresponds to the loss of approximately 24 water molecules and 8 chlorine atoms (theoretical loss = 49.4%). In the temperature range 58-74°C it is possible to notice a weight loss of 9.7%, (1.33 mg of weight loss/starting weight = 13.74 mg), which is related to the loss of approximately 8 water molecules (7.8% exact value). TG analysis of **16** exhibits a steady weight loss over the same temperature range (25-400°C). The total weight loss of 13.7% corresponds to loss of 12 water molecules, calculated 14.1%. The mass spectrometry analysis of **14** and **16** under positive ions conditions showed the parent ion peak and the fragmentation pattern reveals the cluster core remains intact. The parent ion peak of **16** was not observed.

4.3.1.2 Synthesis of galloxanes: $[(2PyPO)_4(2PyPOH)_2Ga_8Cl_{12}(H_2O)_4(thf)_2][GaCl_4]_2(thf)_8$, (17), and $[(2PyPO)_4(2PyPOH)_2GaCl_{12}(thf)_2(OH_2)_2](NO_3)_2(thf)_9$, (18)

Hydrolysis products of gallium have been less well studied than their aluminum counterparts, in part because hydrolysis of gallium(III) structures beyond an OH/Ga ratio of 2.5:1 produces a gel, followed at a ratio of 3:1 by the precipitation of polymeric GaO(OH) built from edge linked GaO_6 units.[175] It has also been found that hydrolytic gallium species do not lend themselves well to crystallization, hence the limited number isolated.[176] Nevertheless, gallium phosphate chemistry is expanding due to the ability of gallium to exist in more variable and expanded coordination modes as opposed to zeolites and aluminophosphates.[156b,157c]

The reaction of gallium(III) chloride with $2PyPOH_2$ in thf followed by work-up in toluene afforded **17** in moderate yield and **18** in low yield, Scheme 4.6. Leaving the reaction mixture in thf and concentration of the thf solution can significantly increase the yield of crystalline **17**.

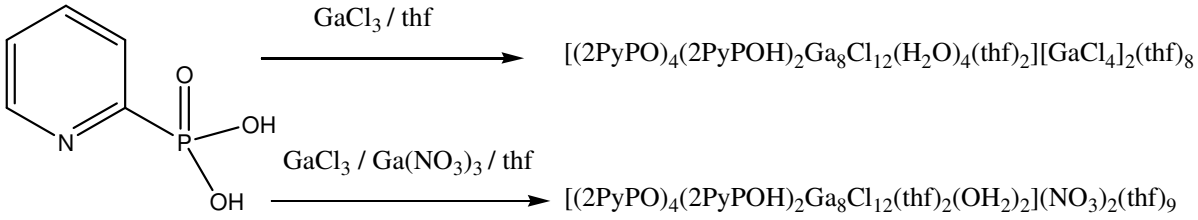

Scheme 4.6 Synthesis of $[(2PyPO)_4(2PyPOH)_2Ga_8Cl_{12}(H_2O)_4(thf)_2][GaCl_4]_2(thf)_8$, (**17**), and $[(2PyPO)_4(2PyPOH)_2GaCl_{12}(thf)_2(OH_2)_2](NO_3)_2(thf)_9$, (**18**).

The main difference between the two structures, **17** and **18**, is the exchange of the counterion $GaCl_4^-$ in **17** to NO_3^- in **18**. This was achieved through using a 1:1 ratio gallium(III) chloride and nitrate in the reaction mixture for formation of **17**. Gallium(III) nitrate was added to the reaction mixture in an attempt to prevent rapid hydrolysis of $GaCl_3$ to $Ga(OH)_3$ which has been documented in gallium hydrolysis chemistry.[175] Unlike in complexes **14-16**, some of the Ga-halide bonds remain intact, in part because of the non-aqueous conditions employed, but also because Ga^{3+} is slightly less acidic than Al^{3+}. The origin of hydrolysis is likely from use of undried solvents.

4.3.1.2.1 Crystal structures of $[(2PyPO)_4(2PyPOH)_2Ga_8Cl_{12}(H_2O)_4(thf)_2][GaCl_4]_2(thf)_8$, (17), and $[(2PyPO)_4(2PyPOH)_2GaCl_{12}(thf)_2(OH_2)_2](NO_3)_2(thf)_9$, (18)

The structural similarities of complexes **17** and **18** are detailed in Table 4.2. In both complexes the cationic core can be broken down into an eight-membered "chairlike" arrangement in which the Ga atoms are bridged by O-P-O groups (See Figure 4.8).

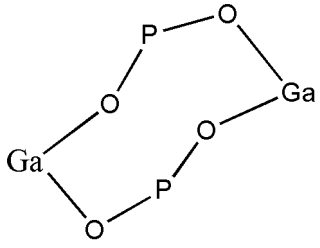

Figure 4.8 Diagram to show the bonding arrangement in the central 'chair'.

Within the Ga_8 cluster, gallium atoms can be observed in two different geometrical environments. The inner gallium atoms exhibit a slightly distorted octahedral geometry,

while the outer gallium atoms ($OGaCl_3$) have close to tetrahedral geometry. In complex **18** the almost octahedral coordination sphere of Ga1 is comprised of four oxo bridges, a pyridyl nitrogen atom, and an oxygen atom of a thf molecule. Ga(3) is coordinated to three oxo bridges, a nitrogen atom of a pyridyl group, and two water molecules. A third pyridyl nitrogen atom, N(1), is not coordinated and bears a proton. Hydrogen bonding exists between the protonated pyridyl nitrogen and a $GaCl_4^-$ counterion in **17** and a NO_3^- counterion in **18**. All phosphonate oxygens are deprotonated, giving a 12^- charge that is balanced by the gallium's positive charge of 24^+ along with 2^+ from the protonated pyridyl nitrogen atoms, 12 chloride atoms, and 2 counteranions. Likewise, in **17** and **18**, there is a difference in P-O bond lengths within the ring and toward the outer edges of the cluster. The external P-O bond lengths are on average longer than the internal P-O bond lengths, most likely because of the structural constraints within the cluster core.

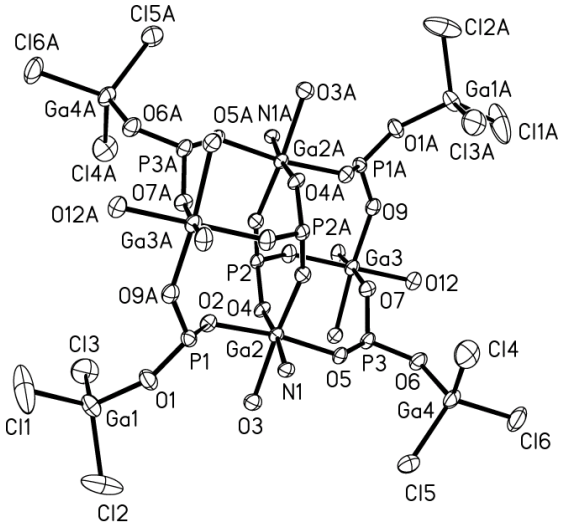

Figure 4.9 A drawing of the cation portion of compound **17**. For clarity it displays only gallium and oxygen atoms. Thermal ellipsoids are drawn at the 30% probability level, hydrogen atoms are omitted for clarity. Selected bond lengths (Å) and angles (°): Ga(1)-Cl(3) 2.157(4), Ga(1)-O(1) 1.830(6), P(1)-O(1) 1.501(6), Ga(2)-N(1) 2.085(6), Ga(2)-O(2) 1.943(5), Ga(2)-O(3) 2.113(6), Cl(3)-Ga(1)-O(1) 108.9(2), O(3)-Ga(2)-N(1) 88.7(2).

Six phosphonate groups support the eight gallium atoms in complexes **17** and **18**. This gives rise to two different phosphorus environments that differ in their P-O coordination

modes to the Ga centers. For example, in **17**, P(2) is connected to an "inner" gallium atom that has a terminal water molecule, while P(3) bonds via O(6) to a $GaCl_3$ molecule (Figure 4.9), and in **18**, P(2) is coordinated to $OGaCl_3$ while P(1) is coordinated through its oxygen atoms to the octahedral Ga atom (Figure 4.10). Unlike the plethora of work available for aluminum phosphonates, the gallium counterparts are less well developed for structural comparison. The asymmetric units of **17** and **18** show structural resemblance to the gallium cluster isolated from the reaction of $^tBu_3Ga$ with phosphonic acid;[177] however, the reaction of $^tBu_3Ga$ with phenylphosphonic acid affords a phosphonate-bridged dimer.[178] Complexes **17** and **18** differ from **14**-**16** in that the pyridyl nitrogen plays a role in cluster stabilization, as four of the six pyridyl N atoms coordinate to Ga atoms and only two pyridyl nitrogen atoms are protonated, while in **14**-**16**, the pyridyl nitrogen atoms are all protonated. Complexes **17** and **18** can be compared with the product from the reaction of phenylphosphonic acid with gallium chloride that afforded a layered lamellar structure.[179]

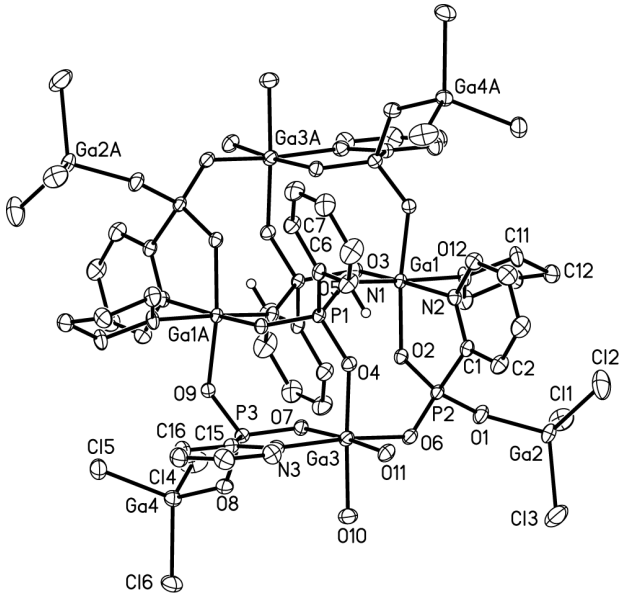

Figure 4.10 Solid-state structure of the cation of **18**. Only the pyridyl hydrogen atoms are shown for clarity. Thermal ellipsoids are drawn at the 30% probability level. Pertinent bond lengths (Å) and angles (°): Ga(2)-Cl(2) 2.1549(16), Ga(2)-O(1) 1.834(3), O(1)-P(2) 1.525(3), Ga(3)-O(10) 1.991(3), Ga(3)-O(6) 1.937(3), Ga(1)-N(2) 2.084(3), Cl(3)-Ga(2)-O(1) 107.24(12), O(10)-Ga(3)-O11 85.42(14).

Table 4.2 Comparison of bond lengths (Å) and angles (^{o}) within the cationic core of **17** and **18**. (In each case the same bonds/ angles are compared).

Compound	$[2PyPO)_4(2PyPOH)_2Ga_8Cl_{12}(H_2O)_4(thf)_2]$ $[GaCl_4]_2(thf)_8$, **(17)**	$[(2PyPO)_4(2PyPOH)_2Ga_8Cl_{12}(thf)_2(OH_2)_2$ $(NO_3)_2(thf)_9$, **(18)**
Ga-O(oxo) (Ga octahedral)	1.943(5)	1.937(3)
Ga-O(thf)	2.113(6)	2.095(3)
Ga-O(H_2O)	1.977(6)	1.991(3)
Ga-N	2.085(6)	2.084(3)
Ga-Cl	2.151(4)	2.1546(19)
Ga-O(tetrahedral)	1.830(6)	1.834(3)
P-O(oxo)	1.501(6)	1.510(3)
P-C	1.811(8)	1.831(4)
P-Ga	3.177	3.254
O(oxo)-Ga-O(oxo) (octahedral Ga)	95.1(2)	95.41(12)
O(oxo)-Ga-O(H_2O) (octahedral Ga)	174.2(3)	172.06(13)
N-Ga-O(thf)	88.7(2)	84.73(14)
Cl-Ga-Cl (Ga tetrahedral)	109.77(13)	109.79(7)
O-P-O	115.0(4)	115.31(16)

4.3.1.2.1.1 Spectroscopic data of 17 and 18

Attempts to observe the two different environments in **17** using ^{31}P NMR revealed peaks at -17.7 ppm and a broad peak at -3 to -5 ppm. Solution ^{31}P NMR on **18** exhibited no phosphorus or proton signals indicating the presence of a possible radical or ligand scrambling leading to immeasurable signals. The hydrogen atom on the pyridyl nitrogen atoms were located from the difference map and confirmed by infrared analysis with a

distinct N-H stretch at 3452 cm^{-1}. Complexes **17** and **18** have low melting points, with **17** melting at 42-43^{o}C and **18** at 80-81^{o}C, this is likely to be due to the presence of coordinated and lattice thf that once lost causes break down of the crystalline lattice. HRMS data of **17**, exhibited no parent ion peak, however peaks could be assigned that indicate that the gallium phosphonate core remains intact, followed by sequential loss of $GaCl_3$.

4.3.1.3 Isolation of the coordination polymer $[4PyCH_2POH)Ga(OH_2)_3](NO_3)_2{\cdot}0.5H_2O\}_x$, (19)

The reactions of $4PyPOH_2$ with gallium chloride were attempted but did not yield any crystals suitable for X-ray crystallography. To determine whether the steric constraints of the ligand were preventing polymer growth, $4PyCH_2PO_3H_2$ was prepared and the reactivity with gallium and aluminum(III) chlorides was investigated but the products from both reactions were oils or amorphous solids. Exchange of the gallium halide salt for gallium(III) nitrate afforded a polymeric species, **19**, Figures 4.11 and 4.12.

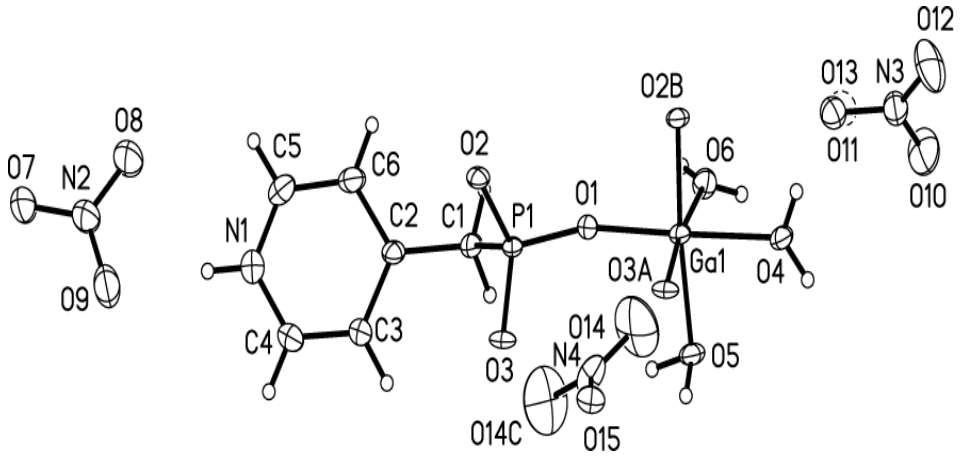

Figure 4.11 Asymmetric unit of **19**. Thermal ellipsoids are drawn at the 50% probability level. There is disorder in the nitrate group {N(3),O(10),O(11),O(12)} which shares the same site with a molecule of water, represented by O(13). Selected bond lengths (Å) and angles (^{o}): Ga(1)-O(1) 1.892(5), Ga(1)-O(3) 1.931(5), Ga(1)-O(4) 1.986(5), Ga(1)-O(5) 2.022(5), Ga(1)-O(6) 2.003(5), P(1)-O(1) 1.508(5), P(1)-O(2) 1.523(5), P(1)-O(3) 1.527(5), O(4)-Ga(1)-O(5) 86.0(2), O(2B)-Ga(1)-O(5) 174.7(2), O(2)-P(1)-O(1) 113.5(3).

Polymer **6** crystallizes in the orthorhombic space group Ib*ca*. In the asymmetric unit is one gallium atom, a phosphonate ligand and two nitrate ions. The repeating unit can be thought of as $[(4PyPOH)_4Ga_4(H_2O)_{12}][NO_3]_8.2H_2O$. The repeating unit is generated by inversion and by the a-glide. It therefore repeats at 9.2230(11)Å, the length of the a axis.

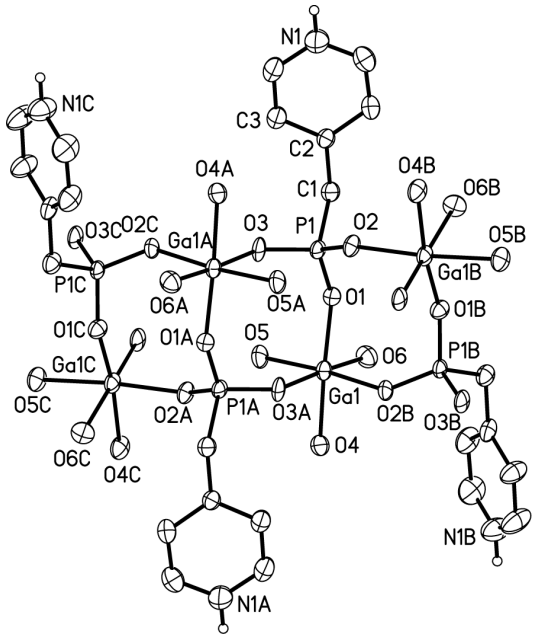

Figure 4.12 Drawing of the $[(4PyPOH)_4Ga_4(H_2O)_{12}]^{8+}$ extended motif. Thermal ellipsoids are drawn at the 50% probability level. Only the pyridyl hydrogen atoms are shown for clarity. Symmetry codes: A = 1-x, 1-y, 1-z; B = ½-x, y, 1-z; C = ½+x, 1 = y, z; D = x-1/2, 1-y, z; E = 3/2-x, y, 1-z.

Each gallium center adopts octahedral coordination geometry with three positions occupied by coordinated water molecules, and the remaining three sites occupied by deprotonated oxygen atoms from the phosphonate moiety. The Ga-O bond lengths are as expected, with the Ga-OH_2 bonds longer than the Ga-O bonds that inter-link the polymer. These distances compare well with related systems.[180] As with many gallium phosphonates the Ga:P ratio is 1:1.[181] Polymer **19** is interesting as a survey of the CCDC reveals only one X-ray structural analysis of a gallium phosphonate with an organophosphonate derivatives.[182] Examination of the hydrogen bonding in **19** reveals the important role that the nitrate ions play; these anions maintain the electroneutrality of the polymer and have an important stabilization role. The anions are positioned between adjacent pyridyl groups and participate

in H-bonding to the coordinated water molecules on the gallium atom and to the deprotonated oxygen atoms of the phosphonate group. This leads to an extensively coordinated network that is relatively thermally robust, melting at 120-125^{o}C.

It is noteworthy to mention the lack of single crystal, structurally characterized molecular or polymeric indium phosphonates.[179,183] Our attempts to crystallize an indium pyridyl phosphonate species were all unsuccessful. From experimental work on thallium(III) halides and nitrates that afford one or two dimensional polymeric species[184] it is possible that indium might be the crossover point in which a mixture of cyclic species and polymeric chains form, leading to insoluble and amorphous material.

4.3.2 Conclusions

The reactions of $2PyPOH_2$ and $4PyPOH_2$ with Al and Ga chlorides afforded alumoxane and galloxane structures that show structural similarity with the single building units of zeolites. In the case of the synthesized alumoxanes, the similarity found in their structure (cubane type arrangement) was a consequence of the protonation of the N-pyridyl atom of the used ligand. Also, it is important to recognize the effect of the counter ion and of coordinating solvents in the stabilization of the cubane structures. The protonation of the N-pyridyl atom possibly limited the isolation of polymeric aluminum phosphonate structures. This issue can be could be partially solved with the use of heterocylic derivatives containing more than one nitrogen atom or by the use of an auxiliary ligand.

For the synthesis of the galloxane species, it was recognized the importance of the use of mild hydrolytic conditions in order to isolate crystalline material avoiding the precipitation polymeric gallium species (e.g. $GaO(OH)_n$). Exchange of the phosphonic acid for the more flexible $4PyCH_2PO_3H_2$ afforded a polymeric structure with a Ga:P ratio of 1:1. This polymeric structure belongs to a limited group of gallium phosphonate polymers.

Future work will be focused on reducing the steric bulk of the phosphonate to look at systems that may mimic the elusive MAO structure (methyl alumoxane).[185] Also, synthetic work is necessary to develop synthetic routes to organic soluble cyclic and cage phosphonates that could act as secondary building units in phosphate materials of group 13 elements. At the same time, the synthesized aluminum and gallium phosphonate cages show promising application for the construction of heteroelemental structures given the possibility of coordinating additional metallic centers through the available coordination sites present in their structures.

Table 4.3 Crystal data and data collection summary for complexes **14**-**16, 17**-**19**

Compound	$[(2PyPOH)_4Al_4(OH_2)_{12}]Cl_8$ $.6H_2O$, **14**	$[(4PyPOH)_4Al_4(OH_2)_{12}]Cl_8$ $.11H_2O$, **15**	$[(2PyPOH)_4Al_4(H_2O)_{12}]$ $[NO_3]_8.7H_2O$, **16**
Chemical Formula	$C_{20}H_{56}Al_4Cl_8N_4O_{30}P_4$	$C_{20}H_{66}Al_4Cl_8N_4O_{35}P_4$	$C_{20}H_{58}Al_4N_{12}O_{55}P_4$
Formula Weight	1348.09	1438.17	1578.58
Crystal System	Monoclinic	Monoclinic	Monoclinic
Space Group	$P2_1/c$	$P2/n$	$P2_1/c$
T(K)	213(2)	213(2)	213(2)
a (Å)	10.9580(12)	14.8394(7)	10.7007(19)
b (Å)	11.8615(13)	11.2851(5)	24.348(4)
c (Å)	42.010(5)	18.3670(9)	25.701(3)
α (^{o})	90	90	90
β (^{o})	93.325(2)	97.887(3)	114.604(11)
γ (^{o})	90	90	90
V (Å ^{3})	5451.2(10)	3046.7(2)	6088.2(16)
Z	4	2	4
Reflections collected	24953	19530	30699
Independent reflections	9854	7233	11001
Data/restraints/parameter ratio	9854/0/631	7233/0/397	11001/11/852
Unique Data (*R int*)	0.0566	0.0239	0.0893
D calc (Mg/m^3)	1.643	1.568	1.722
F(000)	2768	1484	3256
R indices (all data)	R1 = 0.1151, wR2 = 0.1696	R1 = 0.0481, wR2 = 0.0997	R1 = 0.1006, wR2 = 0.1667
Final R indices [$I > 2\sigma(I)$]	R1 = 0.0849, wR2 = 0.1587	R1 = 0.0361, wR2 = 0.0904	R1 = 0.0539, wR2 = 0.1376
Largest difference peak and hole (e Å^{-3})	0.846 and -0.637	0.837 and -0.612	0.669 and -0.739

Compound	$[(2PyPOH)_2(2pypo)_4Ga_8C_{12}(OH_2)_4(thf)_2][GaCl_4]_2.8thf$, **17**	$[(2PyPOH)_2(2Pypo)_4Ga_8Cl_{12}(OH_2)_4(thf)_2](NO_3)_2.9thf$, **18**	$\{[4PyCH_2POH)Ga(OH_2)_3](NO_3)_2.0.5H_2O\}_x$, **19**
Chemical Formula	$C_{70}H_{114}Cl_{20}Ga_{10}N_6O_{32}P_6$	$C_{74}H_{122}Cl_{12}Ga_8N_8O_{39}P_6$	$C_6H_{14}GaN_3O_{12.5}P$
Formula Weight	3143.69	2916.78	428.89
Crystal System	Triclinic	Triclinic	Orthorhombic
Space Group	Pī	Pī	I*bca*
T(K)	213(2)	213(2)	213(2)
a (Å)	14.533(2)	13.2856(10)	9.2230(11)
b (Å)	15.101(3)	15.3643(12)	20.733(3)
c (Å)	19.687(3)	16.9830(13)	29.734(4)
α (°)	68.691(3)	69.1370(10)	90
β (°)	88.293(3)	79.2890(10)	90
γ (°)	61.349(2)	65.0620(10)	90
V (Å ^{3})	3476.8(10)	2934.7(4)	5685.9(10)
Z	1	1	8
Reflections collected	29356	18949	22593
Independent reflections	12481	12818	3490
Data/restraints/parameters	13493/213/588	12818/60/655	3490 / 12 / 236
Unique Data (*R int*)	0.0597	0.0276	0.0838
D calc (Mg/m^3)	1.501	1.650	2.004
F(000)	1572	1476	3472
R indices (all data)	R1 = 0.1578, wR2 = 0.2675	R1 = 0.0857, wR2 = 0.1212	R1 = 0.1381, wR2 = 0.2071
Final R indices [I > 2σ(I)]	R1 = 0.0793, wR2 = 0.2385	R1 = 0.0465, wR2 = 0.1015	R1 = 0.0590, wR2 = 0.1451
Largest difference peak and hole (e $Å^{-3}$)	1.650 and -1.373	0.712 and -0.561	1.202 and -1.045

4.3.3 Experimental

2- and 4-pyridyl phosphonic acids were prepared according to literature procedures.[160] $GaCl_3$ was purchased from Strem Chemicals. All other chemicals were purchased from Aldrich and used as received. The NMR data was recorded on a Varian Mercury 300 NMR spectrometer, IR analyses was conducted on a MIDAC M4000 Fourier transform infrared (FT IR) spectrometer using KBr pellets. Thermogravimetric analyses (TGA) were carried out on a Seiko 220 instrument at a heating rate of 5°C/ min. LR mass spectrometry analysis was carried out using a Bruker Esquire 6000 Mass Spectrometer. HRMS was provided South Carolina Chemistry Department and microanalysis by Schwarzkopf microanalytical laboratory, N.Y. Melting points were determined in capillaries, **14**-**16** under ambient conditions and **17**-**19** under a nitrogen atmosphere and are uncorrected.

4.3.3.1 Synthesis of $[(2PyPOH)_4Al_4(OH_2)_{12}]Cl_8.6H_2O$, (14)

$AlCl_3.6H_2O$ (0.08g, 0.31mmol) and $2PyPOH_2$ (0.05g, 0.31mmol) were added together in an open vial containing 5 mL of water. The clear solution was stirred at 90° for two hours. After two hours, the solution was gravity filtered to remove any solid impurities and left at room temperature for crystallization. From the solution, crystals suitable for X-ray diffraction were obtained. Yield: 0.23 g (56% based on $AlCl_3.6H_2O$), m.p. >250°C, IR (KBr pellets, υ cm^{-1}) 3295(s), 2485(w), 2350(w), 1633(s), 1609(s), 1523(m), 1445(m), 1244(s), 1177(s), 1090(s), 1009(m), 766(m), 729(m). ^1H NMR (300 MHz, 25°C, D_2O): δ 8.79 (d, J = 6 Hz, 1 H), 8.63 (tm, J = 8 Hz, 1 H), 8.27 (t, J = 7.5 Hz, 1 H), 8.11 (t, J = 7.5 Hz, 1 H), $^{31}P\{H\}$ NMR (121 MHz, 25°C, D_2O): δ -6.2. Mass spec: m/z not observed, 444.9 (445) $(2PyPO)_4Al_4(OH_2)_{12}.H_2O$, 262 (262), $(2PyPO)_2Al_2(OH_2)_7Cl$. Elemental Analysis: Obs. (Calc), C 17.15 (17.82), H 4.15 (4.2), N 4.19 (4.2)

4.3.3.2 Synthesis of $[(4PyPOH)_4Al_4(OH_2)_{12}]Cl_8.6H_2O$, (15)

$AlCl_3.6H_2O$ (0.08g, 0.31mmol) and $4PyPOH_2$ (0.05g, 0.31mmol) were added together in an open vial containing 5 mL of water. The clear solution was stirred at 90° for two hours. After two hours, the solution was gravity filtered to remove any solid impurities and left at room temperature for crystallization. From the solution, crystals suitable for X-ray diffraction

were obtained, m p.: >250°C. Yield: 0.28 g (62%, based on $AlCl_3.6H_2O$), IR (KBr pellets, υ cm^{-1}) 3394(s), 1598(s), 1505(m), 1491(s), 1233(s), 1150(s), 1092(s), 1063(m), 1007(w), 730(m), ^1H NMR (300 MHz, 25°C, D_2O, 25 °C,), δ , 8.59 (s, 2H), 7.95 (s, 2H). $^{31}P\{H\}$ NMR (121 MHz, 25°C, D_2O): δ - 0.168.

4.3.3.3 Synthesis of $[(2PyPOH)_4Al_4(OH_2)_{12}](NO_3)_8.7H_2O$, (16)

In a small scintillation vial, solid $Al(NO_3)_3.9H_2O$ (0.23g, 0.62 mmol) had $2PyPOH_2$ (0.1g, 0.62 mmol) added. Approximately, 1-2 mL of deionized water were added. The reaction was warmed to ~70°C for 30 minutes to allow complete dissolution of the reaction and a clear solution was observed. The reaction mixture was gravity filtered to remove any insoluble impurities. Storage at room temperature for 2 days afforded crystalline material of **16** (0.88 g, 90.7 %). Data Analysis of **16**: m.p. > 250°C, ^1H NMR (300 MHz, 25°C, D_2O, 25 °C), 8.10 (d; J = 6.0Hz, 1H), 8.35 (t; J = 7.5Hz, 1H), 8.65, 8.33 (overlapping doublets), 8.81 (d; J = 6.3Hz, 1H), $^{31}P\{H\}$ NMR (121 MHz, 25°C, D_2O): δ −8.32, −13.99 (br.), Mass spec: m/z; obs, (calc.); M+ 1576.9 (1578.4); M-11H_2O = 1380.5 (1381.5), M-19H_2O -8NO_3^- = 743.6 (740.5); IR (KBr pellets, υ cm^{-1}) 3254(s), 1610(m), 1385(s), 1242 (m), 1179(m), 1163(m), 1088(s), 1002(w), 825(w), 769(w), 728(w). Elemental Analysis: obs. (calc), C 14.3 (15.2), H 3.82 (3.67), N 10.51 (10.64), Crystal Data for **16**: Monoclinic, $P2_1/c$, a = 10.7007(19), b = 24.348(4), c = 25.701(3), β = 114.604(11), V = 608802(16) $Å^3$, Z = 4, F(000) 3184, R indices (all data) R1 = 0.1231, wR2 = 0.1955, Final R indices [I > 2σ(I)], R1 = 0.0618, wR2 = 0.1556.

4.3.3.4 Synthesis of $[(2PyPO)_4(2PyPOH)_2Ga_8Cl_{12}(H_2O)_4(thf)_2][GaCl_4]_2(thf)_8$, (17)

$GaCl_3$ (0.25 g, 1.42 mmol) was weighed in the drybox. Under a nitrogen atmosphere, $2PyPOH_2$, (0.22 g, 1.42 mmol) was added along with 15 mL of thf. An immediate reaction as visible, both reactants dissolved and a pale yellow solution resulted. The solution was stirred at ambient temperature for 16 hours, after which time the solvent was removed in-vacuo affording a foamy solid. The solid was extracted into toluene and filtered under nitrogen. Concentration of the solution to ~10 mL and storage at room temperature for 48 hours

afforded colorless crystals of **17**. Yield: 0.65 g (14%), m.p. 42-43°C. IR (KBr pellets, υ cm^{-1}): 3409(s), 2957(s), 2925(s), 2850(w), 1626(s), 1462(s), 1261(s), 1095(s), 1024(s), 804(s). $^{31}P\{H\}$ NMR (121 MHz, 25°C, $CDCl_3$) -17.7 ppm and a broad peak at -3 to -5 ppm, ^{1}H NMR (300 MHz, 25°C, $CDCl_3$, 25 °C), δ (ppm) 1.78 (m; 2H; thf CH_2; J = 6.5 Hz); 3.68 (m; 2H; thf CH_2O; J = 6.7 Hz), 8.02 (br. s), 8.0 (d; J = 6.0Hz), 7.98 (br. s), 7.2 (br. t), Mass spec: m/z not observed, obs (calc), M -$GaCl_4^-$ -4thf, - $22Cl^-$ = 1895.1 (1892.7), HRMS: m/z not observed, cluster core peak at 1460 (calc. 1461), $Ga_7P_5O_{22}N_3Cl_{12}$, 1532 (1531), $Ga_7P_5O_{22}N_3Cl_{12}$ + thf, 1604 (1605), $Ga_7P_5O_{22}N_3Cl_{12}$ + 2thf, 1677 (1677), $Ga_7P_5O_{22}N_3Cl_{12}$ + 3thf, 1028, (1029) $Ga_7P_5O_{22}N_3Cl_{12}$ - $GaCl_3$, - $GaCl_3$ PO_3. The yield of **17** can be increased by addition of thf to $GaCl_3$ under a nitrogen atmosphere, followed by the solid addition of $2PyPOH_2$. Stirring is maintained at room temperature for 5-6 hours, following filtration of the reaction mixture under anaerobic conditions, crystals of **18** can be obtained from the thf solution at room temperature overnight, yield: 0.9 g, 20%, (of crystalline material).

4.3.3.5 Synthesis of $[(2PyPO)_4(2PyPOH)_2GaCl_{12}(thf)_2(OH_2)_2](NO_3)_2(thf)_9$, (18)

To solid $GaCl_3$ (0.25 g, 1.42 mmol), $Ga(NO_3)_3$ (0.19g. 1.42 mmol) and $2PyPOH_2$ (0.22g, 1.42 mmol) were added under stream of $N_{2(g)}$. Tetrahydrofuran was added and resulted in a yellow colored solution Stirring was maintained for 4 hours after which time the yellow solution was filtered from the white precipitate, concentrated and placed at room temperature. After 24 hours, colorless crystals of **18** were isolated. Yield: 0.49g (12%), m.p. 81-82°C, IR (KBr pellets, υ cm^{-1}): 3452(s), 2972(s), 2926(s), 1748(m), 1612(s), 1451(m), 1385(w), 1262(s), 1029(s), 868(w), 803(s), 625(w). No protons or phosphorus nuclei could be detected by the NMR experiments.

4.3.3.6 Synthesis of $[4PyCH_2POH)Ga(OH_2)_3](NO_3)_2.0.5H_2O\}_x$, 19

In an open scintillation vial, $Ga(NO_3)_3$ (0.15g, 0.66 mmol) and $4PyCH_2PO_3H_2$ (0.11g, 0.66 mmol) were dissolved in ~3 mL H_2O and stirred. The resultant clear reaction mixture was heated to ~85°C for 2 hours, after which time the solution was gravity filtered to remove any impurities. Storage of the clear solution at room temperature for 4 days afforded colorless crystals of **19**. Yield: 0.14g (24% based on $Ga(NO_3)_3$), m.p.120-125°C, IR (KBr

pellets, υ cm^{-1}): 3192(s), 2926(s), 1637(s), 1626(m), 1508(m), 1390(s), 1391(s), 1086(m), 1028(s), 952(m), 822(s), 705(m). ^{1}H NMR (300 MHz, 25°C, $CDCl_3$), δ (ppm), messy proton NMR, broad overlapping aromatic signals, 7.59-7.98, $^{31}P\{H\}$ NMR (121 MHz, 25°C, $CDCl_3$) 11.96 (br.)

Chapter 5

Synthesis of homo and hetero metal-phosphonate frameworks from bi-functional aminomethylphosphonic acid

5.1 Introduction

Bi-functional phosphonic acids are of particular interest as the presence of a secondary functional group extends the versatility of metal phosphonates to new and more selective applications and can result in a more porous materials.[186] To the best of our knowledge, the coordination properties of aminomethylphosphonic acid (ampa) have rarely been studied,[187] although diphosphonic acids with amino groups are known to be good chelating agents and have been well researched.[188] Continuing with our research using phosphonic acids,[189] ampa was prepared to examine how the presence of a secondary functional group will affect the structural motif of the metal phosphonate product. The presence of two different functional groups provides numerous chelation modes, Figure 5.1, and we were keen to explore whether this bi-functional ligand could be used to prepare mixed metal polymers. Herein we report the aqueous phase synthesis and characterization of metal phosphonate frameworks from reactions of aminomethylphosphonic acid with metallic precursors of Zn, Cd, Hg, Pb, Ag and Cu.

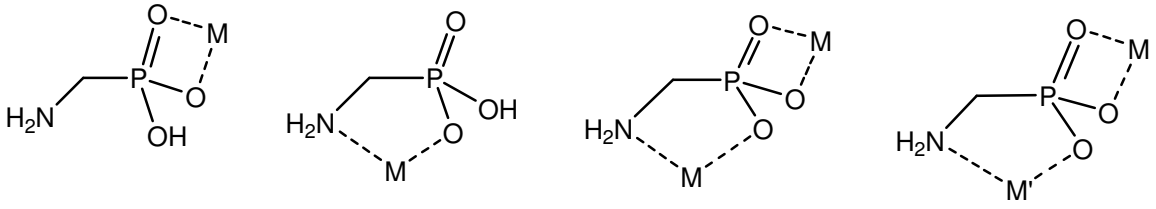

Figure 5.1 Possible co-ordination modes of aminomethylphosphonic acid (ampa)

5.2 Results and discussion

In contrast to traditional hydrothermal methods, we wished to examine the outcome of reactions performed under aqueous conditions at room temperature or with gentle heating. The stoichiometric reactions of aminomethylphosphonic acid (ampa) with $ZnCl_2$, $Cd(NO_3)_2$, $Pb(NO_3)_2$, $Hg(NO_3)_2$, $Ag(SO_3CF_3)$, $AgNO_3$ and $Cu(SO_3CF_3)_2/AgNO_3$ afford a series of two

dimensional polymeric structures **20**-**27**, respectively, scheme 5.1. Complexes **20**-**27** have varied structural motifs ranging from interlinked 12 membered cyclic cores of a zinc chloride phosphonate polymer, **20**, distorted cross linked hexagonal pores of cadmium, **21**, and lead, **22**, a two-dimensional mercury polymer, **23**, with two different mercury environments and a series of complex two-dimensional silver polymers with argentophilic interactions, **24**-**26**. More interestingly, a silver/copper bimetallic framework was isolated from the stoichiometric reaction of ampa with copper triflate and silver nitrate, **27**.

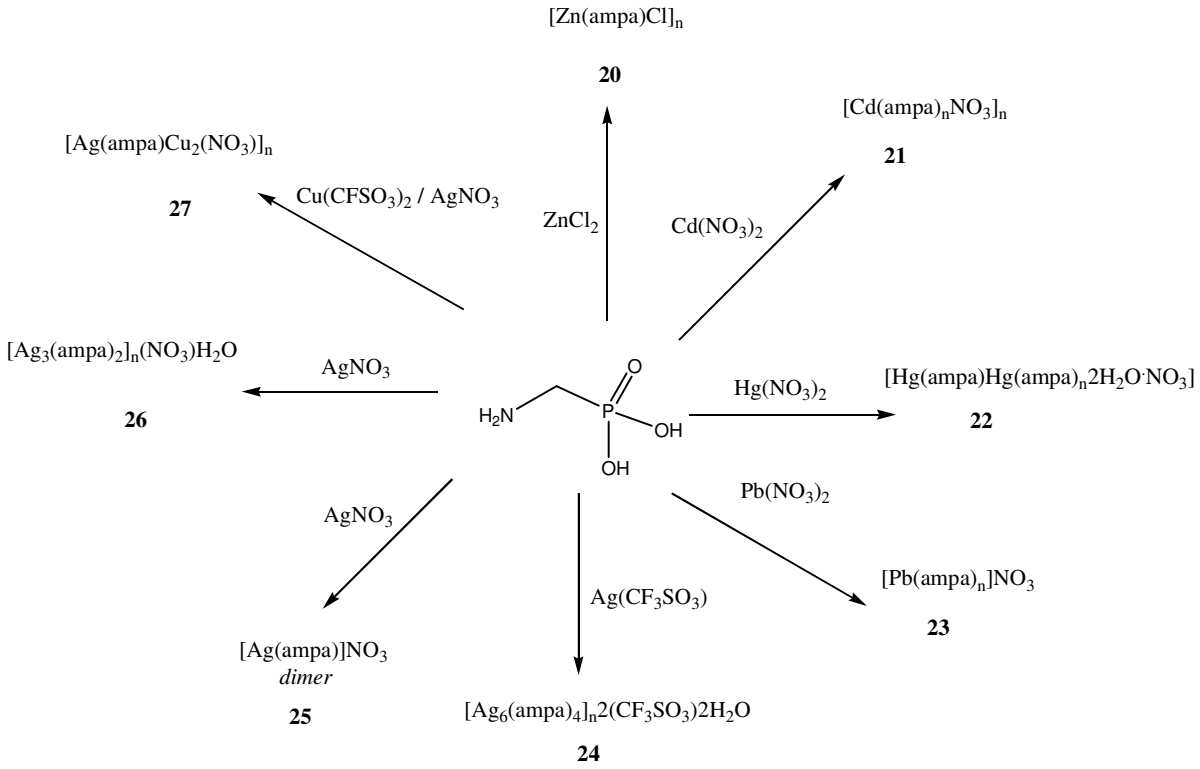

Scheme 5.1 Summary of the reactions of ampa with metal precursors.

5.2.1 Discussion of $[Zn(ampa)Cl]_n$, (20)

The reaction of zinc(II) chloride with aminomethylphosphonic acid (ampa) afforded colorless, monoclinic crystals, (space group $P2_1/c$) of complex **20** in 52% yield, Figure 5.2. Crystallographic analysis revealed the presence of a zinc bi-dimensional framework with each zinc atom in a distorted tetrahedral environment formed by three oxygen atoms from different ampa molecules and one chlorine atom.

The phosphonate group of ampa is doubly deprotonated, but protonated at the amine nitrogen, therefore existing in its zwitterionic form. The existence of the zwitterionic form of the ligand is not too surprising given that a large volume of research has been devoted to employing amines as templating agents for zinc phosphates and phosphonates in which the amines are used for deprotonation of the phosphonic acid and stabilization of the framework through hydrogen bonding.[190] The Zn-O distances are in the range 1.932(2)-1.965(2)Å with each oxygen atom on the phosphonate group coordinated to three different zinc atoms. This arrangement affords tetrahedral units of $[ZnClO_3]$ and $[PCO_3]$ that share common corners creating 12-membered $[Zn\text{-}O\text{-}P\text{-}O]_3$ units that are a common feature of zinc phosphonate polymers.[191] The structural motif of **20** is reminiscent of the zinc chlorophosphonate polymer, $[C_6NH_{14}][ZnClHPO_4]$, prepared by hydrothermal methods and like complex **20** has chlorine atoms perpendicular to the Zn-O-P units.[192] Around every 12-membered unit, a regular symmetrical arrangement can be seen in which the flanking amino groups are arranged on one side of the cyclic core, while on the flip side terminal halides are observed (Figure 5.2).

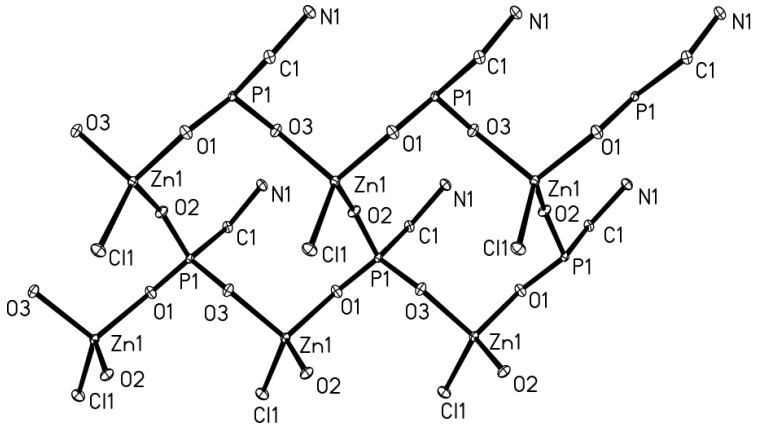

Figure 5.2 Thermal ellipsoid plot of the structural motif of **20**. Hydrogen atoms are omitted for clarity, thermal ellipsoids at 30% probability level

The amine-amine and chloride-chloride separation is ~4.76 Å. The structure shows hydrogen bonding between the chlorine atoms and the amino nitrogen atoms, as well as between one of the amine hydrogen atoms and O(2) of the phosphonate group. The absence

of solvent molecules in **20** affords a thermally stable polymer that has no solvent accessible voids and decomposes at 220-222^{o}C. The thermal stability is confirmed by thermogravimetric analysis (TGA) where minimal weight loss (0.49%) is observed from 50 to 200^{o}C, followed by a sharp weight loss, corresponding to decomposition of the ligand.

5.2.2 Discussion of $[Cd(ampa)NO_3]_n$, (21)

Under similar conditions to the synthesis of **20**, polymer **21** (Figure 5.3) was isolated from the 1:1 reaction of ampa and cadmium(II) nitrate. The cadmium halide precursor was exchanged for the nitrate salt because following the structural analysis of **20** it was thought that the terminal halide was limiting polymer dimensionality, thus employing the coordinating nitrate anion may lend itself to higher dimensional structures.

The isolated 2D cadmium phosphonate polymer displays the cadmium atom in a distorted octahedral coordination sphere consisting of cadmium atoms bonded to an oxygen atom from a nitrate ion and two oxygen atoms from the phosphonate group of the ampa ligand. The symmetry-related equivalents of these oxygen atoms make up the slightly distorted octahedral arrangement. The distortion is attributed to the steric constraints that are imposed by the small bite angle of the ampa group and its limited flexibility.

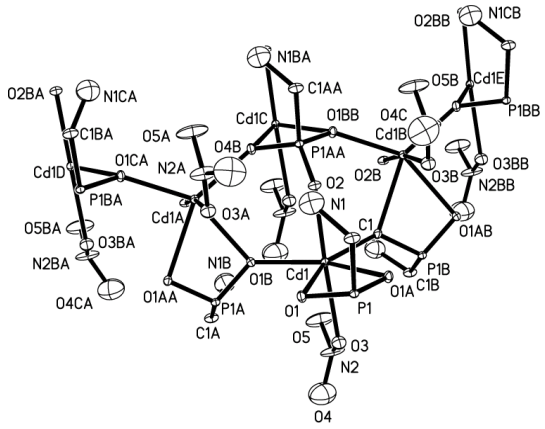

Figure 5.3 Polymeric form of **21**. H atoms are omitted for clarity. Selected bond lengths (Å) and angles (^{o}): Cd(1)-O(1) 2.419(3), Cd(1)-O(2) 2.313(5), Cd(1)-O(3) 2.379(6), Cd(1)-P(1) 3.0002(17), P(1)-O(1) 1.531(3), O(2)-Cd(1)-O(3) 169.93(18), O(2)-Cd(1)-O(1) 87.97(13).

The change from tetrahedral geometry observed around Zn^{2+} in **20** to octahedral geometry around Cd^{2+} in **21** is likely to be associated with the size effect comparing the ionic radii of Zn^{2+}(0.74Å) and Cd^{2+}(0.97Å).[193] The cadmium polymer, **21**, displays three different Cd-O bond lengths, all within expected ranges,[194] and also includes a Cd-P interaction at a distance of 2.9999(12)Å, which is within the sum of their van der Waals radii (3.38Å).[194d] The oxygen atom, O(4), and the amino nitrogen atom have disorder associated with a mirror plane but were satisfactorily refined at half occupancy. The longest Cd-O bond at 2.420(2)Å corresponds to the shortest P-O bond (1.514(3)Å). For charge balance the ligand is doubly deprotonated which is reflected by the P-O bond lengths of P(1)-O(1) and P(1)-O(1A) at 1.528(2)Å, which results in the zwitterionic form of the ligand, with protonation at the nitrogen atom, N(1). The hydrogen atoms on the nitrogen atom were located from the residual electron density difference map, using the non centro-symmetric space group, Pn*a*2_1.[195] The unique environment for the phosphorus atoms is confirmed by the presence of a single peak at 12.30 ppm in the ^{31}P NMR solution experiment, which can be compared to that of the free ligand, that has a ^{31}P chemical shift at 11.49 ppm. The presence of only one peak in the ^{31}P NMR suggests that the polymer remains intact in solution. In cases where ligand loss occurs coinciding with polymer decomposition, usually several peaks are observed in the spectrum. Solid-state infrared spectroscopy revealed strong absorptions in the 1000-1200cm^{-1} corresponding to P=O and P-O stretching vibrations.[196] The cadmium phosphonate polymer is thermally robust, not melting at 250^{o}C. TG analysis confirms this, with negligible weight loss from 50 to 300^{o}C.

5.2.3 Discussion of [Hg(ampa)Hg(ampa)$_n$2H_2O.NO_3], (22)

Mercury(II) as a typically soft cation prefers coordination to soft nitrogen atoms.[197] Given the bi-functional nature of ampa we wished to explore the reaction of ampa with $Hg(NO_3)_2$; firstly, to determine the coordination preference of Hg(II) for comparison with Cd(II) and Zn(II), but also because reports on mercury(II) phosphonates are disproportionately sparse when compared with that of other metals.[198] This paucity is likely to be due to the low solubility of mercury salts and the difficulty in isolating suitable single crystals for X-ray diffraction.[199] From the equimolar reaction of $Hg(NO_3)_2$ with ampa, colorless crystals of a 2D mercury polymer were isolated in 21% yield (Figure 5.4).

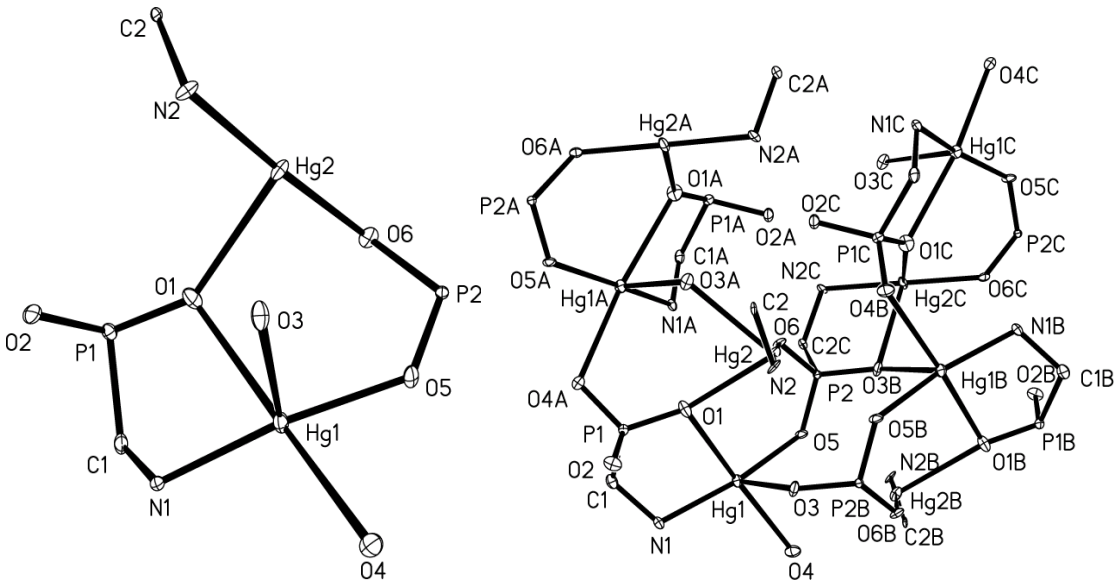

Figure 5.4 Left, solid-state diagram of **22** depicting the atom connectivity. Right, polymeric structure of **22**. Selected bond lengths (Å) and angles (1): Hg(1)-O(1) 2.589(8), Hg(1)-O(3) 2.473(8), Hg(1)-O(4) 2.526(7), Hg(1)-O(5) 2.117(7), Hg(1)-N(1) 2.144(8), Hg(2)-O(1) 2.542(7), Hg(2)-O(6) 2.059(7), Hg(2)-N(2) 2.103(8), P(1)-O(1) 1.513(8), P(1)-O(2) 1.538(8), P(2)-O(5) 1.528(7), P(2)-O(6) 1.537(7), O(5)-Hg(1)-N(1) 164.9(3), N(1)-Hg(1)-O(1) 77.3(3), O(4)-Hg(1)-O(1) 170.9(2), O(6)-Hg(2)-N(2) 176.4(3), O(6)-Hg(2)-O(1) 80.7(3).

The mercury polymer, $[Hg(ampa)Hg(ampa)_n2H_2O.NO_3]$, differs from the previous zinc, **20**, and cadmium, **21**, polymers, because in **22**, one ampa molecule is found to bridge two mercury centers with one mercury atom coordinated to the amine group, while a second mercury center is coordinated to the phosphonate oxygen atoms, (Figure 5.4). An interesting feature of this polymer is that the mercury atoms are in two very distinctive environments. In one case, the mercury atom, Hg(1), is five coordinate, with the sites occupied by a nitrogen atom from an amine group and μ2 oxygen atoms from the ampa. This type of geometry is a common occurrence for mercury complexes.[195] The second environment found for mercury is less often observed[196] and Hg(2) has seesaw geometry, with the N(2)-Hg(2)-O(6) angle, close to linear (176.6(3)). The coordination sphere around Hg(2) consists of a nitrogen atom

and two bridging oxygen atoms from the phosphonate group. The uncoordinated oxygen O(2) atom on P(1) remains protonated, as evidenced by the longer P-O bond of 1.538(8)Å. The net charge of the framework is balanced by the presence of guest nitrate ions in the lattice. The Hg-O bonds vary from 2.117(7) to 2.656(7)Å with those at the longer end substantiating the presence of a weak interaction. The Hg-N bonds average (2.123Å) correspond well to documented Hg-NH_2 interactions.[200] A distance of 3.860Å separates the mercury atoms, which is longer than the sum of their van der Waals radii (rrdW = 1.73Å).[198] Interestingly, despite the different mercury environments, the phosphorus atoms exist in almost identical environments with similar bond lengths and angles. The mercury phosphonate, **22**, has moderate solid-state thermal stability melting at 150-152^{o}C. TGA confirmed this with sharp weight loss (56.4%) between 176 and 180^{o}C corresponding with decomposition of the polymer. In solution the mercury phosphonate has lower stability, with mercury deposition observed at 80-85^{o}C. Following our initial success with the heavier transition metal atoms, we wished to continue the investigation and employed lead nitrate as a possible metallic precursor for comparison with the common oxidation state (2+) of Zn, Cd, and Hg. Furthermore, studies have shown that Pb(II) exhibits different structural chemistry from those of the 2+ transition metals due to the presence of the lone pair of electrons.[201,202] This hypothesis was tested by the aqueous, stoichiometric reaction of $Pb(NO_3)_2$ and ampa.

5.2.4 Discussion of $[Pb(ampa)_n]NO_3$, (23)

The 1:1 aqueous reaction of $Pb(NO_3)_2$ and ampa afforded, **23** (Figure 5.5), a 2D lead phosphonate polymer. It is noteworthy to mention that although lead phosphonates have been previously reported the majority of these are prepared using harsh hydrothermal methods,[203] which can be contrasted to the aqueous synthesis of **23**. Solid state analysis revealed that each lead atom is five coordinate in distorted square pyramidal geometry with oxygen atoms at each vertex and the open side of the pyramid occupied by a lone pair of electrons. The electrostatic repulsions of the lone pair leads to the distorted geometry. The Pb-O distances are in the range 2.356(6)-2.716(6) Å and are comparable with related systems. The Pb-Pb separation of ~4.61Å is too long for any metal-metal interaction.[204] In a similar fashion to the zinc and cadmium polymers, the ampa ligand exists in its zwitterionic form with the phosphonic acid oxygen atoms doubly deprotonated and a protonated NH_2 group. The charge

is balanced by the presence of lattice nitrate ions. A further similarity between the cadmium and lead polymers is the metal-phosphonate repeating unit, which consists of distorted hexagonal-shaped rings, as depicted in Figure 5.5.

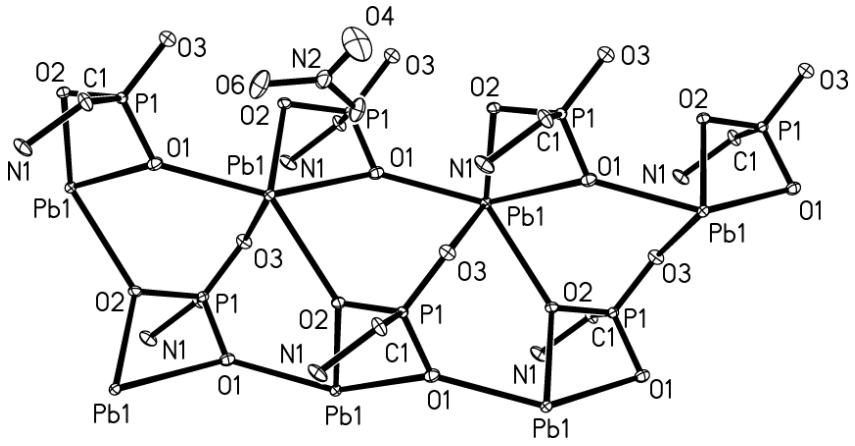

Figure 5.5 Polymeric arrangement of **23**, (thermal ellipsoids at 30% probability level). H atoms are omitted for clarity.

5.2.5 Discussion of $[Ag_6(ampa)_4]_n2(CF_3SO_3).2H_2O$, (24)

Continuing with the exploration of the late transition metals, polymer **24** was obtained from the reaction between silver triflate and ampa in a 1:1 molar ratio. Silver amino phosphonate polymers appear less well characterized than other transition metals, in fact, a survey of the CCDC revealed only one, from the reaction of silver nitrate with N-phosphonomethyl glycine.[205] Complex **24** crystallizes as colorless needles in the triclinic space group, Pī (Figure 5.6). Solid-state analysis of **24** shows six silver atoms in the asymmetric unit, each adopting five coordinate geometry. Four ampa molecules support these six silver atoms, and two triflate anions in the lattice balance the cationic metal charge. The three oxygen atoms on each of the four ampa molecules all coordinate to different silver atoms; for example, the three oxygen atoms on P(1) coordinate to Ag(6), Ag(2), and Ag(1) through O(1), O(2), and O(3), respectively. The phosphorus-oxygen bond lengths are varied, ranging from 1.504(6) to 1.537(5) Å. It is possible that some of the P-O bonds remain protonated, however, no hydrogen atoms for these oxygen atoms could be located. The repeating unit of polymer **24**, consists of a 'silver column' that is generated through edge-

sharing triangles, (Figure 5.7). Similar arrangements of Ag atoms have been observed but most of these are in cages and clusters rather than a polymeric system.[206] The Ag-Ag bonds are in the range 2.9181-3.1642Å that are suggestive of argentophilic interactions.[207] The existence of these argentophilic interactions prompted us to investigate the luminescence of this system. Luminescence of Ag-Ag compounds is a well-known phenomenon, that in part is attributed to the existence of argentophilic interactions.[208] The solution state luminescence was probed at various excitation wavelengths; however, no luminescence was observed and it is possible that low-temperature measurements are required. The presence of non-coordinating guest ions reduce the thermal robustness of the system with complex **24** melting at 140-142^{o}C. However, their presence does promote extensive hydrogen bonding which can be observed between the NH_2-triflate groups, and the phosphonate oxygen atoms with adjacent NH_2 groups. The decreased thermal robustness of **24** is evidenced from TGA data that showed 1.28% weight loss from 117 to 180^{o}C, which is close to the loss of H_2O, theoretical value =1.25%. Broad IR adsorption bands are observed at 3451 cm^{-1} confirming the presence of lattice water molecules.

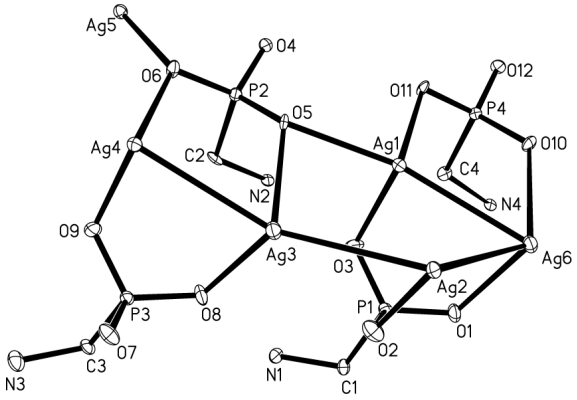

Figure 5.6 Asymmetric unit of **24**, (ellipsoids at 30% probability level), triflate anions, H atoms and lattice water molecules are omitted for clarity. P(1)-O(1) 1.502(6), P(1)-O(2) 1.526(6), P(1)-O(3) 1.518(5), Ag(1)-O(3) 2.224(5), Ag(2)-O(2) 2.184(6), Ag(2)-O(4) 2.514(5), O(3)-Ag(1)-O(5)#3 85.62(19), O(8)-Ag(3)-O(5) 104.81(18), O(6)-Ag(4)-O(9) 105.72(19)

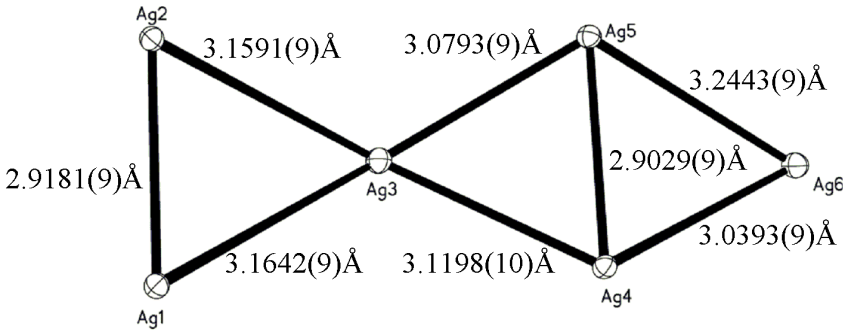

Figure 5.7 Arrangement of silver atoms in **24**.

5.2.6 Discussion of $[Ag(ampa)]NO_3$, (25) and $[Ag_3(ampa)_2]_n(NO_3)H_2O$, (26)

Following the isolation of polymer **24** that has lattice triflate ions, we wished to investigate whether more porous and robust materials could be obtained through exchange of the metal precursor. Because the presence of solvent molecules and anions in the crystalline lattice can limit porosity,[209] in order to harness any future potential applications we wished to investigate the reactions of ampa with a series of silver precursors. The reaction of silver nitrate with ampa (1:1) afforded two different products, a monomeric Ag-ampa complex, **25** (Figure 5.8) and a silver phosphonate polymer, **26** (Figure 5.9).

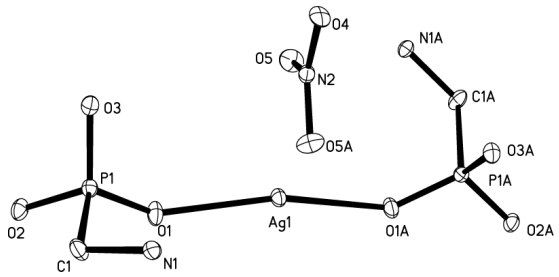

Figure 5.8 Coordination environment of silver in **25**. Hydrogen atoms are omitted for clarity. Thermal ellipsoids drawn at 30% probability level. Selected bond lengths (Å) and angles (^{o}): Ag(1)-O(1) 2.320(3), P(1)-O(1) 1.498(3), P(1)-O(2) 1.568(3), P(1)-O(3) 1.502(3), O(1)-Ag(1)-O(1A) 162.56(14), O(3)-P(1)-O(1) 115.83(17).

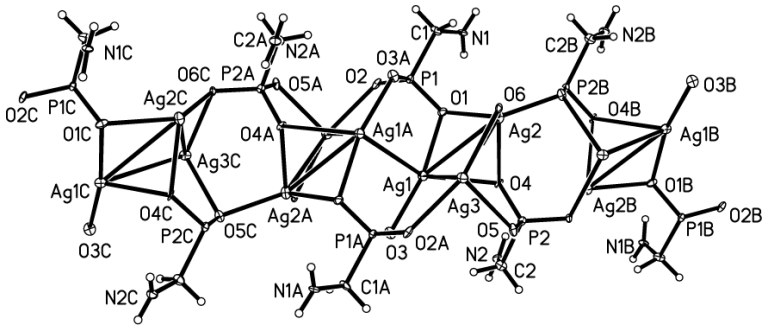

Figure 5.9 Polymeric structure of **26**, thermal ellipsoids at 30% probability level.

These two compounds were obtained from the same reaction vial and were identified under the microscope as two different crystal types. Attempts to separate them by recrystallization were unsuccessful, as were attempts to optimize the yield of each product through reaction temperature. The reaction was performed at room temperature, low temperature (0°C), and high temperature (100°C) but we were only able to obtain a mixture of the same two products. To determine which is the major product the reaction was repeated several times and the crystals were separated by hand using the microscope. In all cases, polymeric **26** was found to be the major product, 78-83%. The major product of the reaction, complex **26** crystallizes in monoclinic space group C2/*c* and the single-crystal analysis revealed a polymeric species displaying a triangular arrangement of silver atoms, each in distorted octahedral environment with argentophilic interactions (Figures 5.9 and 5.10).

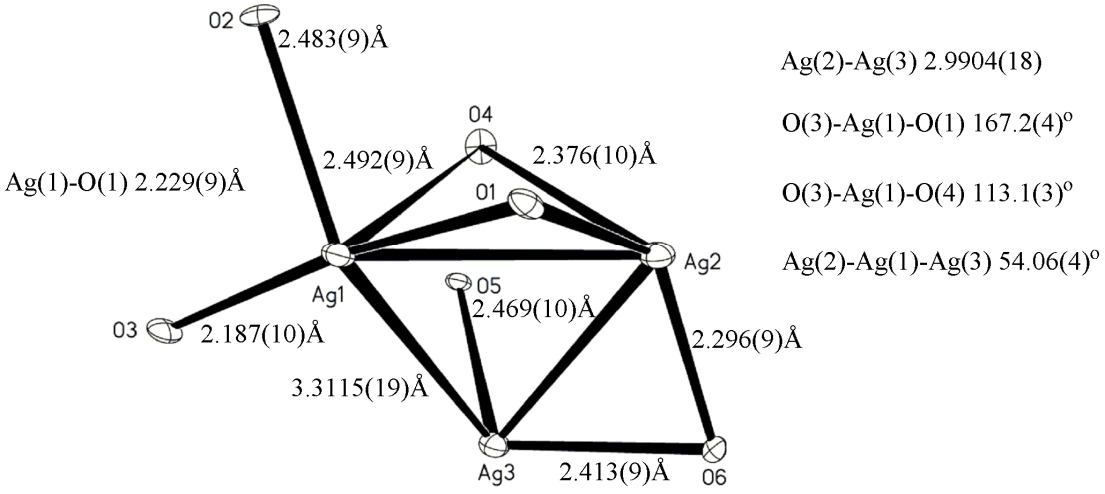

Figure 5.10 Diagram to depict coordination environment, bond lengths (Å) and angles (°) of the silver atoms in **26**. Thermal ellipsoids are drawn at 30% probability level.

The asymmetric unit in **26** has three crystallographically unique silver atoms coordinated to two ampa ligands with a lattice nitrate ion and one molecule of water. Each silver atom is found to adopt seven coordinate geometry with sites occupied by four oxygen atoms and three different silver atoms with Ag-Ag distances in the range 2.997-3.268Å (Figure 5.10). The triangular arrangement of silver atoms observed in **26** is not uncommon for silver coordination polymers with many examples reported with similar Ag-Ag bond lengths to those recorded in **26**.[210]

After considering the various possible coordinate modes of ampa including the N-Hg coordination observed for mercury, we wished to explore the viability of this bi-functional phosphonic acid for bimetallic phosphonate syntheses. We anticipated that through careful selection of the metal precursor, ampa could be used to coordinate different metal centers through both the NH_2 and phosphonate group. To this end, ampa was reacted with silver nitrate and copper(II) triflate in a 1:1:1 ratio and afforded crystalline material of a bimetallic framework: $[Ag(ampa)Cu_2(NO_3)]_n$, **27**. Polymer **27** joins a fairly limited number of structurally characterized bimetallic polymers (Figures 5.11 and 5.12). [211]

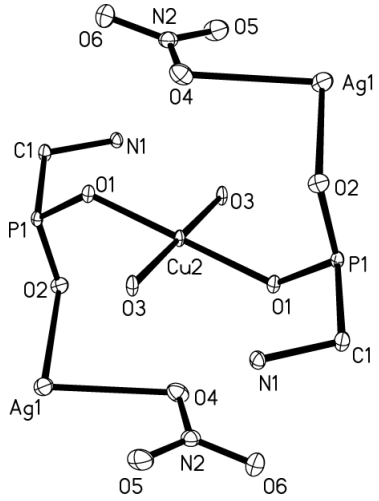

Figure 5.11 Coordination environments of silver and copper in $[Ag(ampa)Cu_2(NO_3)]_n$, **27**. Selected bond lengths (Å) and angles (°). Cu(2)-O(1) 1.938(2), Cu(2)-O(3) 1.9482(19), P(1)-(O1) 1.536(2), P(1)-(O2) 1.515(2), Ag(1)-O(2) 2.353(2), Ag(1)-O(4) 2.513(3), O(1)-Cu(2)-O(1) 180.0, O(3)-Cu(2)–O(3A) 90.51(8), O(2)-Ag(1)-O(4) 85.71(8), O(1)-Cu(2)-O(3) 89.49(8).

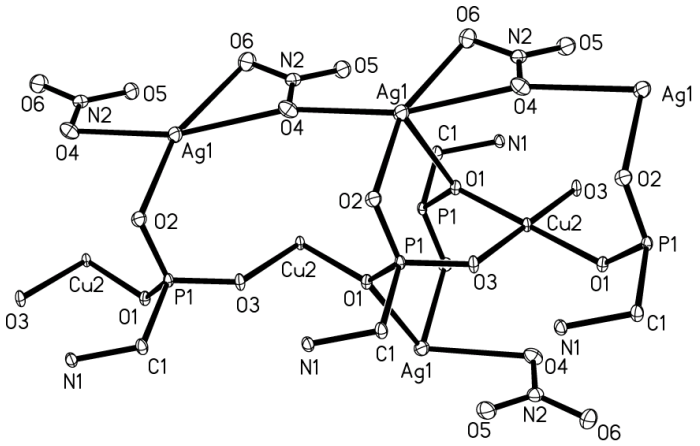

Figure 5.12 Polymeric arrangement of the bimetallic phosphonate, **27**. Hydrogen atoms are omitted for clarity. Thermal ellipsoids drawn at 30% probability level.

Examination of the crystal structure showed that the silver atoms exhibit square pyramidal geometry while the copper atoms are found in square planar geometry. The oxygen atoms coordinated to the silver atom arise from nitrate anions coordinating in a μ2 and μ1 fashion. The phosphonate oxygen atoms, O(1) and O(2), bridge the Ag and Cu atoms. The Ag-O and Cu-O distances are as expected and are in the range 2.353-2.585 and 1.938(2)-1.950(2)Å, respectively.[212] The overall 3+ charge from the metal atoms, is balanced by a doubly deprotonated phosphonate group and a nitrate anion. Hydrogen bonding can be observed between the amine group, N(1)-H(1), and O(3) of the phosphonate moiety (dH···A(A = acceptor), 2.01Å, dD(D = donor)···A, 2.863(3)Å).

5.3 Conclusions

As a result of exploring the chemical behavior of aminomethylphosphonic acid in reactions with different metal salts, it was possible to isolate eight novel metal phosphonate frameworks. These frameworks display specific geometrical characteristics according to the particular stereochemical requirements of the metallic center, the organic ligand and in some cases, the presence of counterions. For example, it was possible to isolate different frameworks having different divalent cations (Zn, Cd, Hg and Pb) displaying the metallic centers in different geometries. These reactions were performed in aqueous media and allowed the study of the zwitterionic behavior of the ampa ligand. The effect of the counterions was analyzed in correspondence with their ability to stabilize the net charge of the synthesized frameworks and in their ability to affect the pore size of the corresponding MOFs. It was possible to recognize that the nitrate ion can display direct coordination to the metallic center allowing the creation of novel architectures. In contrast, the triflate ion has no presence in the coordination sphere of the used metallic centers but has participation in the electrostatic stabilization of the frameworks as well as in modulation of the pore size. In some cases it is possible to find these anions inside the open spaces of the synthesized frameworks.

Given the structural flexibility and the variety of possible coordination modes that the ampa ligand can offer it was possible to isolate a heterometallic phosphonate framework containing the copper and silver atoms in different coordination environments. This result can allow us to evaluate the potential of this bimetallic framework for its use in the development of metalphosphonate materials with optical properties.

Future work will involve the further study of bimetallic phosphonate polymers based in the proper choice of metal precursors and whether extending the length of the carbon chain to aminoethylphosphonic acid or aminopropyl phosphonic acid will lead to more porous structures.

5.4 Experimental

Materials and methods: Aminomethylphosphonic acid was prepared using modified literature methods.[160] Other materials were purchased from Aldrich and used as received. IR spectra were recorded from KBr pellets on a FT-IR spectrometer. Thermogravimetric analysis (TGA) were carried out on a Seiko 220 instrument at a heating rate of 5^{o}C/ min. ^{1}H, ^{31}P{H} were recorded in solution on a Varian Mercury 300 NMR spectrometer. No meaningful ^{13}C data could be collected. Fluorescence was recorded using a Shimadzu 5301PC spectrofluorimeter at ambient temperature. Elemental Analysis was performed by Schwarzkopf Microanalytical Lab, N.Y and was determined for all complexes excluding **25** and **26**.

5.4.1 Synthesis of $[Zn(ampa)Cl]_n$, (20)

Aminomethylphosphonic acid (0.1g, 0.9 mmol) and zinc(II) chloride (0.12g, 0.9 mmol) were added together in an open vial containing 3 mL of water. The reaction mixture was stirred and heated at 70^{o}C for 1 hour. After 1 hour, the reaction mixture was filtered to remove any insoluble material. The final pH of the solution was 3. Colorless crystals suitable for X-ray crystallography analysis were obtained by slow evaporation from the colorless solution at ambient temperature. Yield: 0.092g (52% based on $ZnCl_2$), m.p. 220-222^{o}C (decomposition). IR (KBr pellet, υ cm^{-1}): 3565(s), 3478(s), 3215(s), 3143(s), 2957(m), 2930(m), 2900(w), 1625(m), 1480(s), 1421(s), 1382(m), 1252(s), 1192(s), 1105(s), 1051(s), 835(m), 797(m), 741(s), 700(m). ^{1}H-NMR (D_2O, 300MHz, 25^{o}C) (d, 2H, 3.05ppm, 12.6Hz). ^{31}P-NMR 12.16 ppm (s).

5.4.2 Synthesis of $[Cd(ampa)NO_3]$, (21)

Aminomethylphosphonic acid (0.05g, 0.51mmol) and cadmium(II) nitrate (0.14g, 0.51mmol) were added together in an open vial containing 3 mL of water. The reaction mixture was stirred and heated at 100^{o}C for 1 hour. After 1 hour, the reaction mixture was filtered and the pH recorded, (pH = 3). Suitable crystals for X-ray crystallography were obtained from the solution. Yield: 0.036g (27% based on $Cd(NO_3)_2$). The product has a melting point above 250^{o}C. IR (KBr pellet, υ cm^{-1}): 3561(m), 3478(m), 3238(s), 3094(m), 2805(m), 2698(m), 2611(m), 2565(m), 2344(w), 2128(w), 1622(m), 1606(s), 1523(s),

1523(s), 1363(s), 1252(m), 1191(s), 1101(s), 865(w), 827(m), 816(m), 739(s). ^{1}H-NMR (D_2O, 300MHz, 25^{o}C): (d, 2H, 3.07ppm, 12.6Hz). ^{31}P-NMR 12.29 ppm (s).

5.4.3 Synthesis of [Hg(ampa)Hg(ampa)$_n$2H$_2$O.NO$_3$], (22)

Aminomethylphosphonic acid (0.05g, 0.52mmol) and mercury(II) nitrate (0.13g, 0.52mmol) were dissolved in 3 mL of water. The reaction mixture was stirred and heated at ~ 100^{o}C for 1 hour after which time the clear reaction mixture was gravity filtered. The final pH of the solution was 3. Suitable crystals for X-ray crystallography were obtained from the solution. Yield: 0.12g (21% based on $Hg(NO_3)_2$), m.p. 150-152^{o}C. IR (KBr pellet, υ cm^{-1}): 3120(m), 2903(s), 2618(m), 1633(m), 1528(m), 1384(s), 1165(s), 1108(s), 1032(s), 931(s), 865(m), 827(s), 727(s). ^{1}H-NMR: (D_2O, 300MHz, 25^{o}C) 3.06 ppm (d, 2H, J = 12.6Hz), ^{31}P-NMR 11.99 ppm (s).

5.4.4 Synthesis of [Pb(ampa)$_n$]NO$_3$, (23)

Aminomethylphosphonic acid (0.05g, 0.51mmol) and lead(II) nitrate (0.15g, 0.51mmol) were added together in an open vial containing 2 mL of water. The reaction mixture was stirred and heated at 100^{o}C for 1 hour. After 1 hour, the reaction mixture was filtered and the pH recorded, pH = 3. Suitable crystals for X-ray crystallography were obtained from the solution. Yield: 0.054g (18% based on $Pb(NO_3)_2$), m.p. 200-202^{o}C. IR (KBr pellet, υ cm^{-1}): 3432(m), 2921(s), 2622(m), 1774(w), 1639(s), 1561(m), 1504(m), 1382(s), 1226(w), 1169(m), 1029(s), 952(m), 930(w), 827(w), 800(w), 724(s). ^{1}H-NMR: (D_2O, 300MHz, 25^{o}C) (d, 2H, 3.03 ppm, 12.6Hz). ^{31}P-NMR 12.05ppm (s). TGA measurements recorded minimal weight loss from 50–400^{o}C.

5.4.5 Synthesis of [Ag$_6$(ampa)$_4$]$_n$2(CFSO$_3$).2H$_2$O, (24)

Aminomethylphosphonic acid (0.05g, 0.51mmol) and silver triflate (0.12g, 0.51mmol) were added together in an open vial covered with aluminum foil containing 3 mL of water. The reaction mixture was stirred and heated at 100^{o}C for 1 hour. After 1 hour, the reaction mixture was filtered. The final pH of the solution was 1. Suitable crystals for X-ray crystallography were obtained from the solution. Yield: 0.24g (32% based on Ag triflate). The product decomposes between 140-142^{o}C. IR (KBr pellet, υ cm^{-1}) 3451 cm-1 (m),

3197(m), 2927(s), 2609(w), 1635(m), 1518(m), 1437(w), 1259(s), 1171(s), 1034(s), 938(w), 809(w), 723(m), 645(s), 579(m), 518(s) ^{1}H-NMR (D_2O, 300MHz, 25^{o}C): 3.11 ppm, (d, J = 12.9Hz); ^{31}P-NMR 12.4 ppm (s).

5.4.6 Synthesis of $[Ag(ampa)]NO_3$, (25), and $[Ag_3(ampa)_2]_n(NO_3)H_2O$, (26)

Aminomethylphosphonic acid (0.1g, 0.9mmol) and silver nitrate (0.15g, 0.9mmol) were added together in an open vial covered with aluminum foil containing 3 mL of water. The reaction mixture was stirred and heated at 100^{o}C for 1 hour. After 1 hour, the colorless reaction mixture was filtered. X-ray quality crystals were obtained from slow evaporation of the solution. Yield: 0.11 g of crude product, m.p. 180-191^{o}C. ^{1}H-NMR (D_2O, 300MHz, 25^{o}C): 3.09 ppm, (d, 2H, J = 12.6Hz); ^{31}P-NMR: 12.0 ppm (s).

5.4.7 Synthesis of $[Ag(ampa)Cu_2(NO_3)]_n$, (27)

Aminomethylphosphonic acid (0.06g, 0.51mmol), silver nitrate (0.09g, 0.51mmol) and copper(II) triflate (0.1g, 0.3mmol) were added together in an open vial covered with aluminum foil. The reaction mixture was stirred and heated and 100^{o}C for 1 hour. After 1 hour, the reaction mixture is filtered and the solid residue discarded. From the solution, (*p*H = 1) suitable crystals for X-ray crystallography were obtained. Yield: 0.04g, (13% based on ampa), m.p. 190-192^{o}C (decomp). IR (KBr pellet, υ cm^{-1}): 3515(s), 3398(s), 3084(s), 1610(m), 1514(s), 1353(s), 1252(s), 1175(s), 1119(m), 1087(s), 1030(s) 1256(w), 768(w), 732(m), 645(s), 581(m), 517(s), 467(m). No signals were detected in the ^{1}H-NMR experiment or the ^{31}P-NMR experiment. TGA data: weight loss between 145-150^{o}C % weight loss in this temperature range = 21.8%, corresponding to the loss of two nitrate ions and one water molecule. To confirm the presence of the bimetallic framework in the crude product, energy dispersive X-ray (EDX) analysis was performed and confirmed the presence of both copper and silver. Sulfur contamination from the triflate precursor was also observed.

Table 5.1 Crystal Data for compounds **20-22**

Compound name	$[Zn(ampa)Cl]_n$, **20**	$[Cd(ampa)_nNO_3]$, **21**	$[Hg(ampa)Hg(ampa)_n2H_2O.NO_3]$, **22**[a]
Chemical formula	$C_1H_4ClNO_3PZn$	$CH_6CdN_3O_7P$	$C_2H_9N_3O_{10}P_2Hg_2$[a]
Formula weight	209.86	315.46	698.24
Crystal system	Monoclinic	Orthorhombic	Monoclinic
Space group	$P2_1/c$	P*nma*	C2/*c*
T (K)	213(2)	213(2)	213(2)
a (Å)	4.7551(6)	19.995(3)	23.418(3)
b (Å)	15.6652(19)	6.2770(10)	10.5542(12)
c (Å)	8.1084(9)	5.1508(8)	10.1938(12)
α (°)	90	90	90
β (°)	107.225(6)	90	108.855(2)
γ (°)	90	90	90
V ($Å^3$)	576.90(12)	646.46(18)	2384.2(5)
Z	4	4	8
Reflections collected	3228	3613	6557
Independent reflections	1309	831	2782
Data/restraints/parameter ratio	1309/0/73	831/4/85	2782/5/167
Unique data (R_{int})	0.0319	0.0345	0.0433
D_{calc} (mg/m^3)	2.416	3.241	3.890
F(000)	412	608	2496
R indices (all data)	R1 = 0.0339, wR2 = 0.0755	R1 = 0.0379, wR2 = 0.0995	R1 = 0.0568 wR2 = 0.1101
Final R indices [I >2σ(I)]	R1 = 0.0298, wR2 = 0.0729	R1 = 0.0367, wR2 = 0.0986	R1 = 0.0401, wR2 = 0.0997
Largest difference in peak and hole (e $Å^{-3}$)	0.811 and -0.844	1.163 and -1.054	3.142 and -3.630[b]

[a] H atoms that were not included in the refinement are not included in the chemical formulas.
[b] The large electron density peaks remaining are close in proximity to the heavy metal atoms.

Table 5.2 Crystal Data for compounds **23**-**25**

Compound name	$[Pb(ampa)_n]NO_3$, **23**	$[Ag_6(ampa)_4]_n2(CF_3SO_3).2H_2O$, **24**	$[Ag(ampa)]NO_3$, **25**
Chemical formula	$CH_4N_2O_6PPb$	$C_6H_{22}Ag_6F_6N_4O_{21}P_4S_2$	$C_2H_{12}AgN_3O_9P_2$
Formula weight	378.22	1435.50	391.96
Crystal system	Monoclinic	Triclinic	Orthorhombic
Space group	$P2_1/c$	$P\bar{1}$	Pb*cn*
T (K)	213(2)	213(2)	213(2)
a (Å)	5.1448(10)	7.2789(12)	5.6075(4)
b (Å)	19.182(4)	10.8120(18)	9.0707(7)
c (Å)	8.7258(13)	20.404(3)	21.4778(15)
α (°)	90	89.088(3)	90
β (°)	124.668(8)	83.609(3)	90
γ (°)	90	88.886(3)	90
V ($Å^3$)	708.2(2)	1595.3(5)	1092.45(14)
Z	4	2	4
Reflections collected	3954	9809	5849
Independent reflections	1666	7095	1325
Data/restraints/parameter ratio	1666/0/100	7095/6/461	1325/0/79
Unique data (R_{int})	0.0413	0.0292	0.0312
D_{calc} (mg/m^3)	3.547	2.988	2.383
F(000)	676	1364	776
R indices (all data)	R1 = 0.0475, wR2 = 0.0965	R1 = 0.0863, wR2 = 0.1219	R1 = 0.0436, wR2 = 0.0937
Final R indices [I >2σ(I)]	R1 = 0.0366, wR2 = 0.0914	R1 = 0.0488, wR2 = 0.1044	R1 = 0.0348, wR2 = 0.0888
Largest difference in peak and hole (e $Å^{-3}$)	2.552 and -2.541[a]	1.578 and -1.298	1.084 and -0.682

[a] The large electron density peak remaining in the difference map is associated with the heavy metal center.

Table 5.3 Crystal Data for **26** and **27**

Compound name	$[Ag_3(ampa)_2]_n(NO_3)H_2O$, **26**	$[Ag(ampa)Cu_2(NO_3)]_n$, **27**
Chemical formula	$C_4H_{20}Ag_6N_6O_{19}P_4$	$C_2H_8Ag_2CuN_4O_{12}P_2$
Formula weight	1227.36	621.34
Crystal system	Monoclinic	Triclinic
Space group	C2/*c*	Pī
T (K)	213(2)	213(2)
a (Å)	29.506(13)	5.0294(8)
b (Å)	5.442(2)	7.8443(13)
c (Å)	18.591(8)	9.1189(15)
α (°)	90	72.110(3)
β (°)	123.376(6)	82.240(3)
γ (°)	90	78.176(2)
V ($Å^3$)	2492.8(19)	334.10(9)
Z	4	1
Reflections collected	6829	1940
Independent reflections	2906	1473
Data/restraints/parameter ratio	2906/7/182	1473/0/115
Unique data (R_{int})	0.0522	0.0122
D_{calc} (mg/m^3)	3.270	3.088
F(000)	2320	297
R indices (all data)	R1 = 0.0781, wR2 = 0.2084	R1 = 0.0266, wR2 = 0.0667
Final R indices [I >2σ(I)]	R1 = 0.0624, wR2 = 0.2024	R1 = 0.0254, wR2 = 0.0656
Largest difference in peak and hole (e $Å^{-3}$)	2.450 and -1.92[§]	0.948 and -0.863

[a] The large electron density peak remaining in the difference map is associated with the heavy metal center.

Chapter 6

5-pyrimidyl phosphonic acid as building block for the synthesis of coordination polymers

6.1 Introduction

Our previous work with functionalized organophosphonic acids indicated that these linkers were able to coordinate through both the phosphonate moiety and the secondary functional group.[189] We were interested in the design and synthesis of a tailored organic ligand that would favor predictable self-assembly. A survey of the literature revealed that while pyrazine, pyrimidine and their corresponding carboxylic acids have been successfully employed in supramolecular synthesis,[213] this had not been extended to pyrimidine phosphonic acid derivatives. We wanted to include more coordination centers and concluded that replacing the pyridyl moieties with pyrimidine groups would provide an outer coordination site, allowing the second nitrogen atom to extend polymer dimensionality, through coordination or supramolecular interaction with nearby hydrogen donors, Figure 6.1.

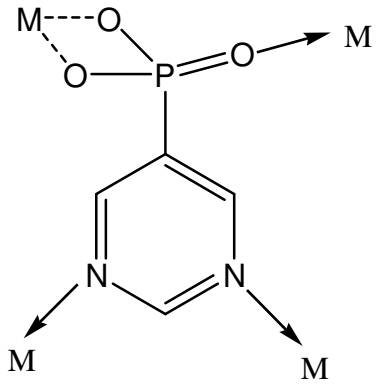

Figure 6.1 Possible coordination modes of 5-pyrimidyl phosphonate ($5PymPO_3H_2$).

Furthermore, one of our primary research goals was the high yielding synthesis of bimetallic systems, as although these are commonly found in nature,[214] bimetallic two- or three-dimensional transition metal frameworks[215] constitute a relatively new class of materials that have potential applications not accessible for single metal systems, for example as biological mimics or novel catalysts. To this end, we investigated the suitability of 5-pyrimidyl phosphonic acid ($5PymPO_3H_2$) for homo and heteroelement polymer synthesis. This hypothesis was demonstrated by the isolation of an ordered mixed-metal, Cu/Ag,

coordination polymer. To enable structural comparison and to determine coordination preference of the ligand, the homometallic copper, silver, zinc and cadmium coordination polymers were synthesized and characterized.

6.2 Results and discussion

6.2.1 Synthetic methods

5-Pyrimidyl phosphonic acid was prepared by a modified Hirao coupling[150] and the purity tested by NMR, elemental analysis and IR. The preparation of complexes **28**-**33** was achieved using one pot aqueous reactions, by combining the ligand with the metal salts in a 1:1 ratio, scheme 6.1.

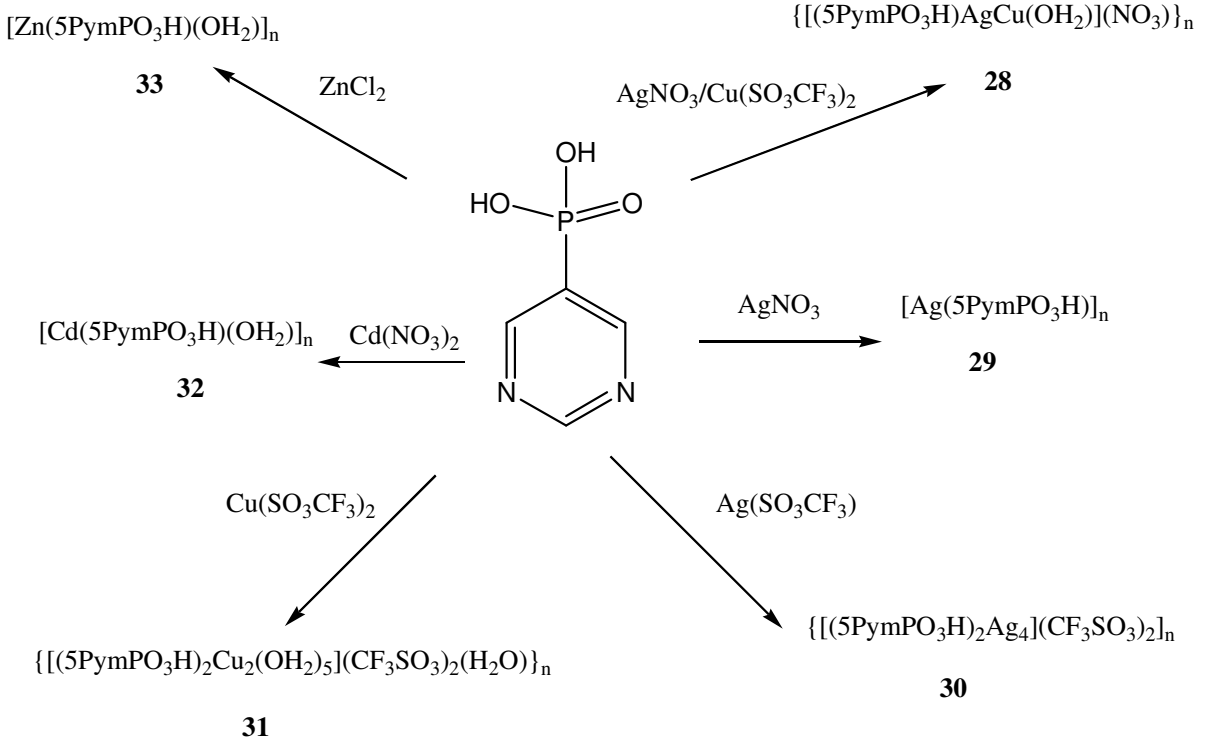

Scheme 6.1 Overview of the synthesis of polymers **28**-**33** using 5-pyrimidyl phosphonic acid.

Single crystals suitable for X-ray diffraction were obtained from slow evaporation of the reaction mixture at room temperature. Metal salts were selected with specific open

coordination sites for coordination to the organic linker. To target bimetallic frameworks, the metal precursors were carefully selected considering solubility, potential metathesis reactions, preferred metal geometry and coordination. 5-Pyrimidyl phosphonic acid ($5PymPO_3H_2$) was specifically selected because the ligand contains a phosphonate moiety for coordination and two heterocyclic nitrogen atoms at the opposite end to the PO_3H_2 group to promote multi-site coordination. We anticipated the ligand would discriminate between small transition metal cations that favor linear (or square planar) geometry or larger octahedral units, and cation bonding preferences, N vs. O.[216] It was thought that transition metal cations such as silver(I) would prefer to be accommodated between the nitrogen atoms in a linear, or T-shaped conformation while cadmium may be bound by both the remote nitrogen atoms or the phosphonate group in octahedral geometry.[217] This expectation was realized by the isolation of pale blue crystals from an equimolar reaction of $AgNO_3$, Cu(II) triflate and $5PymPO_3H_2$. Crystal data for complexes **28**-**33** is detailed in table 6.1 and 6.2.

6.2.1.1 Discussion of $\{[(5PymPO_3H)AgCu(OH_2)](NO_3)\}_n$, (28)

Pale blue crystals of **28** were isolated in 52% yield and found to crystallize in the triclinic space group Pī, Figure 6.2.

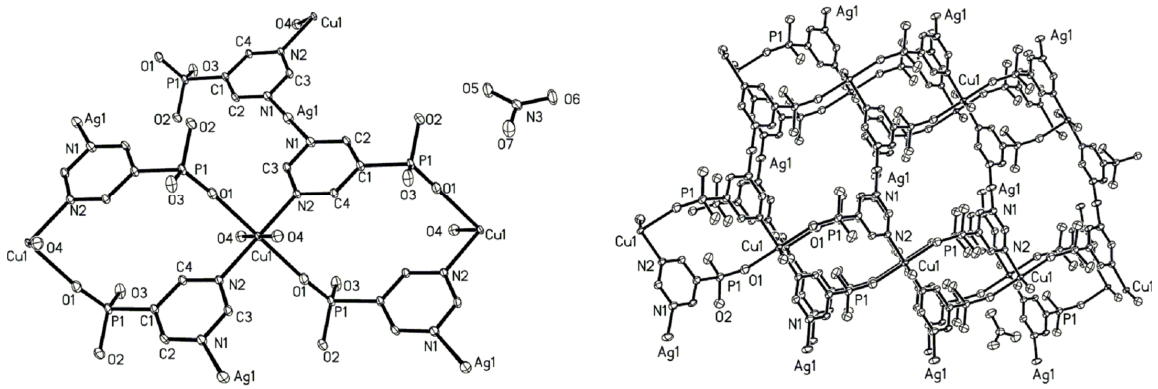

Figure 6.2 The Ag/Cu bimetallic framework, **28**. Selected bond lengths (Å) and angles (^{o}): Ag(1)-N(1) 2.201(3), Cu(1)-N(2) 2.014(3), Cu(1)-O(4) 2.049(3), P(1)-O(1) 1.480(3), P(1)-O(2) 1.551(3), P(1)-O(3) 1.535(3), N(1)-Ag(1)-N(1A) 180.0, O(1)-Cu(1)-O(1A) 180.00, N(2)-Cu(1)-O(4) 89.40(11).

In the asymmetric unit of **28** is found one molecule of $5PymPO_3H$ that is coordinated through its two nitrogen atoms to both copper, Cu(1) (N(2)), and silver atoms, Ag(1), (N(1)) which alternate throughout the polymer. The extended structural motif of **28**, can be described as copper nets supported by linear coordinated silver atoms that act as bridges between the layers. The pyrimidyl rings stack at a distance of ~3.8 Å, (C(1)-C(1A)).

The two available coordination sites around the silver atoms are occupied by a nitrogen atom and the related symmetry equivalent. The copper atoms exhibit octahedral geometry, with the coordination sites being occupied by a pyrimidine nitrogen atom, a water molecule, O(4), and an oxygen atom, O(1), from the phosphonate moiety. Each has a symmetry equivalent, completing the octahedral geometry. The P(1)-O(1) distance of 1.479(3) Å suggests that the PO-Cu interaction is through the P=O group; O3 is deemed to be protonated as reflected by the longer P-O bond length of 1.535(3) Å. To offset the cationic charge the phosphonic acid is singly deprotonated, which along with lattice nitrate ions maintains electroneutrality. Hydrogen-bonding exists from the protonated phosphonate oxygen atoms to the coordinated water molecule and the nitrate ions resulting in a thermally stable material as evidenced by the high melting point of >250^{o}C. Thermal gravimetric analysis of **28**, shows that guest water molecules are eliminated when the temperature is increased from room temperature to 125-148^{o}C corresponding to loss of two coordinated water molecules, (5.9%, calc. 5.6%).

We had expected that the reverse reaction of $5PymPO_3H_2$, Ag triflate and Cu(II) nitrate under similar reaction conditions would afford a similar polymeric structure; however, a homometallic silver polymer was isolated, $[Ag(5PymPO_3H)]_n$, **29**, Figure 6.2. Polymer **29**, can be intentionally isolated from the 1:1 reaction of $AgNO_3$ and $5PymPO_3H_2$, *vide infra*. In an attempt to rationalize the preferred coordination geometries of metals and the ligating preferences of the anions in order to predict structural outcomes, the reactions of silver nitrate, silver triflate, and copper(II) triflate were performed.

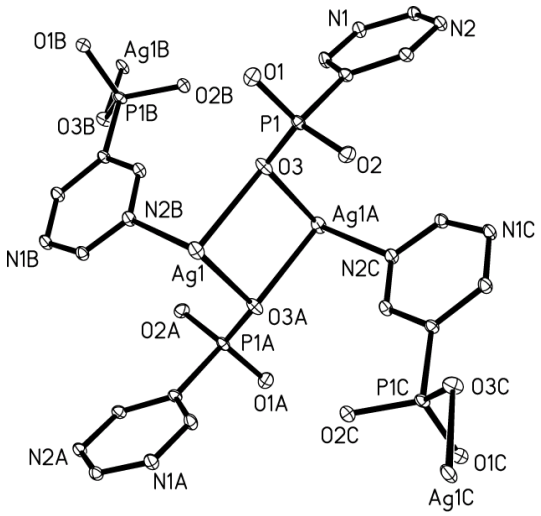

Figure 6.3 Crystal structure of $[Ag(5PymPO_3H)]_n$, **29**. Selected bond lengths (Å) and angles (°): Ag(1)-N(2) 2.2943(16), Ag(1)-O(3) 2.4258(15), P(1)-O(1) 1.5416(16), P(1)-O(2) 1.5307(15), P(1)-O(3) 1.4980(15), N(2)-Ag(1)-O(3) 89.11(5), N(1)-Ag(1)-O(3) 87.71(6).

6.2.1.2 Discussion of $[Ag(5PymPO_3H)]_n$, (29), and $\{[5PymPO_3H)_2Ag_4](CF_3SO_3)_2]_n$, (30)

Silver(I) has been used extensively for assembling coordination polymers because of its flexible coordination sphere which can adopt a wide range of geometries.[218] Although this makes the products less predictable[219] an advantage of this flexibility is that it allows us to investigate how the assembling process is affected by counter-ion. The reaction of $5PymPO_3H_2$ with $AgNO_3$ or $Ag(CF_3SO_3)$ in aqueous conditions at room temperature afforded two, 2D polymers, **29** and **30** respectively, Figures 6.3 and 6.4.

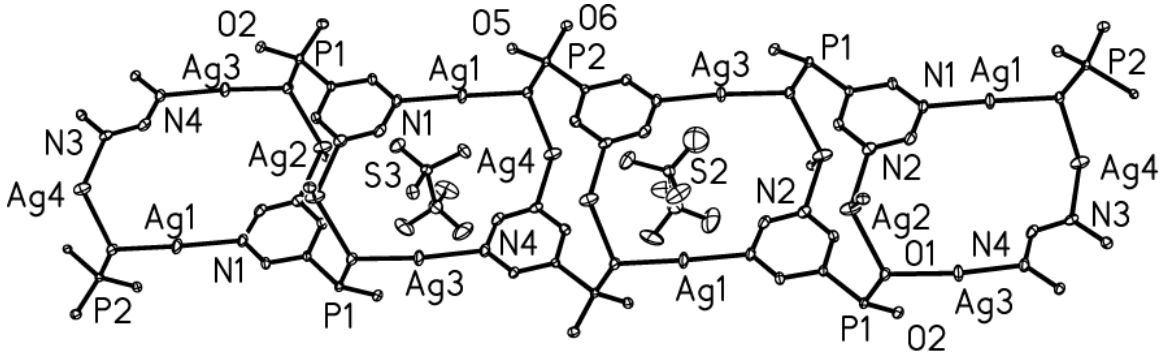

Figure 6.4 Silver triflate polymer, **30**: Ag(1)-O(4) 2.170(4), Ag(1)-N(1) 2.181(5), Ag(2)-O(1) 2.393(4), Ag(3)-N(4) 2.206(5), P(1)-O(1) 1.512(4), P(1)-O(2) 1.562(4), P(1)-O(3) 1.500(4), O(1)-Ag(3)-N(4) 156.00(17), N(2)-Ag(2)-O(1) 113.07(18)

Colorless crystals of **29** were isolated at room temperature and X-ray analysis revealed that they crystallize in the monoclinic space group $P2_1/c$ while crystals from the silver triflate reaction, **30**, are triclinic, Pī. In both polymers **29** and **30**, the anion is displaced from the silver center. For the silver nitrate product, no coordinating or guest nitrate ions are present in the structure, but the larger triflate ions in **30** act as guest anions and sit between the layers of silver atoms, at distances of 2.604Å (Ag(4)-O(10)), 2.661Å (O(11)-Ag(1)), and 2.611Å (O(13)-Ag(2)), from the silver centers, indicating weak, Ag-triflate interactions,[220] Figure 6.4. Polymers **29** and **30** are structurally similar in that the silver atoms, which have a high affinity for soft nitrogen atoms are coordinated to a heterocyclic nitrogen atom and an oxygen atom of the phosphonate group. A further similarity is that each phosphonate group has only one oxygen atom coordinated to each silver atom which corresponds to the shortest P-O bond and that each phosphonate group is singly deprotonated, thus one oxygen remains protonated, O(2) in **30**. The hydrogen atom associated with the protonated phosphonate oxygen could not be refined in **29**. It is interesting to note that the coordination geometry around the silver atoms in **29** and **30** is not as is observed in the bimetallic framework, **28**, highlighting the difficulty in structure prediction when numerous coordination modes of the ligand are possible. The repeat unit in **29**, consists of an Ag-O parallelogram shaped core where the bridging oxygen is from the phosphonate moiety. The Ag-O distance of 2.4258(15)Å is comparable to related systems, but the Ag-Ag distance, 3.740(7)Å, is too great for Ag-Ag interactions.[221] This parallelogram arrangement of Ag-O atoms is found to pack at ~45^o angles to each other which promotes alignment of the pyrimidyl rings. The distance separating the pyrimidine layers is ~3.9Å (aromatic C-aromatic C) which is slightly too long to allow π stacking. In the asymmetric unit of **30** (Ag triflate product) are four crystallographically unique silver atoms, supported by two phosphonate ligands and two guest triflate ions. Two different coordination geometries are observed around the silver atoms, for example, Ag(1) and Ag(3) have two coordinate geometry, while Ag(2) and Ag(4) are three coordinate, with the three coordination sites occupied by a pyrimidine nitrogen atom, and two phosphonate oxygen atoms, in which the Ag(4)-O(4) interaction can be considered as a dative bond.[221] The geometry around the silver centers leaves an open coordination site pointing towards adjacent chains but no interaction between the silver atoms is observed. For example, the silver atoms, Ag(2)-Ag(3), are separated by a distance of

3.871(8)Å which is greater than the Ag-Ag van der Waals radii,[118] (3.44Å). The repeating unit of **30** can be described as a net-like motif made up of two interlinked rectangular shaped units, where the larger rectangle, with the bridged pyrimidine, features four unique silver atoms, while the smaller rectangle, contains only one type of silver atom, Ag(4), Figure 6.5.

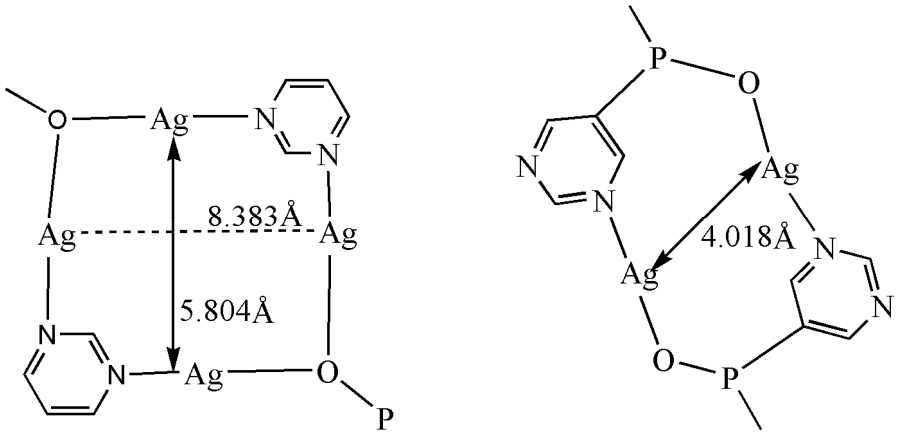

Figure 6.5 Representation of the repeat units in **30**, $\{[5PymPO_3H)_2Ag_4](CF_3SO_3)_2]_n$.

This alternating bi- and tricoordinate geometry is not a new phenomenon. For example, it has been observed in $[Ag_4(\mu\text{-}4,4'\text{-bpp})_3(1,3\text{-bdc})_2]_n2H_2O$, (4,4'-bpp = 2,2'-bis(4-pyridylmethyleneoxy)-1,1'-biphenylene; 1,3 bdc = 1,3benzenedicarboxylate).[222] TG analysis of **29** showed no significant weight loss to 100°C but shows a sharp weight loss between 110-120°C associated with decomposition of the polymer. Polymer **30** exhibited 3.4% weight loss from 93-100°C that corresponds to the loss of two water molecules (calc. 3.5%). Since d^{10} metal organic polymeric species have been found to exhibit photoluminescent properties[223] the luminescent properties of these species were investigated at different excitation wavelengths. However no luminescence was observed, possibly due to the lack of argentophilic interactions. It is noteworthy to mention that other silver precursors with non-coordinating anions such as $AgBF_4$ and $AgPF_6$ were investigated; however, both afforded free, recrystallized ligand, $5PymPO_3H_2$.

6.2.1.3 Discussion of $\{[(5PymPO_3H)_2Cu_2(OH_2)_5](CF_3SO_3)_2(H_2O)\}$, (31)

To compare how the metal center affects the polymeric structural motif, the reaction of $5PymPO_3H_2$ with Cu(II) triflate was performed. Similar to polymer **30**, this polymeric

copper phosphonate has displaced triflate ions that reside as guest molecules along with three lattice water molecules, Figure 6.6.

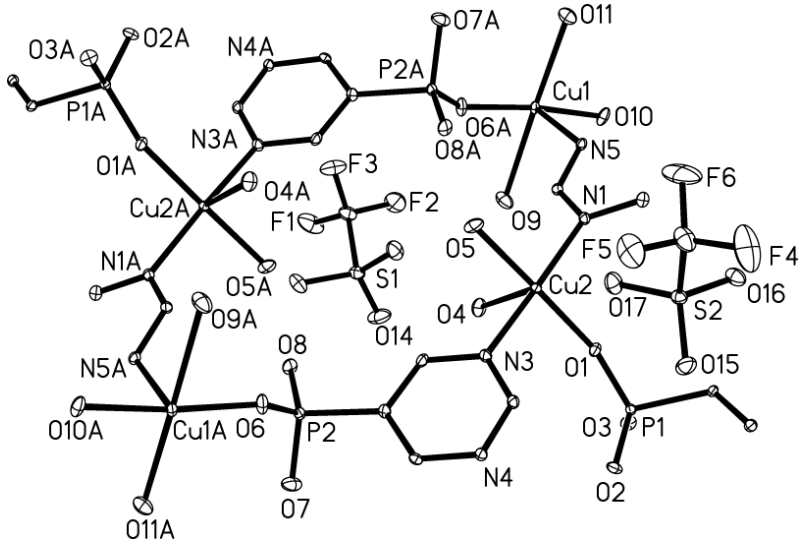

Figure 6.6 Solid-state thermal ellipsoid (30% probability level) of the copper triflate polymer **31**. Hydrogen atoms are omitted for clarity. Selected bond lengths (Å) and angles (°): Cu(1)-N(5) 2.045(2), Cu(1)-O(11) 2.304(2), Cu(2)-O(1) 1.9294(19), Cu(2)-O(5) 1.944(2), Cu(2)-N(3) 2.016(2), P(1)-O(1) 1.494(2), P(1)-O(2) 1.4950(19), P(1)-O(3) 1.571(2), P(2)-O(8) 1.474(2), P(2)-O(8) 1.474(2), O(10)-Cu(1)-N(5) 89.11(8), O(10)-Cu(1)-O(9) 90.81(8), O(1)-Cu(2)-O(5) 178.84(8), O(1)-Cu(2)-N(3) 91.49(9), O(1)-P(1)-O(3) 108.36(11).

Many copper phosphonates exhibit conventional layered or layered pillared structures where the inorganic layers are separated by the organic groups. The inorganic layer usually contains dimers of edgesharing $\{CuO_5\}$ square pyramids which are linked by $\{CPO_3\}$ tetrahedral through corner sharing forming 4- and 8-membered rings.[224] The copper phosphonate, **31**, continues this trend and the resultant polymer can be described as a layered structure in which the triflate ions and a water molecule reside between the layers. However, rather than the typical 4 to 8-membered rings the presence of an additional nitrogen atom in the organic linker results in two interlinked, twisted ring systems; one 12 membered N-Cu-O-P ring, featuring just Cu(2) atoms, while the larger 16 membered ring contains both Cu(2) and Cu(1) atoms (only coordinated atoms that form part of the cyclic structure are counted). The adjacent rings are connected through a pyrimidine bridge (N(3) and N(4)). The dimensions of these repeating units are ~6.86Å, from Cu(2)-Cu(2A) or P(1)-P(1A) in the smaller ring, and ~7.4Å, (Cu(2)-Cu(2A)), and 12.2 Å (Cu(1)-Cu(1A)) in the larger 16-

membered cyclic system. It was expected the Cu atoms would adopt octahedral geometry; however two different coordination environments are revealed. Cu(1) is octahedrally coordinated to an oxygen atom O(6), from a phosphonate group, three water molecules, and two nitrogen atoms from a pyrimidine group. A pyrimidine ring bridges Cu(1) and Cu(2), with the second nitrogen atom coordinated to Cu(2) that has 5-coordinate geometry with one less water molecule than Cu(1). The five coordinate Cu center, Cu(2), is orientated so as the vacant site has a weak interaction with the lattice triflate ion, (Cu(2)-O(17) = 2.613Å), whereas the second anion is located approximately midway between Cu(1) and Cu(2). For charge balance, each 5-pyrimidyl phosphonate is protonated at one of the oxygen atoms, $5PymPO_3(H)$, and similarly to polymers **29** and **30** the shortest P-O bond is the P-O-metal bond. The octahedrally coordinated copper atom, Cu(1), has a coordination environment similar to that observed in the bimetallic framework, **28**. The Cu-N bond lengths are all similar, ranging from 2.015(2)-2.044(2)Å but the Cu-O bond lengths have a wide range from 1.9294(19) to 2.307(2)Å, with the longer values being associated with coordinated water molecules. These values compare well with documented literature values.[225] IR spectroscopy exhibits a strong H_2O stretch and clear bands located at 1264 and 1026 cm^{-1} that are assigned to the asymmetric and symmetric stretching modes of PO_3.[196] TGA of **31** exhibits 19% weight loss from 119-123^oC, associated with loss of water molecules, (calc. 21.1%) followed by a sharp weight loss between 300 and 345^oC that corresponds to polymer decomposition.

6.2.1.4 Discussion of $[Zn(5PymPO_3H)(OH_2)]_n$, (32), and $[Cd(5PymPO_3H)(OH_2)]_n$, (33)

To further examine the structural preference of the late transition metal polymers with $5PymPO_3H_2$ the reactions with $ZnCl_2$, $Zn(NO_3)_2$, $CdCl_2$ and $Cd(NO_3)_2$ were performed. From these reactions, crystalline material was obtained from $ZnCl_2$, **32**, and $Cd(NO_3)_2$, **33**. The single crystal solid-state analysis revealed them to be isostructural. Complexes **32** and **33** crystallize in the orthorhombic space group P*bca*, with octahedral geometry around the metal centers, Figure 6.7.

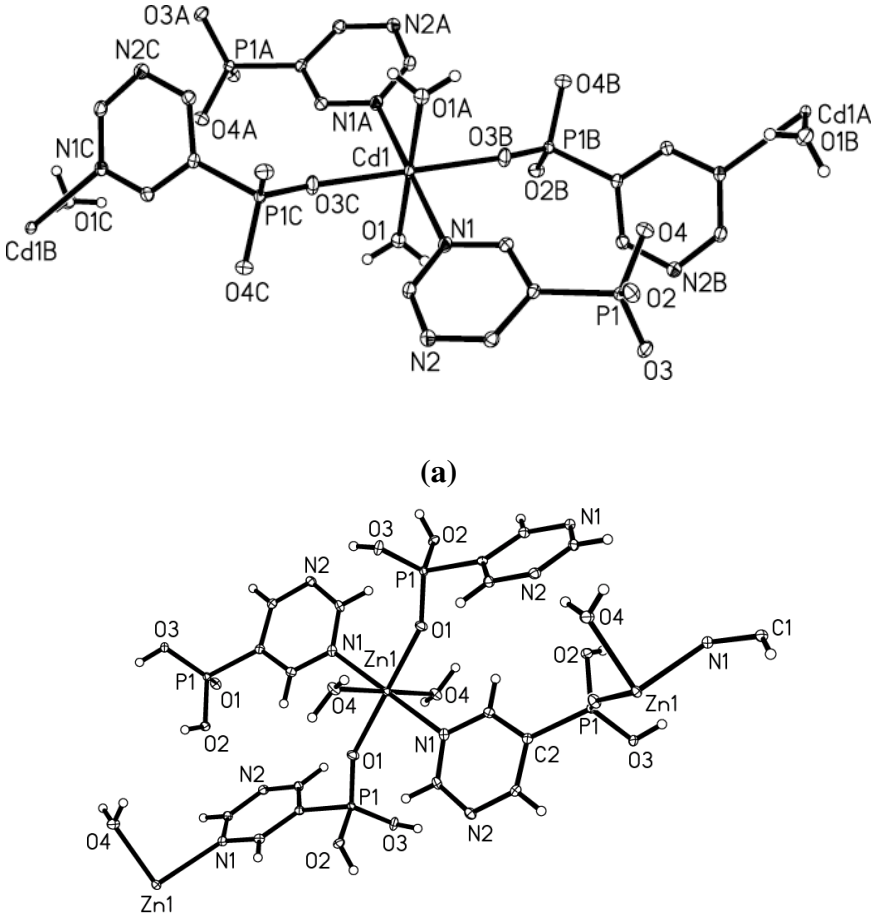

Figure 6.7 X-ray crystal structures of (a) $[Zn(5Pympo)_2(OH_2)]_n$, (**32**) and (b) $[Cd(5Pympo)_2(OH_2)_2]_n$, (**33**). Thermal ellipsoids drawn at 30% probability level.

The metal centers are coordinated to two pyrimidine nitrogen atoms, two phosphonate oxygen atoms and two water molecules. While zinc phosphonates are a well-studied area of research, cadmium phosphonates are less well known.[226] The zinc phosphonate, **32**, differs from reported examples of related zinc systems as these usually exhibit a ring motif, made up of repeating Zn-O-P units.[227] In both **32** and **33**, the +2 charge on the metal center is counteracted by two singly deprotonated ligands (one in the asymmetric unit as Cd(1) and Zn(1) are at half occupancy). Oxygen atoms O(4) in **32** and O(3) in **33** are the remaining protonated oxygen atoms with P-O bonds of 1.569(2)Å, 1.5636(18)Å respectively. Infrared data of **32** and **33** exhibit characteristic stretches for coordinated water molecules at 3592 and 3525 cm^{-1}, **32** also displays symmetric and asymmetric P-OH stretches at 3205 cm^{-1} and deformation at 1609 cm^{-1}. The Cd-Cd separation is ~7.2Å while the Zn-Zn is ~7.1Å, and

corresponds well to the increase in radii from Zn to Cd (1.31Å, Zn and 1.48Å Cd).[194d] Other pertinent bond lengths and angles are compared in Table 6.2. Further evidence of the similarity between **32** and **33** can be obtained from the solution ^{31}P and ^{1}H NMR, with near identical shifts observed in their ^{31}P spectra at 6.28 and 0.98 ppm for Cd and 6.5 and 1.07 ppm for zinc. The presence of two signals in the ^{31}P NMR spectra suggests that upon redissolution in D_2O, polymer decomposition occurs affording signals associated with free and complexed ligand. The complicated overlapping signals in the aromatic region are also attributed to this dissociation. The influence on structural motif by the different functionalities present in $5PymPO_3H_2$ can be examined by comparing the polymeric structures of **32** and **33** with the polymers obtained from the reactions of 5-carboxylic acid pyrimidine,[228] 3-pyridyl phosphonic acid.[229] (which is $5PymPO_3H_2$ minus one nitrogen), and pyrimidine[230] with cadmium(II) and zinc(II) nitrate, although some of these products were obtained from hydrothermal syntheses. The products from these reactions were monomeric $Zn(OH_2)_4(5PymCO_2H)$ where the second nitrogen does not participate in coordination to the metal ion, $[M(NO_3)_2(Pym)(H_2O)_2]_\infty$, that for zinc is a 1D chain but for cadmium a 2D sheet, and a 3D network of [Cd(3-pyridylphosphonate)$_2$]DMSO, where the Cd(II) center is coordinated to both the pyridyl nitrogen and a $\mu_2\eta^2$ phosphonate bridge. Considering the structural diversity of these products it is both surprising and useful that cadmium and zinc afforded isostructural products, as this may lend itself to allowing tailoring of reaction conditions for bimetallic framework syntheses.

6.3 Conclusions

A moderate yielding, aqueous synthesis is described for the synthesis of homo- and bimetallic coordination polymers using 5-pyrimidyl phosphonic acid as the organic linker. This multidentate ligand allowed us the opportunity to explore the behavior of hard and soft coordinating atoms (O and N correspondingly) being part of the same molecule in conjunction with different metal precursors. Simultaneously, it was possible to study the effect of the selected metal precursors for the modulation of the pore size of the synthesized MOFs.

To determine the coordination preference of both the linker and metal cation a series of homometallic metal phosphonates were prepared and structurally characterized. The solid state analyses of the synthesized polymers revealed that the ligand is deprotonated at one of the oxygen atoms and coordination of the phosphonate group occurs primarily through the P=O bond. In these extended structures, the metals displayed a great variety of coordination geometries in which they were coordinated to both the phosphonate group and heterocyclic nitrogen atom, often with the pyrimidine group acting as a bridge between metal centers through the second heterocyclic nitrogen atom. Structural comparisons of the Cu/Ag, bimetallic framework, $\{[(5PymPO_3H)AgCu(OH_2)](NO_3)\}_n$, with the homometallic silver polymers, $[Ag(5PymPO_3H)]_n$ and $\{[(5PymPO_3H)_2Ag_4](CF_3SO_3)_2]_n$, and the copper polymer, $\{[(5PymPO_3H)_2Cu_2(OH_2)_5](CF_3SO_3)_2(H_2O)\}$, show that copper exhibits similar coordination preferences, whereas the coordination geometry for silver is unpredictable and it varies in the aforementioned polymers given the coordinating nature of the nitrate ion and the non-coordinating behavior of the triflate anion which only acts as an electrostatic stabilization agent of the synthesized frameworks.

The reactions between $5PymPO_3H_2$ and zinc(II) and cadmium(II) nitrate were performed in order to contrast the results obtained with Cu and Ag. Interestingly we were able to isolate two isostructural polymers having similar physical characteristics and displaying similar spectroscopic behavior in the NMR experiment. These findings lead us to evaluate their potential for the synthesis of novel heteroelemental polymers containing these late transition elements.

Finally, future work will investigate the utility of $5PymPO_3H_2$ for further main group element polymer or cluster synthesis.

6.4 Experimental

All chemicals were purchased from Aldrich and used as received. NMR data were recorded on a Varian Mercury 300 NMR spectrometer, IR analyses was conducted on a MIDAC M4000 Fourier transform infrared (FT IR) spectrometer using KBr pellets. Thermogravimetric analyses (TGA) were carried out on a Seiko 220 instrument at a heating rate of 5^{o}C/min. Melting points were determined in capillaries under ambient conditions and are uncorrected.

6.4.1 Synthesis of {[(5PymPO$_3$H)AgCu(OH$_2$)](NO$_3$)}$_n$, (28)

5PymPO$_3$H$_2$ (0.1g, 0.62 mmol), 0.11 g of AgNO$_3$ (0.62 mmol), and 0.22 g of Cu(SO$_3$CF$_3$)$_2$ (0.62 mmol) were dissolved in 3 mL of water in an open vial covered with aluminum foil and stirred at 100°C. After 30 minutes, the solution was filtered. From the solution, blue crystals suitable for X-ray diffraction quality crystals were obtained by slow evaporation of the solution at room temperature. Yield: 0.13 g (52% based on 5PymPO$_3$H$_2$), m.p. decomposes at 205-210^{o}C. IR (KBr pellet, υ cm^{-1}) 3447(m), 3068(w), 2919(m), 1560(s), 1418(s), 1261(s), 1178(s), 1033(s), 922(m), 777(m), 769(m), 694(m), 642(s), 567(m), 519(s), 416(m). No signals were detected in the ^{1}H-NMR experiment or the ^{31}P-NMR experiment.

6.4.2 Synthesis of [Ag(5PymPO$_3$H)]$_n$, (29)

5PymPO$_3$H$_2$ (0.1g, 0.62mmol) and 0.11 g of AgNO$_3$ (0.62 mmol) were dissolved in 3 mL of water in an open vial covered with aluminum foil and stirred at 100°C. After 30 min, the reaction mixture was filtered to remove some deposited silver, and the clear solution was left for further crystallization. Colorless crystals suitable for X-ray diffraction quality crystals were obtained by slow evaporation of the solution at room temperature. Yield: 0.04 g (24% based on AgNO$_3$), The product decomposes at 165-170^{o}C. IR (KBr pellet, υ cm^{-1}) 3447(w), 2954 (s), 1574(s), 1377(s), 1250(s), 1188(m), 1087(m), 1054(s), 862(s), 834(s), 697(s), 581(s), 523(m), 416(w), 405(w). ^{1}H NMR (300 MHz, 25°C, D$_2$O): δ (ppm) 6.71 (m, 1H), 7.98 (m, 1H), 8.47 (s, 1H), 8.34 (s, 1H), ^{31}P NMR (121MHz, 25°C, DMSO): δ (ppm) 1.15, 8.05.

6.4.3 Synthesis of $\{[(5PymPO_3H)_2Ag_4](CF_3SO_3)_2]_n$, (30)

$5PymPO_3H_2$ (0.06g, 0.37mmol) and 0.1 g of $Ag(SO_3CF_3)$ (0.37 mmol) were dissolved in 2 mL of water in an open vial covered with aluminum foil and stirred at 100°C for 30 minutes. The clear solution was gravity filtered to remove any insoluble material. Colorless crystals suitable for X-ray diffraction quality crystals were obtained by slow evaporation of the solution at room temperature. Yield: 0.06 g (15 % based on $Ag(SO_3CF_3)$), m.p. 180-185°C. IR (KBr pellet, υ cm^{-1}) 2925(s), 2859(m), 1727(w), 1619(w), 1457(w), 1261(s), 1188(s), 1051(s), 801(w), 640(m), 555(m), 415(w), 403(w). ^{1}H NMR (300 MHz, 25°C, D_2O) δ (ppm) 9.2 (d, 1H), 9.01(s, 1H), 7.81 (s, 1H), ^{31}P NMR (121MHz, 25°C, D_2O) δ (ppm) 1.03, 7.81.

6.4.4 Synthesis of $\{[(5PymPO_3H)_2Cu_2(OH_2)_5](CF_3SO_3)_2(H_2O)\}_n$, (31)

$5PymPO_3H_2$ (0.04g, 0.25mmol) and 0.1g of $Cu(SO_3CF_3)_2$ (0.25 mmol) were dissolved in 2 mL of water in an open vial and stirred at 100°C for 30 minutes. On cooling, the clear blue solution was filtered and stored at room temperature for 5-6 days. Slow evaporation of the solution afforded pale blue crystals of **31**. Yield: 0.08 g (33% based on $Cu(SO_3CF_3)_2$), m.p. 190-195°C. IR (KBr pellet, υ cm^{-1}) 3398(w), 1618(m), 1586(s), 1416(s), 1264(s), 1167(s), 1026(s), 769(s), 693(s), 641(s), 577(s), 518(s). No signals were detected in the ^{1}H-NMR experiment or the ^{31}P-NMR experiment.

6.4.5 Synthesis of $[Zn(5PymPO_3H)(OH_2)]_n$, (32)

$5PymPO_3H_2$ (0.1g, 0.62 mmol) and 0.09 g of $Zn(NO_3)_2$ (0.62 mmol) were dissolved in 2 mL of water in an open vial and stirred at 100°C for 60 minutes. Colorless crystals suitable for X-ray diffraction quality crystals were obtained by slow evaporation of the solution at room temperature. Yield: 0.07 g (35% based on $Zn(NO_3)_2$). The product decomposes at 190-191°C**.** IR (KBr pellet, υ cm^{-1}) 3592(m), 3525(m), 3205(m), 3004(m), 1609(s), 1405(s), 1171(m), 1079(s), 962(m), 785(m), 753(s), 689(s), 508(m). ^{1}H NMR (300 MHz, 25°C, D_2O): δ (ppm)**:** 6.95 (s, 1H) 7.13 (s, 1H) 7.30 (s, 1H) ^{31}P NMR (121MHz, 25°C, D_2O): δ (ppm) 0.98, 6.28.

6.4.6 Synthesis of $[Cd(5PymPO_3H)(OH_2)]_n$, (33)

$5PymPO_3H_2$ (0.1g, 0.62 mmol) and 0.19 g of $Cd(NO_3)_2$ (0.62 mmol) were dissolved in 2 mL of water in an open vial and stirred at 100°C for 30 minutes. The clear solution was gravity filtered and following slow evaporation of the solution over 2 days, colorless crystals of **20** were isolated. Yield: 0.04 g (14% based on $Cd(NO_3)_2$), The product decomposes at 210°C. IR (KBr pellet, υ cm^{-1}) 3525(w), 2929(w), 2728(w), 2392(s), 1763 (s), 1624(w), 1384(s), 1091(w), 824(s), 708(m), 660(m), 563(w), 511(w), 428(m). ^1H NMR (300 MHz, 25°C, D_2O): δ (ppm) 7.77 (t, 2H, J = 27Hz), 8.26 (d, 1H, J = 18Hz), ^{31}P NMR (121MHz, 25°C, D_2O): δ (ppm) 1.07, 6.4.

Table 6.1 Crystal data for compound **28**-**30**

Compound	{[5PymPO$_3$H)AgCu(OH$_2$)](NO$_3$)}$_n$, **28**	[Ag(5PymPO$_3$H)]$_n$, **29**	{[5PymPO$_3$H)$_2$Ag$_4$](CF$_3$SO$_3$)$_2$]$_n$, **30**
Chemical Formula	$C_8H_{10}AgCuN_6O_{14}P_2$	$C_4H_5AgN_2O_3P$	$C_{10}H_7Ag_4F_6N_4O_{12}P_2S_2$
Formula Weight	647.57	264.94	1046.74
Crystal System	Triclinic	Monoclinic	Triclinic
Space Group	P$\bar{1}$	$P2_1/c$	P$\bar{1}$
T(K)	213(2)	213(2)	213(2)
a (Å)	6.6034(10)	9.0075(7)	8.5096(10)
b (Å)	7.6695(12)	8.2037(6)	8.7131(10)
c (Å)	10.5333(16)	11.9721(7)	17.296(2)
α (^{o})	76.055(3)	90	88.498(2)
β (^{o})	85.522(2)	131.358(4)	76.163(2)
γ (^{o})	64.535(2)	90	83.192(2)
V (Å ^{3})	467.24(12)	664.03(8)	1236.4(3)
Z	1	4	2
Reflections collected	2773	6499	7298
Independent reflections	2053	1596	5497
Data/restraints/parameters	2053/ 4/ 159	1596/ 0/ /101	5497/ 0 / 356
Unique Data (*R int*)	0.0145	0.0248	0.0208
D calc (Mg/m^3)	2.301	2.680	2.812
F(000)	318	516	990
R indices (all data)	R1 = 0.0441, wR2 = 0.0812	R1 = 0.0196, wR2 = 0.0513	R1 = 0.0668, wR2 = 0.1354
Final R indices [I > 2σ(I)]	R1 = 0.0326, wR2 = 0.0751	R1 = 0.0187, wR2 = 0.0506	R1 = 0.0495, wR2 = 0.1218
Largest difference peak and hole (e Å^{-3})	0.842 and -0.586	0.516 and -0.847	2.811 and -2.280

Table 6.2 Crystal data for compound **31**-**33**

Compound	{[(5PymPO$_3$H)$_2$Cu$_2$(OH$_2$)$_5$](CF$_3$SO$_3$)$_2$(H$_2$O)}, **31**	[Cd(5PymPO$_3$H)(OH$_2$)]$_n$, **32**	[Zn(5PymPO$_3$H)(OH$_2$)]$_n$, **33**
Chemical Formula	$C_{10}H_{22}Cu_2F_6N_4O_{19}P_2S_2$	$C_8H_{14}CdN_4O_8P_2$	$C_8H_{14}N_4O_8P_2Zn$
Formula Weight	853.46	468.57	421.54
Crystal System	Monoclinic	Orthorhombic	Orthorhombic
Space Group	$P2_1/c$	P*bca*	P*bca*
T(K)	213(2)	213(2)	213(2)
a (Å)	13.9181(15)	12.701(6)	12.5436(14)
b (Å)	11.6269(13)	7.208(4)	7.0918(8)
c (Å)	18.8112(16)	15.998(8)	15.5908(17)
α (°)	90	90	90
β (°)	116.025(6)	90	90
γ (°)	90	90	90
V (Å ^{3})	2735.4(5)	4	1386.9(3)
Z	4	4	4
Reflections collected	15634	13172	8009
Independent reflections	6464	1787	1683
Data/restraints/parameters	6464 / 3 / 395	1787 / 0 / 118	1683 / 3 / 118
Unique Data (*R int*)	0.0328	0.0300	0.0503
D calc (Mg/m^3)	2.072	2.116	2.019
F(000)	1712	928	856
R indices (all data)	R1 = 0.0534, wR2 = 0.0952	R1 = 0.0329, wR2 = 0.0599	R1 = 0.0572, wR2 = 0.0903
Final R indices [I > 2σ(I)]	R1 = 0.0362, wR2 = 0.0857	R1 = 0.0238, wR2 = 0.0542	R1 = 0.0341, wR2 = 0.0783
Largest difference peak and hole (e Å^{-3})	0.581 and -0.838	0.557 and -0.793	0.688 and -0.411

References

1. Hoskins, B. F.; Robson, R. *J. Am. Chem. Soc.* **1990**, *112*, 1546.

2. Janiak, C. *Dalton Trans.* **2003**, 2781.

3. Batten, S. R.; Robson, R. *Angew. Chem. Int. Ed.* **1998**, *37*, 1460.

4. Wang, X.-S.; Ma, S.; Sun, D.; Parkin, S.; Zhou,H.-C. *J. Am. Chem. Soc.* **2006**, *128*, 16474.

5. Rao, L. *Resonance* **2007**, *12*, 30.

6. Yaghi, O. M.; Li, H.; Davis, C.; Richardson, D.; Groy, T. L. *Acc. Chem. Res.* **1998**, *31*, 474.

7. Chui, S. S.-Y.; Lo, S. M.-F.; Charmant, J. P. H.; Orpen, A. G.; Williams, I. D. *Science* **1999**, *283*, 1148.

8. Chen, B.; Eddaoudi, M.; Hyde, S. T.; O'Keeffe, M.; Yaghi, O. M. *Science* **2001**, *291*, 1021.

9. Almeida-Paz, F. A.; Klinowski, J. *Pure Appl. Chem.* **2007**, *79*, 1097.

10. Tranchemontagne, D. J.; Hunt, J. R.; Yaghi, O. M. *Tetrahedron* **2008**, *423*, 705.

11. Bradshaw, D.; Prior, T. J.; Cussen, E. J.; Claridge, J. B.; Rosseinsky, M. J. *J. Am. Chem. Soc.* **2004**, *126*, 6106.

12. Abrahams, B. F.; Jackson, P. A.; Robson, R. *Angew. Chem. Int. Ed.* **1998**, *37*, 2656.

13. Gascon, J.; Aktay, U.; Hernandez-Alonso, M. D.; Van Klink, G. P.; Kapteijn, F. *J. Catal.* **2009**, *261,* 75.

14. Garberoglio, G.; Skoulidas, A. I.; Johnson, J. K. *J. Phys. Chem. B* **2005**, *109,* 13094.

15. Sun, D.; Ma, S.; Ke, Y.; Petersen, T. M.; Zhou, H.-C. *Chem. Comm.* **2005**, 2663.

16. Ingleson, M. J.; Perez-Barrio, J.; Bacsa, J.; Dickinson, C.; Park, H.; Rosseinsky, M. J. *Chem. Comm.* **2008**, 1287.

17. Li, X.-J.; Wang, X.-Y.; Gao, S.; Cao, R. *Inorg. Chem.* **2006**, *45*, 1508.

18. Stein, A.; Keller, S. W.; Mallouk, T. E. *Science* **1993**, *259*, 1558.

19. Ramanan, A.; Whittingham, M. S. *Cryst. Growth Des.* **2006**, *6*, 2419.

20. Qi, Y.; Che, Y.-X.; Zheng, J.-M. *Cryst. Growth Des.* **2008**, *8*, 3602.

21. Choi, E.-Y.; Park, K.; Yang, C.-M.; Kim, H.; Son, J.-H.; Lee, S.W.; Lee, Y.-H.; Min, D.; Kwon, Y.-U. *Chem. Eur. J.* **2004**, *10*, 5535.

22. Batten, S. R. *J. Solid State Chem.* **2005**, *178*, 2475.

23. Forster, P. M.; Thomas, P.M.; Cheetham, A. K. *Chem. Mater.* **2002**, *14,* 17.

24. Ni, Z.; Masel, R. *J. Am. Chem. Soc.* **2006**, *128*, 12394.

25. Li, H.; Eddaoudi, M.; Groy, T. L.; Yaghi, O. M. *J. Am. Chem. Soc.* **1998**, *120*, 8571.

26**.** Pichon, A.; Lazuen-Garay, A; James, S. L. *Cryst. Eng. Comm.* **2006**, *8*, 211.

27. Ferey, G. *J. Solid State Chem.* **2000**, *152*, 37.

28. Collins, D. J.; Zhou, H.-C. *J. Mater. Chem.* **2007**, *17*, 3154.

29. Jones, R. D.; Summerville, A.; Basolo, F. *J. Am. Chem. Soc.* **1978**, *100*, 4416.

30. Miller, J. S.; Vazquez, C.; Jones, N. L.; McLean, R. S.; Epstein, A. J. *J. Mater. Chem.* **1995**, *5*, 707.

31. Belcher, W. J.; Longstaff, C. A.; Neckenig, M. R.; Steed, J. W. *Chem. Comm.* **2002**, 1602.

32. (a) Raymo, F. M.; Stoddart, J. F. *Chem. Rev.* **1999**, *99,* 1643. (b) Loeb, S. J. *Chem. Comm.* **2005**, 1511.

33. Davidson, G. J. E.; Loeb, S. J. *Angew. Chem. Int. Ed*. **2003**, *42*, 74.

34. Moulton, B.; Zaworotko, M. J. *Chem. Rev.* **2001**, *101,* 1629.

35. Lin, W.; Evans, O. R.; Xiong, R.-G.; Wang, Z. *J. Am. Chem. Soc.* **1998**, *120*, 13272.

36. Masciocchi, N.; Castelli, F.; Forster, P. M.; Tafoya, M. M.; Cheetham, A. K. *Inorg. Chem.* **2003**, *42*, 6147.

37. Costes, J. P.; Dahan, F.; Laurent, J. P. *Inorg. Chem.* **1991**, *30*, 1887.

38. (a) Frisch, M.; Cahill, C. L. *Dalton Trans.* **2005**, 1518. (b) Cahill, C. L.; de Lill, D. T.; Frisch, M. *CrystEngComm.* **2007**, *9*, 15.

39. Li, H.; Eddaoudi, M.; O'Keeffe, M.; Yaghi, O. M. *Nature* **1999**, *402*, 276.

40. Dan, M.; Cottereau, G.; Rao, C. N. R. *Solid State Sci.* **2005**, *7*, 437.

41. Cheetham, A. K.; Rao, C. N. R.; Feller, R. K. *Chem. Comm.* **2006**, 4780.

42. Schlapbach, L.; Zuttel, A. *Nature* **2001**, *414*, 353.

43. Hydrogen, Fuel Cells, & Infrastructure Technologies Program: Multiyear Research, Development, and Demonstration Plan; U.S. Department of Energy, February 2005, Chapter 3, http://www.eere.energy.gov/hydrogenandfuelcells/mypp/.

44. Wong-Foy, A. G.; Matzger, A. J.; Yaghi, O. M. *J. Am. Chem. Soc.* **2006**, *128*, 3494.

45. Dinca, M.; Long, J. R. *Angew. Chem. Int. Ed*. **2008**, *47*, 6766.

46. Navarro, J. A. R.; Barea, E.; Salas, J. M.; Masciocchi, N.; Galli, S.; Sironi, A.; Ania, C. O.; Parra, J. B. *Inorg. Chem*. **2006**, *45*, 2397.

47. Yang, C.; Wang, X.; Omary, M. A. *J. Am. Chem. Soc*. **2007**, *129*, 15454.

48. Mehrotra, R. C.; Bohra. R. Metal Carboxylates, Academic Press Inc. London, **1983.**

49. Kaye, S. S.; Long, J. R. *J. Am. Chem. Soc*. **2008**, *130*, 806.

50. Mulfort, K. L.; Hupp, J. T. *J. Am. Chem. Soc.* **2007**, *129*, 9604.

51. Chen, B.; Liang, C.; Yang, J.; Contreras, D. S.; Clancy, Y. L.; Lobkovsky, E. B.; Yaghi, O. M.; Dai, S. *Angew. Chem.* **2006**, *118*, 1418.

52. (a) Li, W.; Li, M.-X.; Shao, M.; Wang, Z.-X., Liu, H. J. *Inorg. Chem. Comm.* **2008**, *11*, 954. (b) Fuentes-Cabrera, M.; Nicholson, D. M.; Sumpter, B. G. *J. Chem. Phys.* **2005**, *123*, 124713.

53. Poulsen, R. D.; Bentien, A.; Graberb, T.; Iversen, B. B. *Acta Cryst.* **2004**, *A60*, 382.

54. Evans, O. R.; Ngo, H. L.; Lin, W. *J. Am. Chem. Soc*. **2001**, *123*, 10395.

55. Seo, J. S.; Whang, D.; Lee, H.; Jun, S. I.; Oh, J.; Jeon, Y. J.; Kim, K. *Nature* **2000**, *404*, 982.

56. (a) Noro, S.; Kitagawa, S.; Yamashita, M.; Wada, T. *Chem. Comm.* **2002**, 222. (b) Kitaura, R.; Onoyama, G.; Sakamoto, H.; Matsuda, R.; Noro, S.; Kitagawa, S. *Angew. Chem. Int. Ed.* **2004**, *43*, 2684.

57. Kitaura, R.; Fujimoto, K.; Noro, S.-I.; Kondo, M.; Kitagawa, S. *Angew. Chem. Int. Ed.* **2002**, *41*, 1.

58. Chapman, M. E.; Ayyappan, P.; Foxman, B. M.; Yee, G.T.; Lin, W. *Cryst. Growth Des.* **2001**, *1*, 159.

59. Hasegawa, S.; Horike, S.; Matsuda, R.; Furukawa, S.; Mochizuki, K.; Kinoshita, Y.; Kitagawa, S; *J. Am. Chem. Soc.* **2007**, *129*, 2607.

60. Dinca, M.; Dailly, A.; Liu, Y.; Brown, C. M.; Neumann, D. A.; Long J. R. *J. Am. Chem. Soc.* **2006**, *128*, 16876.

61. Horike, S.; Dinca, M.; Tamaki, K.; Long, J. L. *J. Am. Chem. Soc.* **2008**, *9*, 5854.

62. Roswell, J. L. C.; Yaghi, O. M. *Angew. Chem. Int. Ed.* **2005**, *44*, 4670.

63. Loiseau, T.; Serre, C.; Huguenard, C.; Fink, G.; Taulelle, F.; Henry, M.; Bataille, T.; Ferey, G. *Chem. Eur. J.* **2004**, *10*, 1373.

64. Hsu, K.-F.; Wang, S.-L. *Inorg. Chem.* **2000**, *39*, 1773.

65. Sassoye, C.; Marrot, J.; Loiseau, T.; Ferey, G. *Chem. Mater.* **2002**, *14,* 1340.

66. Harvey, H. G.; Herve, A. C.; Hailes, H. C.; Attfield, M. P. *Chem. Mater.* **2004**, *16,* 3756.

67. Chippindale, A. M.; Walton, R. *J. Chem. Soc. Chem. Comm*. **1994**, 2453.

68. Stork, J. R.; Thoi, V. S.; Cohen, S. M. *Inorg. Chem.* **2007**, *46*, 11213.

69. Gabbai, F. P.; Schier, A.; Riede, J. *Angew. Chem. Int. Ed.* **1998**, *37*, 622.

70. Gomez-Lor, B.; Gutierrez-Puebla, E.; Iglesias, M.; Monge, M. A.; Ruiz-Valero, C.; Snejko, N. *Inorg. Chem.* **2002**, *41*, 2429.

71. Gomez-Lor, B.; Gutierrez-Puebla, E.; Iglesias, M.; Monge, M. A.; Ruiz-Valero, C.; Snejko, N. *Chem. Mater*. **2005**, *17*, 2568.

72. Ai, W.; He, H.; Liu, L.; Liu, Q.; Lv, X.; Li, J.; Sun, D. *CrystEngComm.* **2008**, *10*, 1480.

73. Ellsworth, J. M.; Zur Loye, H.-C. *Dalton Trans.* **2008**, 5823.

74. (a) Atwood, J. L.; Bennet, F. R.; Jones, C.; Koutsantonis, G. A.; Raston, C. L. *Chem. Comm.* **1992**, 541. (b) Atwood, J. L.; Jones, C.; Butz, K. W.; Gardiner, M. G.; Koutsantonis, G. A. *Inorg. Chem.* **1993**, *32*, 3482. (c) Lorbeth, J.; Dorn, R.; Wocaldo, S.; Massa, W.; Gobel, E. O.; Marschner, T.; Stotz, W. *Adv. Mater.* **1992**, *4*, 576. (d) O'Hare, D.; Foord, J. S.; Page, T. C. M.; Whitaker, T. J. *Chem. Comm.* **1991**, 1445.

75. Zanius, S.; Raptopoulou, C. P.; Terzis, A.; Zafiropoulus, T. F. *Inorg. Chem. Commun.* **1999**, 248.

76. Samanamu, C.; Richards, A.F. *Polyhedron* **2007**, *26*, 923.

77. Yang, S.; Li, G.; Tian, S.; Liao, F.; Lin, F. *J. Solid State Chem.* **2005**, *178*, 3703.

78. Lin, Z.; Jiang, F. L.; Chen, L.; Yuan, D. Q.; Hung, M.C. *Inorg. Chem.* **2005**, *44*, 73.

79. Lin, Z. Z.; Jiang, D. Q.; Yuan, L.; Chem, L. *Eur. J. Inorg. Chem*. **2005**, *10*, 1927.

80. Lin, Z.; Chen, L.; Yue, C.; Yuan, D.; Jiang, F.; Hong, M. *J. Solid Sate Chem.* **2006**, *179*, 1154.

81. Tran, Y. Q.; Cai, C.-X.; Yuan, X.-J.; Li, Y.-Z.; Wang, T.-W.; You, X.-Z. *Chem. Lett.* **2003**, *32*, 796.

82. Walton, R. H. *Inorg. Chem.* **1967**, 640.

83. For examples see: (a) Werner, H.; Otto, H.; Kraus, H. J. *J. Organomet. Chem.* **1986**, *315*, C57. (b) Harvey, S.; Raston, C. L.; Skelton, B. W.; White, A. H.; Lappert, M. F.; Srivastava, G. *J. Organomet. Chem.* **1987**, *328*, C1. (c) Dastiti-Momertz, A.; Neumeller, B.; Melle, S.; Haase, D. *Z. Anorg. Allg. Chem.* **1999**, *625*, 1828.

84. (a) Jeffs, S. E.; Small, R. W.H.; Worrall, I. J. *Acta Crystallogr.* **1984**, *C40*, 1329. (b) Bermejo, M. S.; Castrienas, A.; Fernandez, M. I.; Gomez, M. E. *Acta Crystallogr*. **1991**, *C47*, 1406.

85. Ma, G.; Molla-Abbassi, A.; Kritikos, M.; Ilyukhin, A.; Jalilehvand, F.; Kessler, V.; Skripkin, M.; Sandstrom, M.; Glaser, J.; Naslund, J.; Persson, I. *Inorg. Chem.* **2001**, *40*, 6432.

86. (a) G. M. Sheldrick, SHELXS-97, Program for the solution of crystal structures; University of Göttingen: Germany, 1997. (b) G. M. Sheldrick, SHELXL-97, Program for the refinement of crystal structures.

87. Hughes, M. N., The inorganic chemistry of biological processes, 2nd ed., Wiley:New York, 1972.

88. Chowdhury, A.; Pateanu,L.; Webb, M. A.; Loppnow, G. R. *J. Phys. Chem. B*, **2001**, *105*, 527.

89. Harris, R. L.; Eady, R. R.; Hasnain, S. S.; Sawers, R. G. *Arch Microbiol.* **2006**, *186*, 241.

90. Holland, P. L.; Tolman, W. B. *J. Am. Chem. Soc.* **2000**, *122*, 6331.

91. Chowdhury, A.; Peteanu, L. A.; Webb, M. A.; Loppnow, G. R. *J. Phys. Chem. B* **2001**, *105*, 527.

92. Beinert, H. *Eur. J. Biochem.* **1997**, *245*, 521.

93. Solomon, E. I.; Sundaram, U. M.; Machonkin, T. E. *Chem. Rev.* **1996**, 2563.

94. Hay, M. T.; Milberg, R. M; Lu, Y. *J. Am. Chem. Soc.* **1996**, *118*, 11976.

95. Chowdhury, S.; Patra, G. K.; Drew, M. G. B.; Chattopadhyay, N.; Datta, D. *J. Chem. Soc*. *Dalton Trans*. **2000**, 235.

96. Lucchese, B.; Humphreys, K. J.; Lee, D. H.; Incarnto, C. D.; Sommer, R. D.; Rheingold, A. L.; Karlin, K.D. *Inorg. Chem.* **2004**, *43*, 5987.

97. Chesnut, D. J.; Kusnetzow, A.; Birge, R. R.; Zubieta, J. *Inorg. Chem.* **1999**, *38*, 2663.

98. Graham, P. M.; Pike, R. D.; Sabat, M.; Bailey, R. D.; Pennington, W. *Inorg. Chem*. **2000**, *39*, 5121.

99. Healy, C.; Pakawatchai, R.I.; Papasergio, V. A.; Patrick, A. H.; White, C. *Inorg. Chem.* **1984**, *23*, 3769.

100. Cabeza, J. A.; Llamazares, A.; Riera, V.; Trivedi, R. *Organomet.* **1998**, *17*, 550.

101. Raston, C. L.; White, A. H. *J. Chem. Soc. Dalton Trans.* **1976**, 2153.

102. Umakoshi, K.; Kinoshita, I.; Ooi, S. *Inorg. Chim. Acta* **1987**, *127*, L41.

103. Kawano, T.; Kuwana, J.; Ueda, I. *Bull. Chem. Soc. Japan* **2003**, *76*, 789.

104. Portela, A. A.; Carballo, R.; Casas, J. S.; Garcia-Martinez, E.; Gomez-Alonso, C.; Sanchez-Gonzalez, A.; Sordo, J.; Vuzques-Lopez, E. M. *Z. Anorg. Allg. Chem.* **2002**, *628*, 939.

105. Barnett, S. A.; Blake, A. J.; Champness, N. R.; Wilson, C. *Chem. Comm.* **2002**, 1640.

106. Lu, J. Y. *Coord. Chem. Rev.* **2003**, *246*, 327.

107. Wang, Q.-M.; Guo, G.-C.; Mak, T. C. W. *Chem. Comm*. **1999**, 1849.

108. Zhang, X.-M.; Hao, Z.-M.; Wu, H.-S. *Inorg. Chem.* **2005**, *44*, 7301.

109. Power, K. N.; Lennigar, T. C.; Zanarotko, M. J. *Chem. Comm.* **1998**, *48*, 95.

110. Kinoshita, I.; Wright, L. J.; Kubo, S.; Kimura, K.; Sakata, A.; Yano, T.; Miyamoto, R.; Nishioka, T.; Isobe, K. *Dalton Trans.* **2003,** 1993.

111. Zhang, B.-Y.; Yang, Q., Nie, J.-J. *Acta Cryst. E* **2008**, *E64*, m7.

112. Zhang, X.-M.; Fang, R.-Q.; Wu, H.-S. *J. Am. Chem. Soc.* **2005**, *127*, 7670.

113. Kappenstein, C.; Hugel, R. P. *Inorg. Chem.* **1977**, *16*, 250.

114. Hibble, S.; Chippendale, A. M. *Z. Anorg. Allg. Chem*. **2005**, *631*, 542.

115. Blake, A. J.; Champness, N. R.; Khlobystov, A.; Lemenovskii, D. A.; Li, W.-S., Schroder, M. *Chem. Comm*. **1997**, 2813.

116. Peindy, H. N.; Guyon, F.; Khatyr, A.; Knorr, M.; Strohmann, C. *Eur. J. Inorg. Chem*. **2007**, 1823.

117. (a) Dai, J.; Munakata, M.; Wu, L.-P.; Kuroda-Sowa, T.; Suenga, Y. *Inorg. Chim. Acta* **1997**, *258*, 65. (b) Caradoc-Davies, P. L.; Hanton, L. R., Hodgkiss, J. M.; Spicer, M. D. *J. Chem. Soc. Dalton Trans.* **2002**, 1581.

118. Bondi, A. *J. Phys. Chem*. **1964**, *68,* 441.

119. Hanton, L. R.; Richardson, C.; Robinson, T.; Turnbull, J. M. *Chem. Comm*. **2000**, 2465.

120. Teichert, O.; Sheldrick, W. S. *Z. Anorg. Allg. Chem*. **2000**, *626*, 2196.

121. Moreno, J. M.; Suarez-Valera, J.; Colacio, J. C.; Avila-Roson, M. A.; Hildago, D.; Martin-Ramos, D. *Can. J. Chem*. **1995**, *73*, 1591.

122. Blake, A. J.; Brooks, N. R.; Champness, N. R.; Crew, M.; Hanton, L. R.; Hubbersley, P.; Parsons, S.; Schröder, M. *J. Chem. Soc. Dalton Trans.* **1999,** 2813.

123. Shi, J.-M.; Xu, W.; Zhao, B.; Cheng, P.; Liao, D.-Z.; Chen, X.-Y. *Eur. J. Inorg. Chem*. **2005**, 55.

124. de Castro, V. D.; de Lima, G. M.; Filgueiras, C. A. L.; Gambardella, M. T. P. *J. Molec. Struct*. **2002**, *609*, 199.

125. Zheng, Y.; Du, M.; Li, J.-R.; Zhang, R.-H.; Bu, X. H. *Dalton Trans.* **2003**, 1509.

126. Hartley, F.R. (Ed). *The Chemistry of Organophosphorus compounds*, Vol.4, Wiley: New York, 1996.

127. Quin, L. D. A. *Guide to organophosphorus chemistry*, Wiley: New York, 2000.

128. Clearfield, A. *Prog. Inorg. Chem.* **1998**, *47*, 371.

129. Clearfield, A., Wang, Z. *J. Chem. Soc., Dalton. Trans*. **2002**, 2937.

130. Minimol, M. P.; Rao, K.P.; Sai, Y. R.; Vidysagar, K. *Proc. Indian Acad. Sci.* (*Chem. Sci.*), **2003**, *115*, 419.

131. Cao, G.; Lee, H.; Lynch, V. M; Mallouk, T. E. *Inorg. Chem.* **1988**, *27*, 2781.

132. Cao, G.; Lee, H.; Lynch, V. M; Mallouk, T. E. *Solid State Ionics* **1988**, *26*, 63.

133. Martin, K. J.; Squattrito, P. J.; Clearfield, A. *Inorg. Chim. Acta* **1989**, *155*, 7.

134. Cabeza, A.; Aranda, M. A. G.; Bruque, S.; Poojary, D. M.; Clearfield, A. *Mater. Res. Bull.* **1998**, *33*, 1265.

135. Cabeza, A.; Aranda, M. A. G.; Bruque, S.; Poojary, D. M.; Clearfield, A.; Sanz, J. *Inorg. Chem*. **1998**, *37*, 4168.

136. Cunningham, D.; Hennelly, P. J. D.; Deeney, T. *Inorg. Chim. Acta* **1979**, *37*, 95.

137. Raki, L.; Detellier, C. *Chem. Comm*. **1996**, 2475.

138. Poojary, P. M.; Hu, H. L.; Campbell, F. L.; Clearfield, A. *Acta Cryst. B* **1993**, *49*, 996.

139. Maeda, K. *Micropor. Mesopor. Mater.* **2004**, *73*, 47.

140. Amicangelo, J.C.; Leenstra, W.R. *Inorg. Chem*. **2005**, *44*, 2067.

141. Chandrasekhar, V., Sasikumar, P., Boomishankar, R., Anantharamar, G. *Inorg. Chem*. **2006**, *45*, 3344.

142. Drumel, S.; Janvier, P.; D. Deniaud, D.; Bujoli, B. *J. Chem. Soc. Chem. Comm.* **1995**, 1051. (b) Drumel, S.; Janvier, P.; Barboux, P.; Bujoli-Doeuff, M.; Bujoli, B. *Inorg. Chem*. **1995**, *34*, 148. (c) Hartman, S.J.; Todorov, E.; Cruz, C.; Sevov, S.S. *Chem. Comm.* **2000**, 1213.

143. (a) Clearfield, A. *Chem. Mater.* **1998**, *10*, 2801. (b) Hix, G. B.; Kariuki, B. M; Kitchin, S.; Tremayne, M. *Inorg. Chem.* **2001**, *40*, 1477.

144. Menaa, B.; Shannon, I. J. *J. Mater. Chem.* **2002**, *12*, 350.

145. Bellitto, C.; Bauer, E. M.; Righini, G. *Inorg. Chim. Acta* **2008**, *361*, 3785.

146. (a) Michaelis, A.; Kaehene, R. *Chem. Ber.* **1898**, *31*, 1408. (b) Arbuzov, A. E. *J. Russ. Phys. Chem. Soc.* **1906**, *38*, 687.

147. Bhattacharya, A. K.; Thyagarajan, G, *Chem. Rev.* **1981**, *81*, 415.

148. McKenna, C. E. *Chem. Comm.* **1979**, 739.

149. Hirao, T.; Masunaga, T.; Ohshiro, Y.; Agawa, T. *Tet. Lett*. **1980**, *21*, 3595.

150. Hirao, T.; Masunaga, T.; Yamada, N. *Bull. Chem. Soc. Jpn*. **1982**, *55*, 909.

151. Gelman, D. *Org. Letters* **2003**, *5*, 2315.

152. Huang, C.; Tang, X.; Fu, H.; Jiang, Y.; Zhao, Y. *J. Org. Chem.* **2006**, *71*, 5020.

153. Rao, C. N. R. *Chem. Eur. J.* **2006**, *12*, 3636.

154. Franz, G. *AAPS PharmaSci* **2001**, *3*, 2.

155. Cassidy, J. E.; Jarvis, J. A. J.; Rothon, R.N. *J. Chem. Soc. Dalton Trans.* **1975**, 1497.

156. (a) Roesky, H. W.; Walawalkar, M. G.; Murugavel, R. *Acc. Chem. Res*. **1999**, *32*, 117. (b) Storre, J.; Klemp, A.; Roesky, H. W.; Fleischer, R.; Stalke, D. *Organomet.* **1997**, *16*, 3074. (c) González-Gallardo, S.; Jancik, V.; Cea-Olivares, R.; Toscano, R. A.; Moy-Cabrera, M. *Angew. Chem. Int. Ed.* **2007**, *46*, 2895. (d) Chakraborty, D.; Horchler, S.; Roesky, H. W.; Noltemeyer, M.; Schmidt, H-G. *Inorg. Chem.* **2000**, *39*, 3995.

157. (a) Harlan, C. J.; Mason, M. R.; Barron, A. R. *Organomet.* **1994**, *13*, 2957. (b) Landry, C. C.; Harlan, C. J.; Bott, S. G.; Barron, A. R. *Angew. Chem. Int. Ed. Engl.* **1995**, *34*, 1201. (c) Koide, Y.; Barron, A. R. *Organomet.* **1995**, *14*, 4026. (d) Keys, A.; Bott, S.; Barron, A. R. *Chem. Comm.* **1996**, 2339.

158. (a) Lii, K.-H.; Huang, Y.-F. *Inorg. Chem.* **1999**, *38*, 1348. (b) Maeda, K.; Akimoto, J.; Kiyozumi, Y.; Mizukami, F. *Angew. Chem. Int. Ed*. **1995**, *34*, 1199. (c) Maeda, K.; Akimoto, J.; Kiyozumi, Y.; Mizukami, F. *J. Chem. Soc. Chem. Comm*. **1995**, *20*, 1033.

159. (a) Kratochvil, J.; Necas, M.; Petricek, V.; Pinkas, J. *Inorg. Chem.* **2006**, *45*, 6562. (b) Josien, L.; Simon-Masseron, A.; Gramlich, V.; Patarin, J.; Rouleau, L. *Chem. Eur. J.* **2003**, *9*, 856. (c) Hix, G. B.; Wragg, D. S.; Wright, P. A.; Morris, R. E. *J. Chem. Soc. Dalton Trans.* **1998**, 3359. (d) Lin, C.-H.; Wang, S-L.; Lii, K-H. *J. Am. Chem. Soc.* **2001**, *123*, 4649 .

160. (a) Redmore, D. *J. Org. Chem.* **1970**, *35*, 4114. (b) Chen, D.; Martell, A. E.; Motekaitis, R. J.; McNamus, D. *Can. J. Chem.* **1998**, *76*, 445. (c) Bulot, J. J.; Elia Aboujaoude, E.; Collignon, N.; Savignac, P. *Phosphorus and Sulfur* **1984**, *21*, 197. (d) A. Viinikanoja, J. Lukkari, T. Aeaeritalo, T. Laito, J. Kankare, *Langmuir* 2003, 19, 2768.

161. (a) Fawcett, J.; Platt, A. W. G.; Vickers, S. *Polyhedron* **2003,** *22*, 1431. (b) Bianchi, E. M.; Sajadi, S. A. A.; Song, B.; Sigel, H. *Chem. Eur. J.* **2003**, *9*, 881. (c) Xiang, J. F.; Li, M.; Si-min, W.; Jie, Y. L.; Sun, J. *Coord. Chem.* **2007**, *60*, 1867. (d) Wu, J.; Hongwei, H.; Huayun, F.; Fan, Y. *Inorg. Chem.* **2007**, *46*, 7960. (e) Fredoueil, F.; Penicaud, V.; Bujoli-Doeuff, M.; Bujoli, B. *Inorg. Chem.* **1997**, *36*, 4702. (f) Gan, X.-M.; Rapko, B. M.; Fox, J.; Binyamin, I.; Pailloux, S.; Duesler, E. N.; Paine, R. T. *Inorg. Chem*. **2006**, *45*, 3741

162. Ion exchange of phosphonates: (a) Clearfield, A. *New Developments in Ion Exchange Materials*; Abe, M.; Kataoka, T.; Suzuki, T.; Eds.; Kodansha, Ltd.: Tokyo: Japan, 1991. (b) Ortiz-Avila, C. Y.; Bhardwaj, C.; Clearfield, A. *Inorg. Chem.* **1994**, *33*, 2499. For catalysis examples see: (c) Wan, B.-Z.; Anthony, R. G.; Peng, G.-Z.; Clearfield, A. *J. Catal.* **1994**, *101*, 19. (d) Colon, J. L.; Thakur, D. S.; Yang, C.-Y.; Clearfield, A. *J. Catal.* **1990**, *124*, 148. (e) Deniaud, D.; Schollorn, B.; Mansuy, D.; Rouxel, J.; Battioni, P.; Bujoli, B. *Chem. Mater.* **1995**, *7*, 995. Applications as ion sensors. (f) Cao, G.; Hong, H.; Mallouk, T. E. *Acc. Chem. Res.* **1992**, *25*, 420. (g) Alberti, G.; Polombari, R. *Solid State Ionics* **1989**, *35*, 153. (h) Alberti, G.; Casciola, M.; Polombari, R. *Solid State Ionics* **1992**, *52*, 291. (i) Thompson, M. E. *Chem. Mater.* **1994**, *6*, 1168.

163. (a) Ungashe, S. B.; Wilson, W. L.; Katz, H. E.; Scheller, G. R.; Putvinski, T. M. *J. Am. Chem. Soc.* **1992**, *114*, 8717. (b) Clearfield, A. *Comments Inorg. Chem.* **1990**, *10*, 114. (c) Alberti, G.; Costantino, U.; Allulli, S.; Tomassini, J. *J. Inorg. Nucl. Chem.* **1978**, *40*, 1113. (d) S. Yamanaka, *Inorg. Chem.* **1976**, *15*, 2811.

164. Konar, S.; Zo, J.; Provirin, A. V.; Dunbar, K. R.; Clearfield, A. *Inorg. Chem.* **2007**, *46*, 5229.

165. Samanamu, C. R.; Richards, A. F. *Inorg. Chim. Acta* **2007**, *360*, 4037.

166. (a) Kaminsky, W.; Sinn, H.; Proc. IUPAC, IUPAC, *Macromol. Symp.* **1982**, *28*, 247. (b) Wehmschulte, R. J; Power, P. P. *J. Am. Chem. Soc.* **1997**, *119,* 8387. (c) Wu, F.-J.; Simeral, L. S.; Mrse, A. A.; Eilertsen, J. L.; Negureanu, L.; Gan, Z.; Fronczek, F. R.; Hall, R. W.; Butler, L. G. *Inorg. Chem.* **2007**, *46*, 44.

167.Mason, M. R.; Smith, J. M.; Bott, S. G.; Barron, A. R.; *J. Am. Chem. Soc.* **1993**, *15*, 4971.

168. Albrecht, M.; Dehn, S.; Fröhlich, R. *Angew. Chem. Int. Ed.* **2006**, *45*, 2792.

169. (a) Lin, C-H.; Wang, S-L.; *Inorg. Chem.* **2005**, *44*, 251. (b) Josien, L.; Masseron, A. S.; Gramlic, V.; Patarin, J. *Chem. Eur. J.* **2002**, *8*, 1614. (c) Davis, M. E.; Saldarriaga, C.; Montes, C.; Garcès, J.; Crowder, C. *Zeolites,* **1988**, *8*, 362. (d) Hui, Q.; Xu, R.; Li, S.; Ma, Z.; Thomas, J. M.; Jones, R. H.; Chippindale, A. M. *J. Chem. Soc. Chem. Comm*. **1992**, 876. (e) Lin, C. H.; Wang, S. L.; Lii, K. H. *J. Am. Chem. Soc*. **2001**, *123*, 4649.

170. Johannson, G. *Ark. Kemi* **1962**, *20*, 305. (b) Alluche, L.; Gerardin, C.; Loiseau, T.; Ferey, G.; Taulelle, F.; *Angew Chem. Int. Ed.* **2000**, *39*, 511. (c) Seichter, W.; Mogel, H.-J.; Brand, P.; Salah, D.; *Eur. J. Inorg. Chem.* **1998**, 795. (d) Heath, S. L.; Jordan, P. A.; Johnson, I. D.; Moore, G. R.; Powell, A. K.; Helliwell, M. *J. Inorg. Biochem.* **1995**, *59*, 785.

171. (a) Atwood, J. L.; Hrncir, D. C.; Priester, R. D; Rogers, R. D. *Organomet.* **1983**, *2*, 985. (b) Casey, W. H.; Olmstead, M. M.; Phillips, B. L. *Inorg. Chem*. **2005**, *44*, 4888.

172. Pasynkiewicz, A. *Polyhedron* **1990**, *9*, 429.

173. Aranda, M. A. G.; Losilla, E. R.; Cabeza, A.; Bruque, A. J. *J. Appl. Crystallogr.* **1998**, *31*, 16.

174. Reactions were attempted in NH_4OH, by addition of NaOH, pyridine or triethylamine. Reactions were also performed at neutral pH but no crystalline material could be isolated.

175.Vitse, P.; Galy, J.; Potier, A. *C. R. Chim.* **1973**, *277*, 159.

176. (a) Goodwin, J. L.; Teal, S. J.; Heath, S. L.; *Angew Chem. Int. Ed.* **2004,** *43*, 4037. (b) Gerasko, O. A.; Mainicheva, E. Q.; Naumov, D. Y.; Kuratieva, N. V.; Sokolov, M. N.; Fedin, V. P. *Inorg. Chem.* **2005**, *44*, 4133.

177. Landry, C. C.; Cleaver, W. M.; Guzei, I. A.; Rheingold, A. L. *Organomet.* **1998**, *17*, 5209.

178. Mason, M. R.; Perkins, A. M.; Matthews, R. M.; Fisher, J. D.; Mashata, M. S.; Vij, A. *Inorg. Chem.* **1998**, *37*, 3734.

179. Morizzi, J.; Hobday, M.; Rix, C. *J. Mater. Chem.* **2000**, *10*, 1693.

180. Van Poppel, L. H.; Bott, S. G.; Barron, A. R. *Polyhedron*, **2002**, *21*, 1877.

181. (a) Yang, Y.; Liu, Y.; Chen, C.; Wang, W.; Yi, Z.; Pang, W. *Polyhedron*, **2004**, 23, 1535. (b) Chippindale, A.M.; Peacock, K. J.; Cowley, A.R. *J. Solid State Chem*. **1999**, 145, 379. (c) Chen, C-Y.; Chu, P.P.; Lii, K-H. *Chem. Comm*. **1999**, 1473.

182. Bujoli-Doeuff, M.; Evain, M.; Fayon, F.; Alonso, B.; Massiot, D.; Bujoli, B. *Eur. J. Inorg. Chem*. **2000**, 2497.

183. (a) Lii, K.-H.; Huang, Y.-F. *Inorg. Chem.* **1999**, *38*, 1348. (b) Morizzi, J.; Hobday, M.; Rix, C. *J. Mater. Chem.* **1999**, *9*, 863. (c) Mason, M. R. *J. Cluster Sci*. **1998**, *9*, 1.

184. Samanamu, C.R.; Richards, A.F. Unpublished results.

185. (a) Sinn, H.; Kaminsky, W. *Adv. Organomet. Chem.* **1980**, *18*, 99. (b) Feng, T. L.; Gurian, P. L.; Healy, M. D.; Barron, A. R. *Inorg. Chem.* **1990**, *29*, 408. (c) Koide, Y.; Bott, S. G.; Barron, A. R. *Organometallics* **1996**, *15*, 2213. (d) Galimberti, M.; Destro, M.; Fusco, O.; Piemontesi, F.; Camurati, I. *Macromolecules* **1999**, *32*, 258 (e) Kaminsky, W. *Catal. Today* **2000**, *62*, 23 (f) Watanabi, M.; McMahon, C. N.; Harlan, C. J.; Barron, A. R. *Organometallics* **2001**, *20*, 460.

186. (a) Chen, C. L.; Goforth, A. M.; Smith, M. D.; Su, C. Y., Zur Loye, H.-C. *Inorg. Chem.* **2005**, *44*, 8762. (b) Ma, B. Q.; Mulfort, K. L.; Hupp, J. T. *Inorg. Chem.* **2005**, *44*, 4912.

187. (a) Sawka-Dobrowolska, W.; Glowiak, T.; Antonov, A.; Jezowska-Trzebiatowska, B. *Acta Crystallogr. A* **1978**, *34*, S141. (b) Glowiak, T.; Sawka-Dobrowolska, W.; Jezowska-Trzebiatowska, B.; Antonow, A. *Inorg. Chim. Acta* **1980,** *45*, 105. (c) Glowiak, T., Sawka-Dobrowolska, W.; Jezowska-Trzebiatowska, B.; Antonow, A. *J. Cryst. Mol. Struct.* **1980**, *10*, 1.

188. (a) Mao, J.-G.; Clearfield, A. *Inorg. Chem.* **2002**, *41*, 2319. (b) Cabeza, A.; Ouyang, X.; Sharma, K. V. C.; Aranda, M. A. G.; Bruque, S.; Clearfield, A. *Inorg. Chem.* **2002**, *41*, 2325. (c) Mao, J.-G.; Wang, Z.; Clearfield, A. *Inorg. Chem.* **2002**, *41*, 2334. (d) Martinez-Tapia, H. S.; Cabeza, A.; Bruque, S.; Pertierra, P.; Garcia-Granda, S.; Aranda, M. A. G. *J. Solid State Chem.* **2000**, *151,* 122. (e) Bishop, M.; Bott, S. G.; Barron, A. R. *Chem. Mater.* **2003**, *15*, 3074. (f) Kong, D.; Li, Y.; Ouyang, X.; Prosvirin, A.V.; Zhao, H.; Ross Junior, J. H.; Dunbar, K. R.; Clearfield, A. *Chem. Mater*. **2004**, *16*, 3020. (g) Bauer, S.; Muller, H.; Bein, T.; Stock, N. *Inorg. Chem.* **2005**, *44*, 9464. (h) Du, Z.-Y.; Ying, S.-M.; Mao, J.-G. *J. Mol. Struct.* **2006**, *788*, 218. (i) Sharma, C. V. K.; Clearfield, A. *J. Am. Chem. Soc.* **2000**, *122*,

1558. (j) Yang, B.-P.; Mao, J.-G.; Sun, Y.-Q.; Zhao, H.-H.; Clearfield, A. *Eur. J. Inorg.Chem.* **2003**, 4211.

189. (a) Fry, J. A.; Samanamu, C. R., Montchamp, J.-L.; Richards, A. F. *Eur. J. Inorg. Chem.* **2008**, *3*, 463. (b) Samanamu, C. R.; Montchamp, J.-L.; Olmstead, M. M.; Richards, A. F. *Inorg. Chem.* **2008**, *47*, 3879.

190. (a) Choudhury, A.; Natarajan, S.; Rao, C. N. R. *Inorg. Chem.* **2000**, *39*, 4295. (b) Chidambaram, D.; Neeraj, S.; Natarajan, S.; Rao, C. N. R. *J. Solid State Chem.* **1999**, *147*, 154.

191. (a) Yu, Y.; Wang, Y.; Shi, Z.; Xu, R. *Chem. Mater.* **2001**, *13*, 2972. (b) Alexios, M.; Dendrinou-Samara, C.; Raptopoulou, C.P.; Terzis, A. *Inorg. Chem.* **2002**, *41*, 4732. (c) Kubieck, V.; Vojtisek, P.; Rudovsky, J.; Hermann, P.; Lukes, I. *Dalton Trans.* **2003**, 3927. (d) Videra, V.; Chauvin, A.S.; Varbanov, S.; Baux, C.; Scopelith, R. *Eur. J. Inorg. Chem.* **2004**, 2173. (e) Looney, A.; Lornebise, M.; Miller, D.; Parkin, G. *Inorg. Chem.* **1992**, *31*, 989. (f) Poat, J. C.; Slawin, A. M. Z.; Williams, D. J.; Woollins, J. D. *Polyhedron* **1992***, 11*, 2125–2126.

192. Neeraj, S.; Natarajan, S. *J. Mater. Chem.* **2000**, *10*, 1171.

193. Cotton, F. A.; Wilkinson, G.; Murillo, C. A.; Bochmann, M. *Advanced Inorganic Chemistry*; 6th ed., Wiley-Interscience: New York, 1999.

194. (a) Mao, J.-G.; Wang, Z.; Clearfield, A. *Inorg. Chem.* **2002**, *41*, 3713. (b) Mao, J.-G.; Wang, Z.; Clearfield, A. *J. Chem. Soc. Dalton Trans.* **2002**, 4457. (c) Stock, N.; Bein, T. *J. Solid State Chem.* **2002**, *167*, 330. (d) Greenwood, N. N.; Earnshaw, A. *Chemistry of the Elements*; 2nd ed., Butterworth-Heinemann: Massachusetts, 1997.

195. Hydrogen atoms on the cadmium phosphonate polymer could not be satisfactorily refined due to the disorder in the NH_2 group of the ligand. Solution of complex **21** in a non-centro symmetric space group removes the disorder in the amino group and allows the hydrogen atoms to be located and refined. Formula = $C_1H_5Cd_1N_2O_6P$, Orthorhombic, $Pna2_1$, a = 19.981(2), b = 5.1465(6), c = 6.2790(7), Z = 4, Final R [$I>2\sigma(I)$] R1 = 0.0243, wR_2 = 0.0554.

196. (a) Corbridge, D. E. C., *P an outline of its biochemistry and technology*, 4th ed., Elsevier: Amsterdam, 1990; (b) Nakamoto, K. *Infrared Spectra of Inorganic and Coordination Compounds*, Wiley: New York, 1963.

197.(a) Pantenburg, I.; Thosen, C.; Hoge, B. *Z. Anorg. Allg. Chem.* **2002**, *628*, 1785. (b) Tschinkl, M.; Bachman, R. E.; Gabbai, F. P. *Organomet*. **2000**, *19*, 2633. (c) Vojtisek, P.; Rohovec, J.; Lukes, I. *Collect. Czech. Chem. Commun*. **1997**, *62*, 1710. (d) Mather, G. G.; Pidcock, A. *J. Chem. Soc. Dalton* **1978**, 560. (e) Stepnicka, P.; Cisarova, I.; Gyepes, R. *Eur. J. Inorg. Chem.* **2006**, 926.

198. (a) Bowen, S. M.; Deusler, E. N.; Paine, R. T.; Campana, C. F. *Inorg. Chim. Acta* **1982**, *59*, 53. (b) Tikhonova, I. A.; Dolgushin, F. M.; Tugashov, K. I.; Petrovskii, P. V.; Furin, G. G.; Shur, V. B. *J. Organomet. Chem.* **2002**, *654*, 123. (c) Zhu, Z.-B.; Gao, S.; Huo, L.-H.; Ng, S. W. *Acta Crystallogr. E*. **2005**, *65*, m288. (d) Balch, A. L.; Olmstead, M. M.; Rowley, S. P. *Inorg. Chem.* **1988**, *27*, 2275. (e) Byriel, K. A.; Dunster, K. R.; Gahan, L. R.; Kennard, C. H. L.; Latten, J. L. *Inorg. Chim. Acta* **1992**, *196*, 35.

199. (a) Weiss, R.; Kraut, N.; Hampel, F. *J. Organomet. Chem.* **2001**, *617*, 473. (b) Balasubramani, K.; Muthiah, P. T.; Bocelli, G.; Cantoni, A. *Analytical Sciences: X-ray Structure Analysis Online* **2007**, *23*, 129. (c) Hoskins, B. F.; Robson, R.; Sutherland, E. E. *J. Organomet. Chem.* **1996**, *515*, 259. (d) Lobana, T.; Tarlok, S.; Sandhu, K.; Maninderjeet, D. C.; Povey, G. W.; Smith *J. Chem. Soc. Dalton Trans.* **1988**, *12*, 2913.

200. (a) Alcock, N. W.; Lampe, P. A.; Moore, P. *J. Chem. Soc. Dalton Trans.* **1978**, 1324. (b) Bharara, M. S.; Bui, T. H.; Parkin, S.; Atwood, D. A. *Dalton Trans.* **2005**, 3874. (c) Brodersen, K.; Beck, R. *Z. Anorg. Allg. Chem.* **1987**, *553*, 35.

201. (a) Nockemann, P.; Meyer, G. *Z. Anorg. Allg. Chem.* **2003**, *629*, 1294. (b) Brodersen, K.; Zimmerhackl, J. *Z. Naturforsch. B* **1991**, *46*, 1. (c) Kepert, D. L.; Taylor, D.; White, A. H. *J. Chem. Soc. Dalton Trans.* **1973**, 392. (d) Galassi, R.; Bachechi, F.; Burini, A. *J. Mol. Struct.* **2006**, *791*, 82. (e) Canty, A. J.; Deacon, G. B. *Inorg. Chim. Acta* **1980**, *45*, L225.

202. (a) Cabeza, A.; Aranda, M. A. G.; Martinez-Lara, M.; Bruque, S.; Sanz, J. *Acta Crystallogr. B.* **1996,** *52,* 982. (b) Poojary, D. M.; Zhang, B. L.; Clearfield, A. *J. Mater. Chem*. **1996**, *8*, 1333. (c) Cabeza, A.; Aranda, M. A. G.; Bruque, S. *J. Mater. Chem.* **1999**, *2*, 571.

203. (a) Yang, B.-P.; Sun, Z.-M.; Mao, J.-G. *Inorg. Chim. Acta* **2004**, *357*, 1583. (b) Ayyappan, S.; Diaz de Delgado, G.; Cheetham, A. K.; Ferey, G.; Rao, C. N. R. *J. Chem. Soc. Dalton Trans.* **1999**, 2905. (c) Ying, S.-M.; Mao, J.-G. *Eur. J. Inorg. Chem.* **2004**, 1270, 1276. (d) Song, J.-L.; Lei, C.; Sun, Y.-Q.; Mao, J.-G. *J. Solid State Chem.* **2004***, 177*, 2557.

(e) Sun, Z.-M.; Mao, J.-G.; Sun, Y.-Q.; Zheng, H.-Z.; Clearfield, A. *New. J. Chem.* **2003**, *27*, 1326.

204. (a) Mao, J. G.; Wang, Z.; Clearfield, A. *Inorg. Chem.* **2002**, *41*, 6106. (b) Stock, N. *Solid State Sci.* **2002**, *4*, 1089.

205. Sagatys, D.S.; Dahlgren, C.; Smith, G.; Bott, R. C.; White, J. M. *J. Chem. Soc. Dalton Trans.* **2000**, 3404.

206. For an example see: Wang, Q.-M.; Mak, T. C. W. *Chem. Eur. J*. **2003**, *9*, 44.

207. (a) Shi, M.; Jiang, J.-K. *Chirality* **2003**, *15*, 605. (b) Zhao, X.-L.; Mak, T. C. W. *Inorg. Chim. Acta* **2006**, *359*, 3451. (c) Hou, H.; Wei, Y.; Song, Y.; Mi, L.; Tang, M.; Li, L.; Fan, Y. *Angew. Chem. Int. Ed.* **2005**, *44*, 6067. (d) Su, W.; Cao, R.; Hong, M.; Wong, W.-T.; Lu, J. *Inorg. Chem. Commun.* **1999**, *2*, 241. (e) Zhao, X.-L.; Mak, T. C. W. *Polyhedron* **2006**, *25*, 975.

208. (a) Liu, H.-Y.; Wu, H.; Ma, J.-F.; Song, S.-Y.; Yang, J.; Liu, Y.-Y.; Su, Z.-M. *Inorg. Chem.* **2007**, *46*, 7299. (b) Teets, T.S.; Partyka, D. V.; Esswein, A.J.; Updegraff, J. F.; Zeller, M.; Hunter, A. D.; Gray, T. G. *Inorg. Chem.* **2007**, *46*, 6218. (c) Belicchi, M.; Ferrari, F.; Bisceglie, E.; Cavalli, G.; Pelosi, P.; Tarasconi, V.; Verdolino, V. *Inorg. Chim. Acta* **2007**, *360*, 3233. (d) Liu, B.; Chen, W.; Jin, S. *Organomet.* **2007**, *26*, 3660.

209. Kitagawa, S.; Kitaura Ryo, R.; Noro, S. *Angew. Chem. Int. Ed.* **2004**, *43*, 2334.

210. (a) Catalano, V. J.; Malwitz, M. A.; Etogo, A. O. *Inorg. Chem.* **2004**, *43*, 5714. (b) Yam, V. W.-W.; Lo, W.-Y.; Lam, C. H.; Fung, W. K. -M.; Wong, K.M.-C.; Lau, V.C.-Y.; Zhu, N. *Coord. Chem. Rev.* **2003**, *245*, 39. (c) McKee, V.; Nelson, J.; Speed, D. J.; Town, R. M. *J. Chem. Soc. Dalton Trans.* **2001**, 3641. (d) Catalano, V.J.; Malwitz, M.A. *Inorg. Chem.* **2003**, 42, 5483. (e) Catalano, V. J.; Moore, A. L. *Inorg. Chem.* **2005**, *44*, 6558.

211. (a) Noro, S.; Miyasaka, H.; Kitagawa, S.; Wada, T.; Okubo, T.; Yamashita, T.; Mitani, T. *Inorg. Chem.* **2005**, *44*, 133. (b) Toyota, A.; Yamaguchi, T.; Igashira-Kamiyama, A.; Kawamoto, T.; Konno, T. *Angew. Chem. Int. Ed.* **2005**, *44*, 1088. (c) Schultheiss, N.; Barnes, C. L.; Bosch, E. *Cryst. Growth Des.* **2003**, 573. (d) Sylvestre, I.; Wolowska, J.; Kilner, C.A.; McInnes, E. J. L.; Halcrow, M. A. *Dalton Trans.* **2005**, 3241. (e) Zou, Y.; Liu, W.-L.; Lu, C.-S.; Wen, L.-L.; Meng, Q.-J. *Inorg. Chem. Commun.* **2004**, *7*, 985. (f) Brouca-Cabarrecq, C.; Marrot, B.; Mosset, A. *Acta Crystallogr. C*. **1996**, *52*, 1903. (g) Shakibaie-Moghadam, M.; Timper, U.; Heller, G. *Z. Naturforsch, B*. **1994**, *49*, 627.

212. (a) Examples include: Park, Y. J.; Do, Y.; Kim, K. M.; Choi, M.-G.; Jun, M.-J.; Kim, C. *Polyhedron* **2002**, *21*, 33. (b) Yan, B.; Capracotta, M. D.; Maggard, P.A. *Inorg. Chem.* **2005**, *44*, 6509.

213. (a) Rodriguez-Dieguez, A.; Cano, J.; Kivekas, R.; Debdoubi, A.; Colacio, E. *Inorg. Chem.* **2007**, *46*, 2503. (b) Khan, M. I.; Yohannes, E.; Golub, V. O.; O'Connor, C. J.; Doedens, R. J. *Chem. Mater.* **2007**, *19*, 4890. (c) Persky, N. S.; Chow, J. M.; Poschmann, K.A.; Lacuesta, N. N.; Stoll, S. L.; Bott, S. G.; Obrey, S. *Inorg. Chem.* **2001**, *40*, 29.

214. (a) Mancin, F.; Scrimin, P.; Tecilla, P.; Tonellato, U. *Chem. Comm.* **2005**, 2540. (b) Panda, R.; Berlinguette, C. P.; Zhang, Y.; Holm, R. H. *J. Am. Chem. Soc.* **2005**, *127*, 11092. (c) Ciurtin, D.; Smith, M. D.; Zur Loye, H.-C. *Chem. Comm.* **2002**, 74.

215. (a) Carlucci, L.; Ciani, G.; Porta, F.; Proserpio, D. M.; Santagostini, L. *Angew. Chem., Int. Ed.* **2003**, *42*, 317. (b) Carlucci, L.; Ciani, G.; Porta, F.; Proserpio, D. M.; Santagostini, L. *Angew. Chem. Int. Ed.* **2002**, *41*, 1907. (c) Dong, Y. B.; Smith, M. D.; Zur Loye, H.-Z. *Angew. Chem., Int. Ed*. **2000**, *39*, 4271.

216. (a) Young, A. G.; Hanton, L. R. *Coord. Chem. Rev.* **2008**, *252*, 1346. (b) Bowmaker, G.A.; Effendy, K. C.; Lim, B. W.; Skelton, D.; Sukarianingsih, S; White, A. H. *Inorg. Chim. Acta* **2005**, *358*, 4342.

217. (a) Luo, T.-T.; Hsu, L.-Y.; Su, C.-C.; Ueng, C.-H.; Tsai, T.-C.; Lu, K.-L. *Inorg. Chem.* **2007**, *46*, 1532. (b) Dong, Y.-B.; Smith, M. D.; Zur Loye, H.-C. *Inorg. Chem.* **2000**, *39*, 1943.

218. Khlobystov, A. N.; Blake, A. J.; Champness, N. R.; Lemenovskii, D. A.; Majouga, A. G.; Zyk, N. V.; Schroder, M. *Coord. Chem. Rev.* **2001**, *222*, 155.

219. (a) Baxter, P. N. W.; Lehn, J.-M.; Baum, G.; Fenske, D. *Chem. Eur. J.* **2000**, *6*, 4510. (b) Toyota, S.; Woods, C. R.; Benaglia, M.; Haldimann, R.; Warnmark, K.; Hardcastle, K.; Siegel, J. S. *Angew. Chem. Int. Ed.* **2001**, *40*, 751. (c) Hiraoka, S.; Yi, T.; Shiro, M; Shionoya, M. *J. Am. Chem. Soc.* **2002**, *124*, 14510.

220. (a) Su, C.-Y.; Cai, Y.-P.; Chen, C.-L.; Smith, M. D.; Kaim, W.; Zur Loye, H.-C. *J. Am. Chem. Soc.* **2003**, *125*, 8595. (b) Wu, H.-P.; Janiak, C.; Rheinwald, G.; Lang, H. *J. Chem. Soc. Dalton Trans.* **1999**, 183. (c) Jia, C.; Liu, S.-X.; Neels, A.; Labat, G.; Decurtins, S. *Polyhedron* **2005**, *24*, 3032. (d) Brammer, L.; Burgard, M. D.; Rodger, C. S.; Swearingen, J.

K.; Rath, N.P. *Chem. Comm*. **2001**, 2468. (e) Nattinen, K. I.; Linnanto, J.; Rissanen, K. *Eur. J. Inorg. Chem.* **2003**, 4078.

221. Blake, A. J.; Champness, N. R.; Hubberstey, P.; Li, W.-S.; Witthersby, M. A.; Schroder, M. L. *Coord. Chem. Rev.* **1999**, *183*, 138.

222. (a) Bu, X.-H; Xie, Y.-B.; Li, J.-R.; Zhang, R.-H. *Inorg. Chem.* **2003**, *42*, 7422. (b) Gong, Y.-Q.; Chen, J.-T.; Yuan, D.-Q.; Wu, M.-Y.; Huang, Y.-G., Jiang, F.-L.; Hong, M.-C. *Inorg. Chim. Acta* **2007**, *360*, 2207.

223. Cooke, M. W.; Chartrand, D.; Hanan, G. S. *Coord. Chem. Rev.* **2007**, *252*, 903.

224. (a) Wang, Y.; Bao, S.-S.; Xu, W.; Chen, J.; Gao, S.; Zheng, L.-M. *J. Solid State Chem.* **2004**, *177*, 1297. (b) Ma, Y.-S.; Song, Y.; Du, W.-X.; Li, Y. Z.; Zheng, L. M. *Dalton Trans.* **2006**, 3328. (c) Zhang, Y.; Clearfield, A. *Inorg. Chem.* **1992**, *31*, 2821. (d) Le Bideau, J.; Bujoli, B.; Jouanneaux, A.; Payen, C.; Palvadeau, P.; Rouxel, J. *Inorg. Chem.* **1993**, *32*, 4617.

225. (a) Barea, E.; Navarro, J. A. R.; Salas, J. M.; Masciocchi, N.; Galli, S.; Sironi, A. *Polyhedron* **2003**, *22*, 3051. (b) Gamez, P.; Van Albada, G.A.; Mutikainen, I.; Turpeinen, U.; Reedijk, J. *Inorg. Chim. Acta* **2005**, *358*, 1975.

226. (a) Cao, G.; Lynch, V. M.; Yacullo, L. N. *Chem. Mater.* **1993**, *5*, 1000. (b) Lin, Z.-E.; Sun, Y.-Q.; Zhang, J.; Wei, Q.-H.; Yang, G.-Y. *J. Mater. Chem.* **2003**, *13*, 447.

227. Barthelet, K.; Merlier, C.; Serre, C.; Riou- Cavellec, M.; Riou, D.; Ferey, G. *J. Mater. Chem.* **2002**, *12*, 1132.

228. Aakeroy, C. B.; Desper, J.; Levin. B.; Valdes-Martinez, J. *Inorg. Chim. Acta* **2006**, *359*, 1255.

229. Ayyappan, P.; Evans, O. R.; Foxman, B. M.; Wheeler, K. A. *Inorg. Chem.* **2001**, *40*, 5954.

230. (a) Barnett, S.A.; Champness, N. R.; Wilson, C. *Eur. J. Inorg. Chem.* **2005**, 1572. (b) Barnett, S. A.; Blake, A. J.; Champness, N. R.; Wilson, C. *Dalton Trans*. **2005**, 3852.

VITA

Christian Samanamu was born December 14, 1979 in Lima, Peru. He is the only child of Marina Chavez and Roberto Samanamu. In 1996, he graduated with honors from the Parrochial School “Saint Rose of Lima”- Maryknoll Fathers.

He received a Bachelor of Sciences degree in Chemistry from the Pontifical Catholic University of Peru in January 2004.

From February to July 2005 he worked as a Chemistry Lecturer in the Science Department of the Pontifical Catholic University of Peru.

In August 2005, he enrolled in graduate study at Texas Christian University, Fort Worth, Texas, to pursuit a PhD in Inorganic Chemistry. While working on his doctorate degree, he worked as a Graduate Teaching Assistant for four semesters and was awarded the Louis H. and Madlyn B. Barnett Scholarship from the Texas Christian University in the fall of 2007.

ABSTRACT
STUDIES ON THE SYNTHESIS OF MAIN GROUP AND LATE TRANSITION ELEMENT POLYMERS
By Christian Samanamu, Ph.D., 2009
Department of Chemistry
Texas Christian University
Dissertation Advisor: Anne F. Richards, Assistant Professor

Metal organic frameworks (MOFs) are metal-ligand compounds that extend into one, two or three dimensions via metal-ligand bonding that have found numerous technological applications, associated with their open pores and large internal surface area. The work developed in this doctoral thesis consists in the study of methodologies and systematic development of ligands or organic spacers for the synthesis of novel metal organic frameworks.

An introduction to the chemistry, structural features and diverse applications of metal organic frameworks is provided in Chapter 1.

The following chapter, chapter 2 involves the synthesis of gallium, indium and thallium metal organic frameworks using pyrazine, and pyrazine-2-carboxylic acid as organic spacers. The change in the pore size of the synthesized frameworks was studied in correlation with the atomic radii of the selected triel elements.

Chapter 3 describes the work with the flexible, multidentate heteroelemental dipodal ligands: bis(2-pyridylthio)methane, bis(2-pyrimidylthio)methane and bipyrimidyldisulfide. These ligands were reacted with a series of copper halides or pseudo halides for the isolation of cubane clusters and polymers depending on the flexibility of the selected ligands, the stereochemical requirements of the metal center and the preferred coordination modes of the corresponding halide or pseudo halide.

The fourth chapter deals with the use of 2-pyridinephosphonic acid ($2PyPOH_2$), 4-pyridinephosphonic acid ($4PyPOH_2$) and 4-pyridinemethylphosphonic acid ($4PyCH_2PO_3H_2$) for the synthesis of aluminum and gallium phosphonate cages. The isolation of these cages was achieved under careful control of the hydrolytic conditions of the corresponding reaction media.

Chapter 5, details the results of the studies with the ligand aminomethylphosphonic acid (ampa) for the construction of MOFs. The reaction of ampa with salts of Zn, Cd, Hg, Pb, Ag, Cu and Pb afforded new metal-phosphonate polymers with unique structural features and includes the synthesis of a bimetallic MOF containing Ag and Cu.

Finally, chapter 6 analyzes the ligand 5-pyrimidyl phosphonic acid (5-PymPO_3H_2) in the synthesis of homo and heteroelemental MOFs based on its possession of a phosphonate moiety for coordination and two heterocyclic nitrogen atoms at the opposite end to the PO_3H_2 to promote multi-site coordination. As a consequence it was possible to synthesize six coordination polymers, including a two dimensional, Cu/Ag polymer.

All of the MOFs obtained throughout these studies have been characterized by X-ray crystallography along with other spectroscopic techniques, including NMR, IR, UV/Vis, and MS.